Washington University in St. Louis

Washington University Open Scholarship

All Theses and Dissertations (ETDs)

1-1-2011

Studies of fluorescent imaging for mRNA detection in living cells

Zhenghui Wang
Washington University in St. Louis

Follow this and additional works at: https://openscholarship.wustl.edu/etd

WASHINGTON UNIVERSITY IN ST. LOUIS
Department of Chemistry

Dissertation Examination Committee:
Professor John-Stephen Taylor, Chairperson
Professor Mikhail Berezin
Professor Robert Blankenship
Professor Steven Brody
Professor Joshua Maurer
Professor Michael Welch

Title

**Studies of fluorescent imaging for mRNA
detection in living cells**

By

Zhenghui Wang

A dissertation presented to the Graduate
School of Arts and Sciences of Washington
University in partial fulfillment of the
requirements for the degree of Doctor of
Philosophy

August 2011

Saint Louis, Missouri

ABSTRACT

Studies of fluorescent imaging for mRNA
detection in living cells

By

Zhenghui Wang

Doctor of Philosophy in Chemistry

Washington University in St Louis, 2011

Professor John-Stephen Taylor, Chairperson

This dissertation focuses on the study of imaging mRNA in living cells. To achieve this research objective, three approaches have been utilized: (1) Imaging of a transgenic mRNA tagged by multiple repeats of malachite green (MG) binding aptamer. (2) Imaging of inducible nitric oxide synthase (iNOS) mRNA by strand-displacement activated Peptide Nucleic Acid (PNA) probes. (3) Imaging of iNOS mRNA by binary fluorescently labeled PNA probes.

The first approach was based on the work of our former lab member Dr. Huafeng Fang, who had constructed a multiple MG binding aptamer tagged transgene (Flag-mβ2AR-GFP-MGVI), which could also express a green fluorescence protein associated with an adrenergic receptor protein. It has been reported that the tagged aptamer sequence can increase the fluorescence of MG up to 2000 fold by binding to MG. Total RNA extract of the transfected MDCK cells has shown up to 22 times increase of fluorescence in the presence of MG. Confocal fluorescence imaging study has shown that in the

presence of MG, cells expressing the transgene showed both the fluorescence of GFP and enhanced fluorescence of MG. A flow cytometry study detected that in the presence of MG and transfected cells showed 1.3 fold increase of fluorescence compared to the wild type MDCK cells.

The next approach was to use strand-displacement activated PNA probes to detect the iNOS mRNA in living RAW 264.7 mouse macrophage cells. A probe constitutes of an antisense 23-mer fluorescein (FAM) labeled antisense PNA and a 17-mer Dabcyl^{plus} labeled complementary DNA was used. The fluorescence of the FAM was quenched when the two strands hybridized to each other. In the presence of target mRNA, the shorter strand was displaced by the mRNA, which has more base pairs complementary to the PNA. The fluorescence of FAM was restored and thus could be used to detect the mRNA. The probe has been shown to be able to detect the target DNA and *in vitro* transcribed mRNA in solution. Fluorescence in situ hybridization (FISH) showed that the probes showed 3.6 ($\pm$ 1.8)-fold increase of fluorescence between stimulated cells expressing a high level of iNOS mRNA and non-stimulated cells. Cationic Shell-crosslinked Knedel-like (cSCK) nanoparticles were employed to deliver probes into living cells and the fluorescence of the stimulated cells observed by confocal microscopy increased 16.6 ($\pm$ 7.9)-fold. RT-PCR was conducted to determine the absolute copy number of the iNOS mRNA in cells. The detected increase of iNOS mRNA after 18 hours of stimulation was around 100 times, and the actual copy number of the mRNA per cell was around 70000. These results reveal that the under our current systems, strand-displacement probes are not sufficient to report quantitatively on the mRNA copy numbers in living cells, but they can be used to achieve mRNA imaging in living cells.

The third approach was to use fluorescent labeled binary PNA probes to image the iNOS mRNA in living RAW 264.7 cells. PNAs bearing FAM and Cy5 and targeting the adjacent sites of the iNOS mRNA were synthesized and had shown FRET signal upon binding to the DNA target and *in vitro* transcribed iNOS mRNA in solution. The probes were delivered into living cells by hybridizing to their partially complementary DNAs and forming complexes with cSCK nanoparticles. Fluorescent images were taken by confocal microscope. The matched probes showed FRET image for stimulated cells while control probes showed almost no FRET signal and non-stimulated cells treated with matched probes showed weak signal. The average FRET intensity detected in stimulated cells was 3.8 ($\pm$ 0.9) times higher than in non-stimulated cells.

This thesis is dedicated to my beloved family members and my girlfriend

Yiran Dong. Thank you all for supporting and believing in me.

TABLE OF CONTENTS

LIST OF FIGURES

Chapter 4

LIST OF TABLES

Chapter One

Introduction

1.1 Gene expression, antisense inhibition and mRNA imaging

Messenger RNA (mRNA) is a macro-molecule that is involved in gene expression and protein production in almost all species. In eukaryotic cells, mRNA is produced in the nucleus from pre-mRNA which is transcribed from the DNA template with the help of RNA polymerase and several other enzymes. The pre-mRNA transcribed from DNA is then processed by spliceosomes to form the mature mRNA. The DNA coding for the spliced parts are called introns and the intervening parts are referred to as exons. The mature mRNA is then transported to the ribosome in the cytoplasm, where it is translated into protein through the use of aminoacyl transfer RNAs (aa-tRNAs) which align with the mRNA via base pairing between 3-nucleotide segments known as codons. Each aa-tRNA carries a specific amino acid. These amino acids are covalently joined by the ribosome to form a polypeptide. In this way, the sequences of the nucleotides in DNAs specify the sequences of the amino acids in the proteins (**Figure 1.1**).

The important role of mRNA in gene expression has led to the development of a variety of methods for its detection and regulation. For example, researchers use antisense nucleic acids to bind and manipulate mRNAs produced by certain genes [1, 2]. These nucleic acids probes are complementary to mRNA sequences, which are known as "sense" sequences. By hybridizing to the mRNA, the nucleic acid probes can either block the translation of the mRNA or cause enzymatic degradation of the mRNA. The clinical application of these antisense oligonucleotides is termed antisense gene therapy [3]. Researchers have developed various nucleic acid analogs for antisense inhibition, including phosphorothioate DNA [4], 2'-O-methylated RNA [5], peptide nucleic acid (PNA) [6-9], locked DNA (LNA) [10, 11], and other analogs [12] (**Figure 1.2**). Recently,

2

it has been discovered that some short double strand RNAs called "small interfering RNA" (siRNA) can also silence gene expression [13, 14]. These types of RNAs, which are usually 20 to 25 nucleotides in length, can cause the degradation of the targeted mRNA through "RNA interference pathway" that involves the RNA-induced silencing complex (RISC).
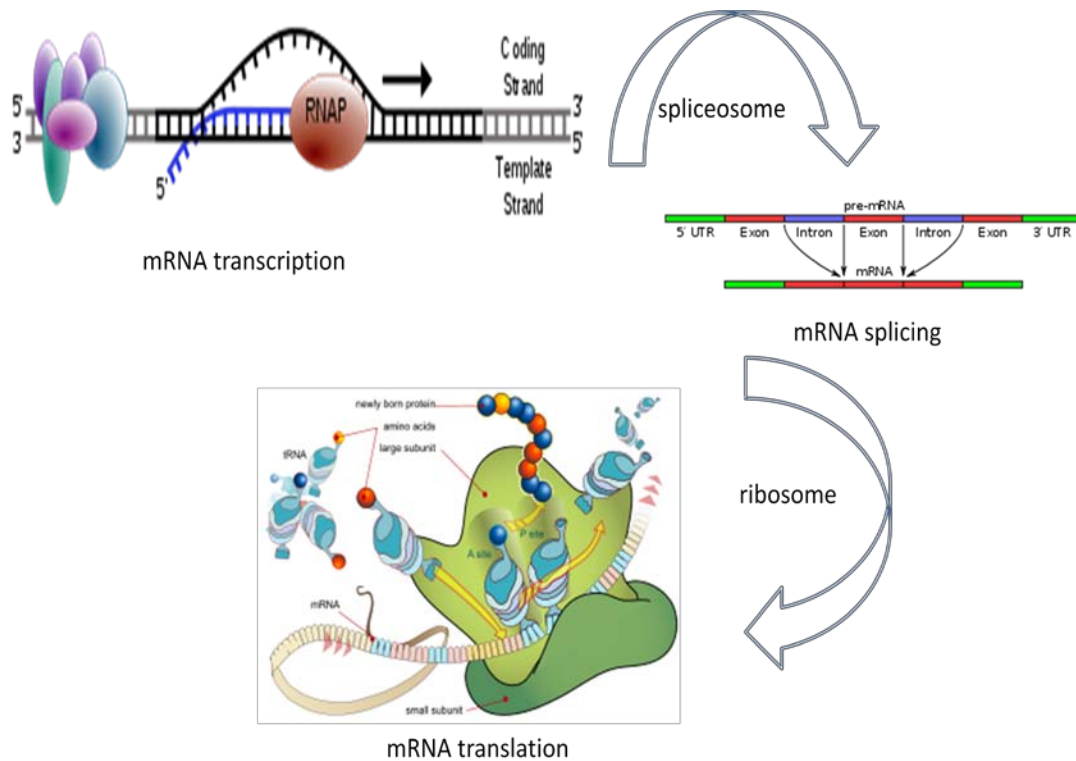
Figure 1.1: A schematic representation for gene expression
(Remixed from Wikipedia under GNU Free Document License)
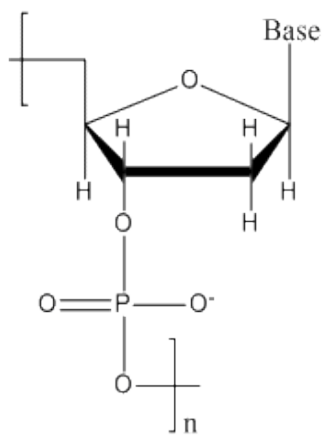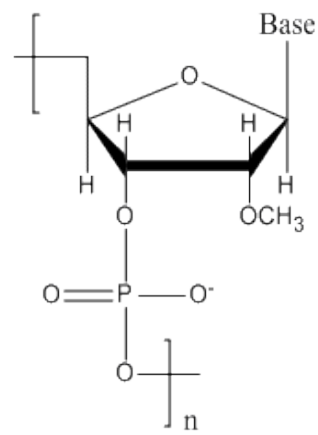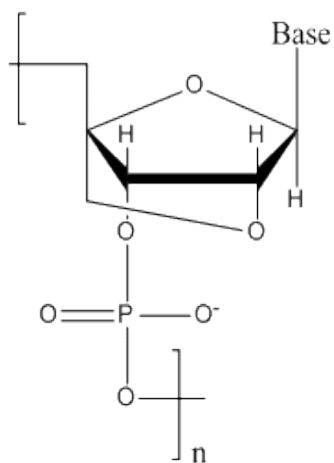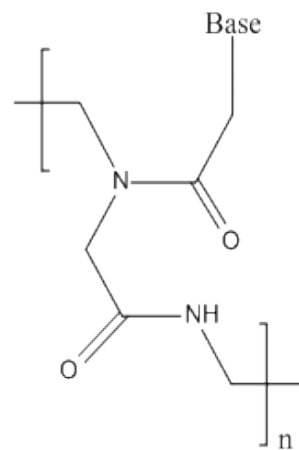
Figure 1.2: Some typical DNA analogs

Besides the antisense inhibition and silencing of mRNA, it is also of interest to be able to measure and image mRNA transcripts. For example, in some diseases or cancers, certain genes may be over-expressed and it would be useful to be able to detect and control the abnormal gene expression [15, 16]. There are many ways to monitor gene expression. For example, researchers can monitor gene expression at protein level via immunohistochemical staining [17], western blot [18], mass spectrometry [19] and other techniques. However, a more direct way to monitor gene expression would be to detect the mRNA. Many techniques have been developed to quantify gene expression at the mRNA level, such as: Northern hybridization (Northern blot) [20], real-time polymerase chain reaction (RT-PCR) [21-23], DNA microarray [16, 24], etc. These techniques have all been proved to be powerful tools to quantitatively measure the change in mRNA expression. Some techniques, for example RT-PCR, can even detect a few copies of mRNA per cell [25]. These methods, however, also have drawbacks. Most of them are time consuming and destructive, requiring lysis of cells or tissue samples. It would be advantageous to have methods that can detect, as well as image, mRNA inside living cells and *in vivo*.

Many techniques have been developed for mRNA imaging and quantification, most of which rely on the detection of optical or radioactive signals. One way to monitor the expression of RNA is to tag a transgene mRNA with aptamers that can increase the signal intensity of a fluorescent probe [26, 27], a strategy that will be discussed in more detail in chapter two. In another approach, a transgene mRNA is tagged with a protein binding sequence, such as the MS2 protein binding sequence, which is then recognized by the protein fused to a fluorescent protein [27]. Another approach is the spliceosome-mediated

RNA transplicing (SMarRT), in which an RNA transcript of a reporter protein (such as a luciferase) is engineered to ligate with a target pre-mRNA during trans-splicing process. The trans-spliced mRNA expression can then be monitored by detecting the signals from the co-expressed reporter protein [28].

Besides the transgenic methods, another general approach is to image endogenous mRNA using antisense nucleic acid probes. These probes achieve their specificity via Watson-Crick base pairing, in which adenine (A) forms a base pair with thymine (T) and guanine (G) pairs with cytosine (C), via hydrogen bonding [29]. The antisense probes are then conjugated to reporter groups and are 20 to 50 nucleotides in length so as to achieve specificity for targeting DNA or RNA. Some of the most commonly used reporter groups are radioactively labeled molecules, which can be detected by radiation sensitive detectors [30-32]. Another type of reporting group are fluorescent molecules [33-36]. Researchers have also developed fluorescent quantum dots that can be conjugated to nucleic acid probes. These quantum dots, usually nanocrystals made from inorganic materials, have higher extinction coefficients and similar quantum yields to the commonly used organic fluorescent molecules. They are usually brighter and have narrower emission lines, making them more suitable for biological imaging [37, 38]. The use of nucleic acid probes to detect and image mRNA will be the main topic of this thesis and will be discussed extensively in the following sections.

1.2 Molecular imaging using nucleic acid probes

Because of the simplicity of targeting mRNA (or DNA) by Watson-Crick base pairing, nucleic acid probes have been widely used for mRNA imaging. The two basic

types of probes are: always-on probes and light-up probes. Details of each of these types of probes will be discussed in the following sections (**Figure 1.3**).

1.2.1 "Always-on" probes

"Always-on" probes are the simplest type of nucleic acid probes. There are usually 25-30 nucleotides for a probe constructed by DNA and around 50 nucleotides for a probe constructed by RNA [36]. To achieve specificity, the probes have to be of certain length, because the shorter the probe, the greater possibility that it will bind to non-target mRNAs that share the same sequences as the target. Also, if the sequence is too short, the melting temperature will be too low for a probe to bind effectively to its target under physiological conditions [39]. The un-paired bases (or mismatch bases) will destabilize the binding, therefore, only the perfectly matched sequences will have the highest binding affinity to the target [40-42]. However, these probes are difficult to enter or exit cells even with modifications. Often delivery involves endocytosis which results in high background signals because most of the probes remain trapped in endosomes. Even if the probes enter the cytoplasm, unbound probes may not be able to exit the cell efficiently, and they can bind non-specifically to proteins and other mRNA/DNAs inside the cytoplasm [30]. Furthermore, DNA and RNA probes are also prone to enzymatic degradation inside cells. Therefore, these probes are often used with cell lysates or in situ hybridization, where intracellular delivery of the probes is not a problem.

One of the most widely used techniques for quantifying mRNA involving always-on probes is fluorescence in situ hybridization (FISH) [43-45]. Cells or tissues are treated with fixatives (such as formaldehyde or methanol) to fix the cellular morphology and

7

allow the probes to penetrate the cell. To reduce the background signal generated by the non-specific binding, stringent washing steps are used. Sometimes an amplification step is used to achieve better signal to noise ratio, in which the probe is conjugated to a molecule that can bind carriers with multi signaling molecules, such as antibodies, biotin/avidin conjugated fluorophores [46], or horseradish peroxidase to catalyze oxidation of tyramide [47, 48].

1.2.2 FRET-based "light-up" probes

To avoid the drawbacks of the always-on probes, researchers have developed probes that only "light-up" upon binding to the target. Examples of these probes include: nucleic acid templated profluorescent probes [49], hybridization triggered fluorogenic probes [50-53], molecular beacon probes [54, 55], strand-displacement probes [56], and binary FRET probes [57, 58], etc. One type of the "light-up" probe that will be investigated extensively in this thesis is the FRET probe, which utilizes a Förster resonance energy transfer (FRET) mechanism to transfer energy from one probe to another through space [58]. This is a nonradiative dipole-dipole coupling process in which energy from an energetically excited molecule is transferred to another molecule in close proximity. As a result, the energy level of the first molecule, known as the "donor", returns to the ground state, rendering the decrease of the fluorescence intensity and lifetime. The second molecule, known as the "acceptor", could either emit fluorescence at longer wavelength than the donor (red-shifted emission), or release the energy without emitting fluorescence (fluorescence quenching) [59-61].

8

The efficiency of the FRET depends on three main factors: the distance between the donor and the acceptor, the overlapping between the donor's emission spectrum and the acceptor's absorption spectrum, and the relative orientation of the donor's emission dipole and the acceptor's absorption dipole moment. The FRET efficiency is the quantum yield of the energy transfer transition, and depends on a number of parameters as shown in the following equation:

$$E = k_{et}/(k_f + k_{et} + \sum k_i)$$

where k_{et} is the rate of energy transfer, k_f is the relative decay rate, and k_i are constants for any other de-excitation pathways. The efficiency E also depends on the distance between the two molecules and is described as [62, 63]:

$$E = 1/(1 + \left(\frac{R}{R_0}\right)^6)$$

where R_0 is the Förster radius for a given pair of donor and acceptor molecules and R is the actual distance between the two molecules. For a given FRET pair, R_0 depends on the overlap integral of the donor emission spectrum with the acceptor absorption spectrum and their mutual molecular orientation, which are described by the following equation:

$$R_0^6 = 8.8 \times 10^{-28} \cdot \Phi(D) \cdot \kappa^2 \cdot \eta^{-4} \cdot J(\lambda)$$

where $J(\lambda)$ is the spectral overlap of donor emission and acceptor excitation, η the index of refraction, $\Phi(D)$ the fluorescence quantum yield of the donor and κ the orientation factor of the donor and acceptor dipole moments.

A typical effective distance for FRET is 1-10 nm, which roughly corresponds to a distance of 3 to 30 nucleotides along the double helix of a DNA molecule. When the

distance between two dyes is close enough, fluorescent quenching can also occur by the formation of a nonfluorescent complex, which is also known as "contact quenching" or "static quenching" [64]. In this quenching phenomenon, the absorption spectra of the two molecules will change when they form a complex, whereas in FRET, the absorption of the two molecules will not change [65]. The following contents will discuss some typical designs of the probes that employ FRET.

1.2.2.1   Binary FRET probes

Binary probes consist of two single-strand molecules, one conjugated to a "donor" and the other to an "acceptor". [57, 63, 66, 67]. When unbound to a target, the two single-strands will not interact with each other, and the emission of the acceptor won't be observed upon the excitation of the donor. Upon binding to a target mRNA, which serves as a molecular template, the two fluorophores are held close to each other so that an effective FRET can occur. The most common way to monitor a FRET signal is via two color ratio imaging (also known as sensitized emission), where the donor is excited and the emission of both donor and acceptor is collected [68].
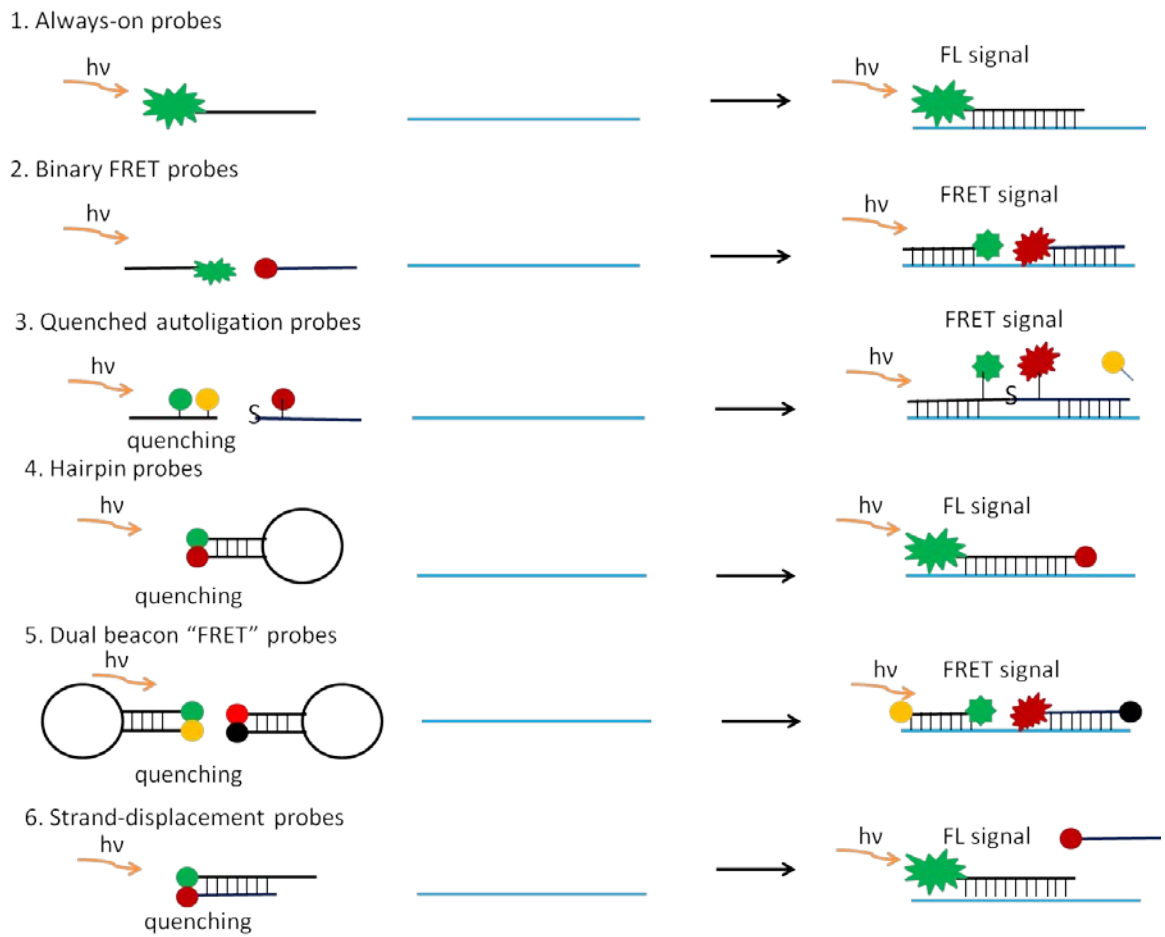
Figure 1.3: Typical designs of optical nucleic acid probes

This FRET system is a great improvement to the single "always-on" probes in that the fluorescence of the donor in the unbound state will cause little interference with the FRET signal arising from the acceptor in the bound donor acceptor pair. Researchers have used this type of FRET probe to detect mRNA both in vitro and in living cells [35, 69]. Sometimes however, the laser that excites the donor will also excite the acceptor, or the fluorescence of the donor may overlap with emission from the acceptor [70], rendering a false positive signal. Therefore, a typical FRET experiment requires a number of controls to eliminate false-positive signals.

There are ways to minimize signals emanating from unbound probes. One way is to measure the fluorescence life time of the donor using a technique called fluorescence lifetime imaging microscopy (FLIM) [68]. Most fluorescent molecules used for FRET exhibit a decay in fluorescence with half life on the nanoseconds scale. The fluorescence lifetime of the donor is sensitive to the outside environment, and will decrease in the presence of an acceptor in FRET. FLIM only measures the fluorescence life time change of the donor, which is indicative of FRET, and will have fewer artifacts compared to measuring the fluorescence intensity of the acceptor [71]. One drawback of this method is that it requires sophisticated instrumentation that can measure fluorescence life time at the nano second time scale. It is also a slower imaging technique, taking a few minutes to obtain each image. Other environmental effects can also alter the fluorescence life time of the donor; so that careful processing is required for live cell imaging.

Another approach to detecting FRET is the acceptor photo bleaching FRET [68, 72]. This method monitors the restoration of fluorescence of the donor after removal of the FRET acceptor by photo bleaching. FRET can also be detected by polarization anisotropy

imaging. When excited by a linearly polarized laser, the fluorescence anisotropy of the molecule can be determined from intensity measurements parallel and perpendicular to the incident polarization. When there is FRET between two molecules, the fluorescence of the donor will be depolarized, and such depolarization can be recorded to monitor the FRET between two molecules. This technique is usually applied to fluorescent protein imaging [68].

Besides two-probe FRET, there is a variation called "tandem FRET" where the FRET occurs between three or more fluorophores [57, 73], with the first one's emission overlapping with the second one's absorption and the second one's emission overlapping the absorption of the third, etc. This design further reduces interference from the emission of the donor, but requires more stringent conditions and has lower overall FRET efficiency.

1.2.2.2 Quenched autoligation FRET probes (QUAL-FRET probes)

A different approach to improving FRET probes involves mRNA templated covalent ligation of a pair of FRET probes in which the ligation reaction activates an otherwise quenched donor probe. In this design, one probe contains a donor fluorophore and a quencher, while the second probe contains an acceptor fluorophore and a nucleophilic group. When simultaneously bound to the target mRNA, the quencher of the donor probe is displaced by the nucleophile that is conjugated to the acceptor probe. The donor, is now no longer quenched, and can transfer its energy to the acceptor dye via FRET. This design further reduced the background signal from the free donor probes. Eric Kool et al. have developed such quenched autoligation or QUAL-FRET probes to

detect rRNA in bacteria and image mRNA in living cells. The ligated probe can dissociate from the template, triggering another round of probe binding and ligating, and the FRET signal can be amplified [74, 75],

1.2.2.3 Molecular beacons (hairpin probes)

Another type of widely used probes is a molecular beacon [76-78]. The molecular beacon is a single-strand probe that forms a "stem and loop" structure, which is also known as a "hairpin". The stem usually comprises 5-7 pairs of complementary nucleotides, with a fluorophore on one end and a quencher on the other. The loop is the recognition part of the probe, and is complementary to the target mRNA sequence. In the absence of the target sequence, the two strands of the stem hybridize together, bringing the two moieties in close proximity so that the fluorescence of the "donor" molecule is quenched by the quencher [64]. In the presence of the target, the hairpin will open and the loop (and maybe part of the stem) will hybridize to the target DNA or mRNA. The conformational change of the beacon will separate the donor and the quencher and the fluorescence of the donor will be restored upon excitation. This is also a "switched-on" probe that will theoretically reduce the background signal when the probe is in its unbound state. A variation of this probe is to conjugate the same fluorophore to both ends of the beacon. Some fluorescent molecules, such as pyrene, whose fluorescent properties depend on proximity, can form "excimers", which will have different fluorescent properties than the monomer [79, 80].

1.2.2.4 Dual beacon FRET probes

Dual beacon "FRET" probes are the combination of the molecular beacon and binary FRET probes. In this design, two FRET probes are made into molecular beacons, and thus the fluorescence of both the donor and the acceptor is quenched in the unbound state. Upon hybridization to a target mRNA, the two beacons open up, and the donor and the acceptor are no longer quenched so that FRET can occur. This design eliminates the background signal of the donor and acceptor in their unbound states. Gang Bao and coworkers have shown that such dual FRET probes can be utilized to image mRNA both *in vitro* and in living cells [81, 82].

1.2.2.5 Strand-displacement probes

Strand-displacement probes are double strand probes with a fluorophore attached to one strand and a quencher attached to a complementary strand [56, 83, 84] and are thus similar to molecular beacons. The fluorescence of the fluorophore is quenched via FRET or, if close enough, via contact quenching [64]. Upon binding to a target, one of the strands will be displaced by the target to form a more stable duplex. The two original strands are no longer hybridized to each other and the fluorescence on the reporter strand will be restored. This is a "switched-on" type of probe, which means that it will only emit fluorescence upon binding to the target. This solves the high background noise problem caused by the "always-on" probe. This probe is also known as "Yin-Yang" probe [85], which means "off-on" in Chinese philosophy. The two strands of the probe are usually of different lengths, which will facilitate the displacement reaction and favor binding of the target [56].

15

1.3. Current obstacles in mRNA imaging and solutions

Despite the rapid development of agents for mRNA imaging using nucleic probes, some problems still exist for using these probes for *in vivo* imaging [27]. The following sections will discuss some obstacles to *in vivo* mRNA imaging using nucleic probes and current approaches to surmounting them.

1.3.1 *In vivo* stability of the probes

Probes made from DNA and RNA are labile to enzymatic degradation under biological conditions. To overcome these drawbacks, researchers have developed a variety of nucleic acid analogs, which, while retaining the recognition features of the probes (Watson-Crick base pairing), have modifications on the backbones of the probes so that they are more resistant to enzymatic activities. Some of the most commonly used modified probes include 2'-O-methylribonucleotides [86, 87], locked DNA (LNA) [88, 89], and peptide nucleic acids (PNA) [90, 91]. Another advantage of these analogs over DNA is that they will not trigger RNase H degradation of the mRNA target, as will DNA [92]. While degradation of the target mRNA might be useful for blocking gene expression, it is not desirable for mRNA imaging purpose. Some of the mimics, such as PNAs and 2'-O-methylribonucleotides, are more resistant to nuclease activity [93], and won't trigger RNase H activity [94], so that the target mRNA will be preserved for imaging purpose. In this thesis, we will focus extensively on using PNA probes for *in vitro* and *in vivo* imaging.

16

1.3.2 Cellular delivery of nucleic acid probes

Another problem with the use of nucleic acid probes *in vivo* is their membrane impermeability. Because most of the nucleic acid probes are neutral or negatively charged, and most of the mammalian cells membranes are also negatively charged, it is difficult for the probes to associate with cell membranes. Nucleic acid probes are also too large and polar to cross the hydrophobic portion of the membrane by diffusion. The following contents will discuss several strategies developed to solve the delivery problem.

1.3.2.1 Delivery of nucleic acid probes by cell penetrating peptide (CPP)

One solution to enhance cell permeation is to attach a cell penetrating peptide (CPP) to the probes [95-99]. CPPs are short peptides that facilitate the cellular uptake of the cargo, such as molecular probes, proteins, or nano-particles. These peptides usually contain many positively charged amino acids, such as lysine, or arginine, and are either covalently [97], or non covalently [100] attached to the probes. The mechanisms by which these CPPs enter cell membranes can be generally categorized into two pathways: energy dependent endocytosis and energy-independent translocation across the lipid bilayer [101]. A recent study on CPP penetrating mechanism has shown that for some commonly used CPPs (TAT, arginine 9, and the antennapedia/penetrating peptide etc.), multiple pathways may be involved, such as macropinocytosis, clathrin mediated endocytosis and caveolae/lipid raft mediated endocytosis [102]. Although a comprehensive understanding of the CPP penetrating mechanism is still under study, CPPs have been proved to enhance the delivery of cargo probes across the cell membranes, for example, Gang Bao and coworkers have constructed a molecular beacon

conjugated to TAT-1 peptide via both cleavable and uncleavable bonds and utilized such peptide-linked beacon probes to image the GAPDH mRNA inside living cells [103].

1.3.2.2 Delivery of nucleic acid probes by lipids

Taking advantage of the fact that viruses can efficiently carry their genome and invade host cells, researchers have achieved gene delivery via recombinant viral vectors [104]. This has triggered the research on developing synthetic vectors to delivery cargos (probes, proteins or drugs) into cells. One type of such delivery system is to use cationic lipids [105, 106]. Because DNA probes are negatively charged, they can associate with the cationic lipids via electrostatic interactions to form lipoplexes. These lipoplexes then interact with cell membranes and the cargo is then released into the cytoplasm when the liposomes fuse with anionic cell membranes [105]. For probes that are not negatively charged, such as PNA probes, an alternative method is to hybridize the probes with negatively charged DNA probes to form negatively charged heteroduplexes so that they will interact with positively charged lipids [107]. These lipoplexes can achieve effective delivery of the gene or antisense probes, however, their stability, cytotoxicity and ability to form homogeneous liposomes still need to be improved [108].

1.3.2.3 Delivery of probes by nanoparticles

Another type of synthetic vector for probe delivery are cationic polymers (nanoparticles). These polymers, usually containing protonated primary, secondary or tertiary amines, are positively charged and interact with the negatively charged DNA or siRNA to form polyplexes [109, 110]. These polyplexes can also protect the nucleic acid

18

cargo from degradation by various enzymes in the cellular environment [111]. Some particles have tunable pH adjustability, which facilitate the endosomal escape of the delivered cargo [112]. Typical examples of the nanoparticles used for nucleic acid delivery include: polyethyleneimine (PEI) polymer [113], polyamidoamine (PAMAM) dendrimers [114, 115], comb-like amphiphilic nanoparticles [116], etc. Recently, the Wooley group has developed a cationic shell-cross-linked (cSCK) nanoparticle. Through collaborative work with their lab, we have proved that cSCK nanoparticles can effectively deliver plasmid and PNA into mammalian cells [110, 117]. In chapter three and four, cSCK nanoparticles will be used to deliver PNA probes into living cells.

One advantage of these synthetic particles is that they can be modified to carry multi-functional groups for various purposes. For example, to improve the serum circulation, researchers have attached polyethylene glycol (PEG) to particles [118]. To improve specificity in cell targeting, receptor binding ligands can be attached to particles. This can also help the cellular uptake of the particles via receptor mediated endocytosis [119, 120]. These particles can also incorporate agents such as fusogenic peptides that can facilitate endosomal escape of the probes [121, 122]. Researchers have also conjugated nucleic acid probes to the nanoparticles via bioreductively-cleavable bonds, such as disulfide bond, which will enable the release of the probes after delivering them into the cells and enhance the antisense effect [110]. Some polyplexes are also degradable, making them usefully tools for clinical gene therapies and *in vivo* imaging [123]. **Figure 1.4** depicts the general use of nanoparticles for the delivery of nucleic probes and mRNA imaging.

19

Besides cationic polymers, another type of nanoparticle used for antisense imaging is to use gold nanoparticles. Researchers have modified the surface of gold nanoparticles with various ligands, including single strand DNA. In one type of construct, the ODNs are conjugated to fluorophores to form a beacon on the gold surface, The fluorescence of the fluorophores is quenched by the gold nanoparticles and is restored when the ODNs bind to target mRNA inside cells [124]. In other circumstances, the ODNs can hybridize to nucleic acid probes and carry these probes into the cells [26, 125].
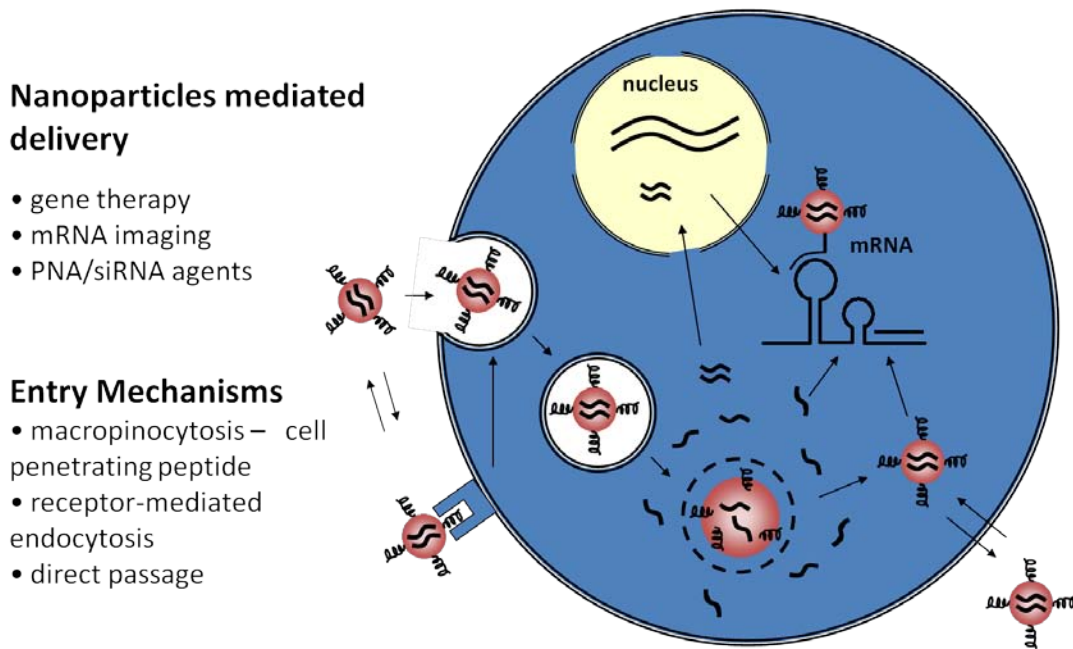
Figure 1.4: Schematic representation of nanoparticles mediated cellular delivery

1.3.2.4 Other methods and chemicals for cellular delivery

There are some other techniques and methods to achieve cellular delivery of nucleic acid probes. One method is microinjection, which uses a needle 0.5 to 5 micrometers in diameter to inject the probes into a single cell [93, 126]. This method ensures that the probes are injected into the cytoplasm or nucleus; however, it is time consuming and cannot be applied to large scale transfection. Another method is to use pore forming chemicals. Studies have shown that some chemicals in the exotoxin family, such as streptolysin O (SLO), can cause reversible pores on cell membrane [127, 128]. Studies have shown that treating certain type of cells with SLO can effectively deliver probes into membrane and image mRNA in living cells, with minimum damage to the cells after recovery. Another way to form pores on the membrane is through electroporation, which uses electrical pulses to stimulate the cells and form trans-membrane pores on the cell surface so that the molecular probes can enter the cytoplasm of the cells [129, 130]. Besides the three methods mentioned above, there is another way to load the probes called "pinocytic cell-loading" [131, 132]. This method induces pinocytosis of the cells by treating the cells with buffer containing probes and high concentration of glucose. After taking up the probes, cells are treated with diluted medium (lysis buffer) that will induce the burst of the endosomes to release probes into the cytoplasm. This method can produce homogeneous distribution of the probes inside cells; however, such method of delivery requires high concentration of the probes, which may be expensive to synthesize.

1.3.3 Enhancing endosomal escape of nucleic acid probes

Another obstacle for antisense inhibition and imaging of mRNA expression is the release of probes after delivery via endocytosis mechanisms. Although other pathways exist for cellular delivery of nucleic acid probes, a lot of lipoplexes and polyplexes (nanoparticles) enter into the cells via endocytosis [108]. As the endosomes form and develop from the early stage to the late stage, the pH inside the vesicles decreases from 7 to around 5.5. Then the late endosomes fuse with lysosomes and the nucleic acid probes are prone to be degraded in lysosomes or exported out from cells. Therefore, to achieve better delivery efficiency, it is necessary to disrupt endosomes at early stage to release their cargos into the cytoplasm. Researchers have developed many approaches to facilitate the endosomal release of the cargos, however, the effectiveness of this process remains a major problem for mRNA imaging in living cells and *in vivo* [133].

One way to induce endosomal escape is to use fusogenic agents, including fusogenic lipid, peptides or proteins. For example, researchers have incorporated a fusogenic lipid dioleoylphosphatidylethanolamine (DOPE) into polymers and found this to enhance the delivery of nucleic acids in the polyplexes [134, 135]. Some peptides, like haemagglutinin, will change conformation from a hydrophilic to a hydrophobic coil when the pH drops from 7 to 5. This change causes the peptide to fuse with endosome membranes when the endosomes acidify, which helps the cargo to pass across the endosomal membrane barrier [136]. Another example is the influenza –derived fusogenic peptide diINF-7, which has been shown to enhance the endosomal escape of certain siRNAs and increase their effect on gene silencing [137].

Another way to promote endosomal escape is by the "proton sponge" effect [138]. It hypothesized that amine groups have certain buffering capacity between pH 7 and 5. As an endosome acidifies, these amino groups "absorb" extra protons, buffering against acidification and maintaining the pH at a higher level inside the endosome. This effect induces the ATPase to "pump" in more protons into the endosome, and more counter ions to balance the protons. The enrichment of counter ions will cause the osmotic swelling and rupture of the endosome, causing the release of the probes. One typical polymer that employs the proton sponge effect is polyethyleneimine (PEI), which has been widely used for gene delivery [113, 139]. Other chemicals containing secondary and/or tertiary amine groups such as chloroquine [140] and histidine [141], have also been used to improve the endosomal escape of the probes.

A third way to promote endosome rupture is to use photosensitive molecules. Photochemical internalization (PCI) is a technology designed to promote endosome rupture and cytosol release by photosensitizers. These molecules, upon stimulation of light, become excited and help to form reactive oxygen species, which have a very short lifetime, and will break the endosome membranes without damaging other parts of the living cells [142]. For example, mixing one photosensitizer, meso-tetraphenylchlorin disulphonate (TPCS2a), together with siRNA has been proved to promote endosomal escape of the siRNA in the human epidermoid carcinoma cell line A431 upon exposure to light source [143].

1.3.4 Other issues regarding antisense mRNA imaging

Despite the fast development in molecular imaging and cellular delivery of the probes, there are still some issues calling for researchers' attention in antisense mRNA imaging. One of the issues is secondary structure of mRNAs. Because of their large size and complicated structure, mRNAs usually fold differently under different conditions [144]. The secondary structure of mRNAs have profound influence on their biological functions [145], and can also affect antisense probe binding [146]. When self-complementary segments of mRNA fold together via Watson-Crick base pairing, they may not be fully accessible to antisense probes. To design an effective antisense probe for mRNA imaging, one needs to avoid those non-accessible sites. One tool that many researchers use is computer-generated mRNA structure prediction software. Some of the computational programs are based on minimal free energy (such as m-fold) and probability of the alignment. These computational algorithms have helped researchers in designing antisense probes [82, 128], however, they still cannot provide accurate prediction of mRNA structure *in vivo*. A better approach is to determine the structure experimentally, such as through the use of oligonucleotide probes to map the accessible sites [147, 148]. For example, our group has successfully mapped antisense-accessible sites on native mRNAs isolated from cells using a modified reverse transcriptase random oligodeoxynucleotide (RT-ROL) assay called MASL. This assay has lead to the design of siRNAs and antisense PNAs with high binding affinity to the iNOS mRNA [149]. Other methods include RNase H cleavage mapping, and use of molecular beacons to screen for antisense binding sites [150].

Another challenge for mRNA imaging is the low copy numbers of mRNA inside cells, which range from less than ten to a few thousand copies [151]. It is almost impossible to image mRNAs with low copy number inside living cells without amplification. In addition to RT-PCR, researchers have developed other amplification methods to detect mRNA *in vitro* using nucleic acid probes. For example, researchers have used a DNA molecular beacon to detect mRNA in solution with the assistance of exonuclease III, which preferably digests one strand of the DNA/DNA or DNA/RNA duplex from 3' blunt end but not the intruding single strand. When the beacon binds to the mRNA, they form a blunt end at the beacon's 3' side, but the 3' end of the mRNA becomes an overhang strand. Therefore the beacon is digested by the enzyme, leaving mRNA intact and able to bind another beacon molecule. The digested beacon will release the fluorophore and the fluorescent signal is amplified each time the enzyme digests the DNA beacon binding to the mRNA [152]. Another design is called "invasive cleavage assay", which uses a sequence specific 5' nuclease to remove the quencher from the DNA probes after they bind to the mRNA target. The cleaved probes become permanently fluorescent and are then replaced by intact probes. The turnover of this process amplifies the fluorescent signal [153].

In some cases, certain mRNAs become over-expressed in cells under stimulating conditions [154] or in cancer cells [155]. These over-expressed mRNAs are usually the proper targets for *in vivo* imaging and are of crucial importance for diagnostic and therapeutic purposes.

1.4. Conclusion and the subjects of this thesis.

Much effort and progress has been seen in the field of mRNA imaging [27], especially the antisense imaging using hybridization probes. Various derivatives of nucleic acids have been developed to improve the stability of probes inside cells. New fluorescent dyes in the near infrared region [156], quantum dots, and radioactive agents have been incorporated to increase the sensitivity of the probes. There are also new designs, imaging methods and instruments designed to produce reliable *in vivo* images with high signal to noise ratios. Developments in nanotechnology have led to new particles that can carry multiple functional groups for *in vivo* imaging purposes. Researchers now are able to achieve multi-color multi-sites imaging by FISH [44], single molecule sensitive imaging for RNA in living cells [157], and ratiometric quantification of fluorescence in living cells [158]. However, there remain hurdles for mRNA imaging *in vivo*. Effective cellular delivery and endosomal release of nucleic acid probes, specific and fast hybridization of the probes, as well as sensitive and quantitative detection methods remain to be challenging issues for researchers in this field [33].

The overall goal of this thesis was to investigate methods that can quantitatively image mRNA in living cells, which will provide foundation for noninvasive *in vivo* imaging. We have investigated several strategies to image mRNA *in vitro*, *in situ* and in cells by using different imaging agents, including fluorescence enhancing aptamer tags, strand-displacement activated fluorescent PNA-DNA probes, and PNA FRET probe pairs. We have also investigated several approaches to facilitate the cellular delivery of the probes. Although compared with some other methods such as RT-PCR, the strategies we exploited are less sensitive for quantitatively measuring mRNA in living cells. They can

26

provide researchers with spatial and temporal information of gene expression. These studies will also help researchers to image gene expression in human by nucleic acid probes with minimum damage, which is the ultimate goal of this research.

In chapter two, we will demonstrate a method to image a transgene RNA tagged with an aptamer that can bind to malachite green (MG) and strongly enhance its fluorescence. We have shown that the aptamer can bind to MG in solution and in total RNA extracted from transgene containing cells. MG was delivered into the cells via free diffusion as well as by the "influx" cell loading method. We have shown that by introducing MG into the cells, we can detect the transgene inside living cells both by confocal microscopy and flow cytometry.

In chapter three, we will show our work to image mouse inducible nitric oxide synthase (iNOS) mRNA in RAW264.7 cells using strand-displacement activated PNA probes. The probes consist of a 23-mer fluorescently labeled PNA hybridized to a 17-mer complementary DNA conjugated to a quencher. The fluorescence of the duplex probe is quenched and can only be restored upon hybridizing to the target mRNA, which causes the shorter DNA quencher strand to be displaced. We have shown that this type of probe can detect DNA and *in vitro* transcribed mRNA in solution. We have used the strand-displacement probes to image iNOS mRNA by fluorescence in situ hybridization (FISH). For the live cell imaging, cSCK nanoparticle was used as the delivering agent and we have shown the fluorescent images of iNOS mRNA in mouse macrophage RAW 264.7 cells.

In chapter four, we will demonstrate the use of fluorescently labeled PNA probes to image iNOS mRNA in living cells by FRET. We have optimized the best position for two

FRET PNA probes to achieve the optimal FRET efficiency, and have shown that the FRET pairs can bind to the iNOS mRNA *in vitro*. We then delivered the two probes into cells by hybridizing them to the partially complementary DNAs and complexing them with cSCK nanoparticles. FRET images of iNOS mRNA inside cells were obtained by confocal microscope and average FRET intensity of selected regions of interests (ROIs) were used to detect the increase of iNOS mRNA in living RAW 264.7 cells after stimulation by lipopolysaccharide (LPS) and gamma interferon (γ-IFN).

In chapter five we will summarize our work on mRNA imaging using fluorescent molecule and optical nucleic acid probes and propose future work in this field.

References:

1. Dias, N. and C.A. Stein, *Antisense oligonucleotides: basic concepts and mechanisms.* Mol Cancer Ther, 2002. **1**(5): p. 347-55.

2. Phillips, M.I. and Y.C. Zhang, *Basic principles of using antisense oligonucleotides in vivo.* Methods Enzymol, 2000. **313**: p. 46-56.

3. Goyenvalle, A., et al., *Therapeutic approaches to muscular dystrophy.* Hum Mol Genet.

4. Matsukura, M., et al., *Selective binding of trisamine-modified phosphorothioate antisense DNA to target mRNA improves antisense activity and reduces toxicity.* Biochem Biophys Res Commun, 2002. **293**(5): p. 1341-7.

5. Kawasaki, A.M., et al., *Uniformly modified 2'-deoxy-2'-fluoro phosphorothioate oligonucleotides as nuclease-resistant antisense compounds with high affinity and specificity for RNA targets.* J Med Chem, 1993. **36**(7): p. 831-41.

6. Braasch, D.A. and D.R. Corey, *Novel antisense and peptide nucleic acid strategies for controlling gene expression.* Biochemistry, 2002. **41**(14): p. 4503-10.

7. Good, L. and P.E. Nielsen, *Peptide nucleic acid (PNA) antisense effects in Escherichia coli.* Curr Issues Mol Biol, 1999. **1**(1-2): p. 111-6.

8. Larsen, H.J., T. Bentin, and P.E. Nielsen, *Antisense properties of peptide nucleic acid.* Biochim Biophys Acta, 1999. **1489**(1): p. 159-66.

9. Nielsen, P.E., *Antisense properties of peptide nucleic acid.* Methods Enzymol, 2000. **313**: p. 156-64.

10.   Braasch, D.A., Y. Liu, and D.R. Corey, *Antisense inhibition of gene expression in cells by oligonucleotides incorporating locked nucleic acids: effect of mRNA target sequence and chimera design.* Nucleic Acids Res, 2002. **30**(23): p. 5160-7.

11.   Rapozzi, V., S. Cogoi, and L.E. Xodo, *Antisense locked nucleic acids efficiently suppress BCR/ABL and induce cell growth decline and apoptosis in leukemic cells.* Mol Cancer Ther, 2006. **5**(7): p. 1683-92.

12.   Seitz, O., *Chemically Modified Antisense Oligonucleotides-Recent Improvements of RNA Binding and Ribonuclease H Recruitment.* Angew Chem Int Ed Engl, 1999. **38**(23): p. 3466-3469.

13.   Hamilton, A.J. and D.C. Baulcombe, *A species of small antisense RNA in posttranscriptional gene silencing in plants.* Science, 1999. **286**(5441): p. 950-2.

14.   Elbashir, S.M., et al., *Duplexes of 21-nucleotide RNAs mediate RNA interference in cultured mammalian cells.* Nature, 2001. **411**(6836): p. 494-8.

15.   Yamamoto, T., et al., *Over-expression of facilitative glucose transporter genes in human cancer.* Biochem Biophys Res Commun, 1990. **170**(1): p. 223-30.

16.   Kauraniemi, P., et al., *New amplified and highly expressed genes discovered in the ERBB2 amplicon in breast cancer by cDNA microarrays.* Cancer Res, 2001. **61**(22): p. 8235-40.

17.   Gillett, C., et al., *Amplification and overexpression of cyclin D1 in breast cancer detected by immunohistochemical staining.* Cancer Res, 1994. **54**(7): p. 1812-7.

18.   Kern, S.E., et al., *Oncogenic forms of p53 inhibit p53-regulated gene expression.* Science, 1992. **256**(5058): p. 827-30.

19. Paša-Tolic, L., et al., *High Throughput Proteome-Wide Precision Measurements of Protein Expression Using Mass Spectrometry.* Journal of the American Chemical Society, 1999. **121**(34): p. 7949-7950.

20. Streit, S., et al., *Northern blot analysis for detection and quantification of RNA in pancreatic cancer cells and tissues.* Nat Protoc, 2009. **4**(1): p. 37-43.

21. Livak, K.J. and T.D. Schmittgen, *Analysis of relative gene expression data using real-time quantitative PCR and the 2(-Delta Delta C(T)) Method.* Methods, 2001. **25**(4): p. 402-8.

22. Giulietti, A., et al., *An overview of real-time quantitative PCR: applications to quantify cytokine gene expression.* Methods, 2001. **25**(4): p. 386-401.

23. Stirling, D., *Qualitative and quantitative PCR: a technical overview.* Methods Mol Biol, 2003. **226**: p. 181-4.

24. Schena, M., et al., *Quantitative monitoring of gene expression patterns with a complementary DNA microarray.* Science, 1995. **270**(5235): p. 467-70.

25. Wagatsuma, A., et al., *Determination of the exact copy numbers of particular mRNAs in a single cell by quantitative real-time RT-PCR.* J Exp Biol, 2005. **208**(Pt 12): p. 2389-98.

26. Zheng, D., et al., *Aptamer nano-flares for molecular detection in living cells.* Nano Lett, 2009. **9**(9): p. 3258-61.

27. Tyagi, S., *Imaging intracellular RNA distribution and dynamics in living cells.* Nat Methods, 2009. **6**(5): p. 331-8.

28.   Bhaumik, S., et al., *Molecular imaging of gene expression in living subjects by spliceosome-mediated RNA trans-splicing.* Proc Natl Acad Sci U S A, 2004. **101**(23): p. 8693-8.

29.   Paroo, Z. and D.R. Corey, *Imaging gene expression using oligonucleotides and peptide nucleic acids.* J Cell Biochem, 2003. **90**(3): p. 437-42.

30.   de Vries, E.F., et al., *Synthesis and evaluation of a fluorine-18 labeled antisense oligonucleotide as a potential PET tracer for iNOS mRNA expression.* Nucl Med Biol, 2004. **31**(5): p. 605-12.

31.   Sun, X., et al., *MicroPET imaging of MCF-7 tumors in mice via unr mRNA-targeted peptide nucleic acids.* Bioconjug Chem, 2005. **16**(2): p. 294-305.

32.   Dewanjee, M.K., N. Haider, and J. Narula, *Imaging with radiolabeled antisense oligonucleotides for the detection of intracellular messenger RNA and cardiovascular disease.* J Nucl Cardiol, 1999. **6**(3): p. 345-56.

33.   Bao, G., W.J. Rhee, and A. Tsourkas, *Fluorescent probes for live-cell RNA detection.* Annu Rev Biomed Eng, 2009. **11**: p. 25-47.

34.   Robertson, K.L., et al., *Fluorescent PNA probes as hybridization labels for biological RNA.* Biochemistry, 2006. **45**(19): p. 6066-74.

35.   Tsuji, A., et al., *Direct observation of specific messenger RNA in a single living cell under a fluorescence microscope.* Biophys J, 2000. **78**(6): p. 3260-74.

36.   Raj, A., et al., *Imaging individual mRNA molecules using multiple singly labeled probes.* Nat Methods, 2008. **5**(10): p. 877-9.

37.   Michalet, X., et al., *Quantum dots for live cells, in vivo imaging, and diagnostics.* Science, 2005. **307**(5709): p. 538-44.

38.   Resch-Genger, U., et al., *Quantum dots versus organic dyes as fluorescent labels.* Nat Methods, 2008. **5**(9): p. 763-75.

39.   Proudnikov, D., et al., *Optimizing primer--probe design for fluorescent PCR.* J Neurosci Methods, 2003. **123**(1): p. 31-45.

40.   Ali, M.F., et al., *DNA hybridization and discrimination of single-nucleotide mismatches using chip-based microbead arrays.* Anal Chem, 2003. **75**(18): p. 4732-9.

41.   Gotoh, M., et al., *A new approach to determine the effect of mismatches on kinetic parameters in DNA hybridization using an optical biosensor.* DNA Res, 1995. **2**(6): p. 285-93.

42.   Wang, J., et al., *Mismatch-sensitive hybridization detection by peptide nucleic acids immobilized on a quartz crystal microbalance.* Anal Chem, 1997. **69**(24): p. 5200-2.

43.   Tanke, H.J., R.W. Dirks, and T. Raap, *FISH and immunocytochemistry: towards visualising single target molecules in living cells.* Curr Opin Biotechnol, 2005. **16**(1): p. 49-54.

44.   Levsky, J.M. and R.H. Singer, *Fluorescence in situ hybridization: past, present and future.* J Cell Sci, 2003. **116**(Pt 14): p. 2833-8.

45.   Femino, A.M., et al., *Visualization of single molecules of mRNA in situ.* Methods Enzymol, 2003. **361**: p. 245-304.

46.   Kerstens, H.M., P.J. Poddighe, and A.G. Hanselaar, *A novel in situ hybridization signal amplification method based on the deposition of biotinylated tyramine.* J Histochem Cytochem, 1995. **43**(4): p. 347-52.

47.   van de Corput, M.P., et al., *Sensitive mRNA detection by fluorescence in situ hybridization using horseradish peroxidase-labeled oligodeoxynucleotides and tyramide signal amplification.* J Histochem Cytochem, 1998. **46**(11): p. 1249-59.

48.   van de Corput, M.P., et al., *Fluorescence in situ hybridization using horseradish peroxidase-labeled oligodeoxynucleotides and tyramide signal amplification for sensitive DNA and mRNA detection.* Histochem Cell Biol, 1998. **110**(4): p. 431-7.

49.   Pianowski, Z., et al., *Imaging of mRNA in live cells using nucleic acid-templated reduction of azidorhodamine probes.* J Am Chem Soc, 2009. **131**(18): p. 6492-7.

50.   Afonina, I.A., et al., *Minor groove binder-conjugated DNA probes for quantitative DNA detection by hybridization-triggered fluorescence.* Biotechniques, 2002. **32**(4): p. 940-4, 946-9.

51.   Lukhtanov, E.A., et al., *Novel DNA probes with low background and high hybridization-triggered fluorescence.* Nucleic Acids Res, 2007. **35**(5): p. e30.

52.   Franzini, R.M. and E.T. Kool, *Efficient nucleic acid detection by templated reductive quencher release.* J Am Chem Soc, 2009. **131**(44): p. 16021-3.

53.   Li, H., et al., *Templated chemistry for sequence-specific fluorogenic detection of duplex DNA.* Chembiochem. **11**(15): p. 2132-7.

54.   Kuhn, H., et al., *Hybridization of DNA and PNA molecular beacons to single-stranded and double-stranded DNA targets.* J Am Chem Soc, 2002. **124**(6): p. 1097-103.

55.   Socher, E., et al., *Low-noise stemless PNA beacons for sensitive DNA and RNA detection.* Angew Chem Int Ed Engl, 2008. **47**(49): p. 9555-9.

56.   Li, Q., et al., *A new class of homogeneous nucleic acid probes based on specific displacement hybridization.* Nucleic Acids Res, 2002. **30**(2): p. E5.

57.   Marti, A.A., et al., *Design and characterization of two-dye and three-dye binary fluorescent probes for mRNA detection.* Tetrahedron, 2007. **63**(17): p. 3591-3600.

58.   Didenko, V.V., *DNA probes using fluorescence resonance energy transfer (FRET): designs and applications.* Biotechniques, 2001. **31**(5): p. 1106-16, 1118, 1120-1.

59.   Ha, T., et al., *Probing the interaction between two single molecules: fluorescence resonance energy transfer between a single donor and a single acceptor.* Proc Natl Acad Sci U S A, 1996. **93**(13): p. 6264-8.

60.   Selvin, P.R., *Fluorescence resonance energy transfer.* Methods Enzymol, 1995. **246**: p. 300-34.

61.   Livak, K.J., et al., *Oligonucleotides with fluorescent dyes at opposite ends provide a quenched probe system useful for detecting PCR product and nucleic acid hybridization.* PCR Methods Appl, 1995. **4**(6): p. 357-62.

62.   Haugland, R.P., J. Yguerabide, and L. Stryer, *Dependence of the kinetics of singlet-singlet energy transfer on spectral overlap.* Proc Natl Acad Sci U S A, 1969. **63**(1): p. 23-30.

63.   Selvin, P.R., *The renaissance of fluorescence resonance energy transfer.* Nat Struct Biol, 2000. **7**(9): p. 730-4.

64.   Marras, S.A., F.R. Kramer, and S. Tyagi, *Efficiencies of fluorescence resonance energy transfer and contact-mediated quenching in oligonucleotide probes.* Nucleic Acids Res, 2002. **30**(21): p. e122.

65.   Johansson, M.K., et al., *Intramolecular dimers: a new strategy to fluorescence quenching in dual-labeled oligonucleotide probes.* J Am Chem Soc, 2002. **124**(24): p. 6950-6.

66.   Blanco, A.M., et al., *A FRET-based assay for characterization of alternative splicing events using peptide nucleic acid fluorescence in situ hybridization.* Nucleic Acids Res, 2009. **37**(17): p. e116.

67.   Oquare, B.Y. and J.S. Taylor, *Synthesis of peptide nucleic acid FRET probes via an orthogonally protected building block for post-synthetic labeling of peptide nucleic acids at the 5-position of uracil.* Bioconjug Chem, 2008. **19**(11): p. 2196-204.

68.   Piston, D.W. and G.J. Kremers, *Fluorescent protein FRET: the good, the bad and the ugly.* Trends Biochem Sci, 2007. **32**(9): p. 407-14.

69.   Sei-Iida, Y., et al., *Real-time monitoring of in vitro transcriptional RNA synthesis using fluorescence resonance energy transfer.* Nucleic Acids Res, 2000. **28**(12): p. E59.

70.   Ruttinger, S., et al., *Accurate single-pair Forster resonant energy transfer through combination of pulsed interleaved excitation, time correlated single-photon counting, and fluorescence correlation spectroscopy.* J Biomed Opt, 2006. **11**(2): p. 024012.

71.   Ng, T., et al., *Imaging protein kinase Calpha activation in cells.* Science, 1999. **283**(5410): p. 2085-9.

72.   Snapp, E.L. and R.S. Hegde, *Rational design and evaluation of FRET experiments to measure protein proximities in cells.* Curr Protoc Cell Biol, 2006. **Chapter 17**: p. Unit 17 9.

73.   Hohng, S., C. Joo, and T. Ha, *Single-molecule three-color FRET.* Biophys J, 2004. **87**(2): p. 1328-37.

74.   Abe, H. and E.T. Kool, *Flow cytometric detection of specific RNAs in native human cells with quenched autoligating FRET probes.* Proc Natl Acad Sci U S A, 2006. **103**(2): p. 263-8.

75.   Silverman, A.P. and E.T. Kool, *Quenched autoligation probes allow discrimination of live bacterial species by single nucleotide differences in rRNA.* Nucleic Acids Res, 2005. **33**(15): p. 4978-86.

76.   Yao, G., et al., *Monitoring molecular beacon DNA probe hybridization at the single-molecule level.* Chemistry, 2003. **9**(22): p. 5686-92.

77.   Summerer, D. and A. Marx, *A molecular beacon for quantitative monitoring of the DNA polymerase reaction in real-time.* Angew Chem Int Ed Engl, 2002. **41**(19): p. 3620-2, 3516.

78.   Zhang, P., T. Beck, and W. Tan, *Design of a Molecular Beacon DNA Probe with Two Fluorophores This work was partially supported by the Office of Naval Research Young Investigator Award N00014-98-1-0621 and by an NSF Career Award (CHE-9733650). We would like to thank Dr. Richard Hogrefe, Paul Imperial, Kelly Christianson, and the Trilink Oligonucleotide Synthesis group for producing the molecular beacons used in this study.* Angew Chem Int Ed Engl, 2001. **40**(2): p. 402-405.

79.   Samain, F., et al., *Spectroscopic properties of pyrene-containing DNA mimics.*
       Bioorg Med Chem, 2008. **16**(1): p. 27-33.

80.   Haner, R., et al., *A highly sensitive, excimer-controlled molecular beacon.* Angew
       Chem Int Ed Engl. **49**(7): p. 1227-30.

81.   Santangelo, P.J., et al., *Dual FRET molecular beacons for mRNA detection in
       living cells.* Nucleic Acids Res, 2004. **32**(6): p. e57.

82.   Jones, R., et al., *Molecular beacons can assess changes in expression and 3'-
       polyadenylation of human eNOS mRNA.* Am J Physiol Cell Physiol, 2009. **296**(3):
       p. C498-504.

83.   Mo, Z.H., et al., *A nanogold-quenched fluorescence duplex probe for
       homogeneous DNA detection based on strand displacement.* Anal Bioanal Chem,
       2007. **389**(2): p. 493-7.

84.   He, F., et al., *Selective and homogeneous fluorescent DNA detection by target-
       induced strand displacement using cationic conjugated polyelectrolytes.* Anal
       Chem, 2008. **80**(6): p. 2239-43.

85.   Ranasinghe, R.T. and T. Brown, *Fluorescence based strategies for genetic
       analysis.* Chem Commun (Camb), 2005(44): p. 5487-502.

86.   Prater, C.E. and P.S. Miller, *3'-methylphosphonate-modified oligo-2'-O-
       methylribonucleotides and their Tat peptide conjugates: uptake and stability in
       mouse fibroblasts in culture.* Bioconjug Chem, 2004. **15**(3): p. 498-507.

87.   Novopashina, D., et al., *Conjugates of oligo(2'-O-methylribonucleotides) with
       minor groove binders as new sequence-specific agents recognizing both grooves*

of double-stranded DNA. Nucleosides Nucleotides Nucleic Acids, 2003. **22**(5-8): p. 1179-82.

88.   Braasch, D.A. and D.R. Corey, *Locked nucleic acid (LNA): fine-tuning the recognition of DNA and RNA.* Chem Biol, 2001. **8**(1): p. 1-7.

89.   Nielsen, C.B., et al., *The solution structure of a locked nucleic acid (LNA) hybridized to DNA.* J Biomol Struct Dyn, 1999. **17**(2): p. 175-91.

90.   Hanvey, J.C., et al., *Antisense and antigene properties of peptide nucleic acids.* Science, 1992. **258**(5087): p. 1481-5.

91.   Nielsen, P.E., M. Egholm, and O. Buchardt, *Peptide nucleic acid (PNA). A DNA mimic with a peptide backbone.* Bioconjug Chem, 1994. **5**(1): p. 3-7.

92.   Walder, R.Y. and J.A. Walder, *Role of RNase H in hybrid-arrested translation by antisense oligonucleotides.* Proc Natl Acad Sci U S A, 1988. **85**(14): p. 5011-5.

93.   Bratu, D.P., et al., *Visualizing the distribution and transport of mRNAs in living cells.* Proc Natl Acad Sci U S A, 2003. **100**(23): p. 13308-13.

94.   Bonham, M.A., et al., *An assessment of the antisense properties of RNase H-competent and steric-blocking oligomers.* Nucleic Acids Res, 1995. **23**(7): p. 1197-203.

95.   Turner, J.J., et al., *Cell-penetrating peptide conjugates of peptide nucleic acids (PNA) as inhibitors of HIV-1 Tat-dependent trans-activation in cells.* Nucleic Acids Res, 2005. **33**(21): p. 6837-49.

96.   Lundberg, P., K. Kilk, and U. Langel, *Cell-Penetrating Peptide-Mediated Delivery of Peptide Nucleic Acid (PNA) Oligomers.* CSH Protoc, 2008. **2008**: p. pdb prot4889.

97.   Patel, L.N., et al., *Conjugation with cationic cell-penetrating peptide increases pulmonary absorption of insulin.* Mol Pharm, 2009. **6**(2): p. 492-503.

98.   Richard, J.P., et al., *Cell-penetrating peptides. A reevaluation of the mechanism of cellular uptake.* J Biol Chem, 2003. **278**(1): p. 585-90.

99.   Zorko, M. and U. Langel, *Cell-penetrating peptides: mechanism and kinetics of cargo delivery.* Adv Drug Deliv Rev, 2005. **57**(4): p. 529-45.

100.   Marsden, H.R., et al., *Noncovalent triblock copolymers based on a coiled-coil peptide motif.* J Am Chem Soc, 2008. **130**(29): p. 9386-93.

101.   Fonseca, S.B., M.P. Pereira, and S.O. Kelley, *Recent advances in the use of cell-penetrating peptides for medical and biological applications.* Adv Drug Deliv Rev, 2009. **61**(11): p. 953-64.

102.   Duchardt, F., et al., *A comprehensive model for the cellular uptake of cationic cell-penetrating peptides.* Traffic, 2007. **8**(7): p. 848-66.

103.   Nitin, N., et al., *Peptide-linked molecular beacons for efficient delivery and rapid mRNA detection in living cells.* Nucleic Acids Res, 2004. **32**(6): p. e58.

104.   Vile, R.G., A. Tuszynski, and S. Castleden, *Retroviral vectors. From laboratory tools to molecular medicine.* Mol Biotechnol, 1996. **5**(2): p. 139-58.

105.   Koltover, I., et al., *An inverted hexagonal phase of cationic liposome-DNA complexes related to DNA release and delivery.* Science, 1998. **281**(5373): p. 78-81.

106.   Zabner, J., *Cationic lipids used in gene transfer.* Adv Drug Deliv Rev, 1997. **27**(1): p. 17-28.

107. Borgatti, M., et al., *Cationic liposomes as delivery systems for double-stranded PNA-DNA chimeras exhibiting decoy activity against NF-kappaB transcription factors.* Biochem Pharmacol, 2002. **64**(4): p. 609-16.

108. Pack, D.W., et al., *Design and development of polymers for gene delivery.* Nat Rev Drug Discov, 2005. **4**(7): p. 581-93.

109. Wagner, E., et al., *Transferrin-polycation-DNA complexes: the effect of polycations on the structure of the complex and DNA delivery to cells.* Proc Natl Acad Sci U S A, 1991. **88**(10): p. 4255-9.

110. Fang, H., et al., *Cationic shell-cross-linked knedel-like (cSCK) nanoparticles for highly efficient PNA delivery.* Mol Pharm, 2009. **6**(2): p. 615-26.

111. Abdelhady, H.G., et al., *Direct real-time molecular scale visualisation of the degradation of condensed DNA complexes exposed to DNase I.* Nucleic Acids Res, 2003. **31**(14): p. 4001-5.

112. Wang, X.L., et al., *A multifunctional and reversibly polymerizable carrier for efficient siRNA delivery.* Biomaterials, 2008. **29**(1): p. 15-22.

113. Boussif, O., et al., *A versatile vector for gene and oligonucleotide transfer into cells in culture and in vivo: polyethylenimine.* Proc Natl Acad Sci U S A, 1995. **92**(16): p. 7297-301.

114. Esfand, R. and D.A. Tomalia, *Poly(amidoamine) (PAMAM) dendrimers: from biomimicry to drug delivery and biomedical applications.* Drug Discov Today, 2001. **6**(8): p. 427-436.

41

115. Bielinska, A., et al., *Regulation of in vitro gene expression using antisense oligonucleotides or antisense expression plasmids transfected using starburst PAMAM dendrimers.* Nucleic Acids Res, 1996. **24**(11): p. 2176-82.

116. Lin, Y.L., et al., *Degradable, pH-sensitive, membrane-destabilizing, comb-like polymers for intracellular delivery of nucleic acids.* Biomaterials. **31**(27): p. 7150-66.

117. Zhang, K., et al., *Cationic shell-crosslinked knedel-like nanoparticles for highly efficient gene and oligonucleotide transfection of mammalian cells.* Biomaterials, 2009. **30**(5): p. 968-77.

118. Ogris, M., et al., *PEGylated DNA/transferrin-PEI complexes: reduced interaction with blood components, extended circulation in blood and potential for systemic gene delivery.* Gene Ther, 1999. **6**(4): p. 595-605.

119. Ferkol, T., et al., *Receptor-mediated gene transfer into macrophages.* Proc Natl Acad Sci U S A, 1996. **93**(1): p. 101-5.

120. Leamon, C.P., D. Weigl, and R.W. Hendren, *Folate copolymer-mediated transfection of cultured cells.* Bioconjug Chem, 1999. **10**(6): p. 947-57.

121. Lee, H., J.H. Jeong, and T.G. Park, *A new gene delivery formulation of polyethylenimine/DNA complexes coated with PEG conjugated fusogenic peptide.* J Control Release, 2001. **76**(1-2): p. 183-92.

122. Vaysse, L., et al., *Improved transfection using epithelial cell line-selected ligands and fusogenic peptides.* Biochim Biophys Acta, 2000. **1475**(3): p. 369-76.

123. Shen, Y., et al., *Degradable poly(beta-amino ester) nanoparticles for cancer cytoplasmic drug delivery.* Nanomedicine, 2009. **5**(2): p. 192-201.

124. Jayagopal, A., et al., *Hairpin DNA-functionalized gold colloids for the imaging of mRNA in live cells.* J Am Chem Soc. **132**(28): p. 9789-96.

125. Seferos, D.S., et al., *Nano-flares: probes for transfection and mRNA detection in living cells.* J Am Chem Soc, 2007. **129**(50): p. 15477-9.

126. Perlette, J. and W. Tan, *Real-time monitoring of intracellular mRNA hybridization inside single living cells.* Anal Chem, 2001. **73**(22): p. 5544-50.

127. Walev, I., et al., *Delivery of proteins into living cells by reversible membrane permeabilization with streptolysin-O.* Proc Natl Acad Sci U S A, 2001. **98**(6): p. 3185-90.

128. Lennon, F.E., et al., *Use of molecular beacons to image effects of titanium surface microstructure on beta1 integrin expression in live osteoblast-like cells.* Biomaterials. **31**(30): p. 7640-7.

129. Neumann, E., et al., *Gene transfer into mouse lyoma cells by electroporation in high electric fields.* EMBO J, 1982. **1**(7): p. 841-5.

130. Tryfona, T. and M.T. Bustard, *Enhancement of biomolecule transport by electroporation: a review of theory and practical application to transformation of Corynebacterium glutamicum.* Biotechnol Bioeng, 2006. **93**(3): p. 413-23.

131. Okada, C.Y. and M. Rechsteiner, *Introduction of macromolecules into cultured mammalian cells by osmotic lysis of pinocytic vesicles.* Cell, 1982. **29**(1): p. 33-41.

132. Park, R.D., P.C. Sullivan, and B. Storrie, *Hypertonic sucrose inhibition of endocytic transport suggests multiple early endocytic compartments.* J Cell Physiol, 1988. **135**(3): p. 443-50.

133. Varkouhi, A.K., et al., *Endosomal escape pathways for delivery of biologicals.* J Control Release.

134. Heyes, J., et al., *Cationic lipid saturation influences intracellular delivery of encapsulated nucleic acids.* J Control Release, 2005. **107**(2): p. 276-87.

135. Carmona, S., et al., *Controlling HBV replication in vivo by intravenous administration of triggered PEGylated siRNA-nanoparticles.* Mol Pharm, 2009. **6**(3): p. 706-17.

136. Wiley, D.C. and J.J. Skehel, *The structure and function of the hemagglutinin membrane glycoprotein of influenza virus.* Annu Rev Biochem, 1987. **56**: p. 365-94.

137. Oliveira, S., et al., *Fusogenic peptides enhance endosomal escape improving siRNA-induced silencing of oncogenes.* Int J Pharm, 2007. **331**(2): p. 211-4.

138. Sonawane, N.D., F.C. Szoka, Jr., and A.S. Verkman, *Chloride accumulation and swelling in endosomes enhances DNA transfer by polyamine-DNA polyplexes.* J Biol Chem, 2003. **278**(45): p. 44826-31.

139. Read, M.L., et al., *A versatile reducible polycation-based system for efficient delivery of a broad range of nucleic acids.* Nucleic Acids Res, 2005. **33**(9): p. e86.

140. Shen, G., et al., *Phospholipid conjugate for intracellular delivery of peptide nucleic acids.* Bioconjug Chem, 2009. **20**(9): p. 1729-36.

141. Pack, D.W., D. Putnam, and R. Langer, *Design of imidazole-containing endosomolytic biopolymers for gene delivery.* Biotechnol Bioeng, 2000. **67**(2): p. 217-23.

142.   Berg, K., et al., *Photochemical internalization: a novel technology for delivery of macromolecules into cytosol.* Cancer Res, 1999. **59**(6): p. 1180-3.

143.   Oliveira, S., et al., *Photochemical internalization enhances silencing of epidermal growth factor receptor through improved endosomal escape of siRNA.* Biochim Biophys Acta, 2007. **1768**(5): p. 1211-7.

144.   Laederach, A., et al., *Distinct contribution of electrostatics, initial conformational ensemble, and macromolecular stability in RNA folding.* Proc Natl Acad Sci U S A, 2007. **104**(17): p. 7045-50.

145.   Winkler, W.C., S. Cohen-Chalamish, and R.R. Breaker, *An mRNA structure that controls gene expression by binding FMN.* Proc Natl Acad Sci U S A, 2002. **99**(25): p. 15908-13.

146.   Lima, W.F., et al., *Implication of RNA structure on antisense oligonucleotide hybridization kinetics.* Biochemistry, 1992. **31**(48): p. 12055-61.

147.   Allawi, H.T., et al., *Mapping of RNA accessible sites by extension of random oligonucleotide libraries with reverse transcriptase.* RNA, 2001. **7**(2): p. 314-27.

148.   Zhang, H.Y., et al., *mRNA accessible site tagging (MAST): a novel high throughput method for selecting effective antisense oligonucleotides.* Nucleic Acids Res, 2003. **31**(14): p. e72.

149.   Fang, H., Y. Shen, and J.S. Taylor, *Native mRNA antisense-accessible sites library for the selection of antisense oligonucleotides, PNAs, and siRNAs.* RNA. **16**(7): p. 1429-35.

150. Gifford, L.K., et al., *Identification of antisense nucleic acid hybridization sites in mRNA molecules with self-quenching fluorescent reporter molecules.* Nucleic Acids Res, 2005. **33**(3): p. e28.

151. Lewis, M.R. and F. Jia, *Antisense imaging: and miles to go before we sleep?* J Cell Biochem, 2003. **90**(3): p. 464-72.

152. Zuo, X., et al., *Sensitive and selective amplified fluorescence DNA detection based on exonuclease III-aided target recycling.* J Am Chem Soc. **132**(6): p. 1816-8.

153. Eis, P.S., et al., *An invasive cleavage assay for direct quantitation of specific RNAs.* Nat Biotechnol, 2001. **19**(7): p. 673-6.

154. Farber, J.M., *A collection of mRNA species that are inducible in the RAW 264.7 mouse macrophage cell line by gamma interferon and other agents.* Mol Cell Biol, 1992. **12**(4): p. 1535-45.

155. Palmieri, D., et al., *Her-2 overexpression increases the metastatic outgrowth of breast cancer cells in the brain.* Cancer Res, 2007. **67**(9): p. 4190-8.

156. Weissleder, R., et al., *In vivo imaging of tumors with protease-activated near-infrared fluorescent probes.* Nat Biotechnol, 1999. **17**(4): p. 375-8.

157. Santangelo, P.J., et al., *Single molecule-sensitive probes for imaging RNA in live cells.* Nat Methods, 2009. **6**(5): p. 347-9.

158. Chen, A.K., et al., *Ratiometric bimolecular beacons for the sensitive detection of RNA in single living cells.* Nucleic Acids Res. **38**(14): p. e148.

Chapter Two

Multimeric aptamer cassettes for transgene mRNA detection by malachite green (MG)

ABSTRACT

The ability to tag mRNAs with functional segments in the un-translated region has enabled a wide range of studies on behavior and distributions of specific mRNAs in living cells. Herein we report the design and construction of repeated aptamer sequences (cassettes) for tagging mRNA transcripts and show that they can be used to image a transgene mRNA by the small molecule malachite green (MG), whose fluorescence increases upon binding to the aptamer. We have shown that the aptamer in transfected cells can be detected in the presence of MG by confocal microscopy and flow cytometry. This multimeric cassette strategy can also be used to enhance RNA imaging by molecular beacons, FRET probes, and fluorogenic agents.

INTRODUCTION

Messenger RNA (mRNA) plays an indispensable role in gene expression and protein production for most biological species. It is therefore of great interest to be able to spatially and temporally monitor mRNA *in vivo*. One approach to nondestructively image endogenous mRNA in real time is to use fluorescently or radioactively labeled antisense probes designed to bind mRNA by Watson-Crick base pairing [1]. Because endogenous mRNA sequences have complex secondary and tertiary structures and are also bound by proteins *in vivo*, it often requires a fair amount of effort to identify high affinity antisense binding sites suitable for mRNA imaging [2]. Even when a suitable antisense agent is identified, there remains the challenge to obtain good signal to noise ratio as mRNAs are usually present at very low concentration inside cells [3], making it difficult to distinguish signals generated by specific binding from signals from free reporters and nonspecific binding. To overcome this problem, investigators have developed binary FRET and molecular beacon-based systems [4-6], which are designed to emit fluorescence only upon binding to the target mRNA. Nonetheless, achieving high sensitivity and signal to noise still remain as major problems for imaging mRNA using nucleic acid probes [7].

Another way to image and track mRNA inside cells is to use a tagged transgene. Unlike endogenous genes, which have a defined sequence and limited number of copies, transgenes can be constructed to afford control over copy numbers and sequence [8-10]. For example, one way to study the behavior of mRNAs in living cells in real time is to biosynthetically tag the mRNA of interest with multiple repeats of the MS2 coat protein that binds to an RNA stem loop. The mRNA can then be imaged by using a cell line

49

expressing an MS2 protein fused with a green fluorescent protein. In this way, the movement of the mRNA can be monitored by observing the fluorescence of GFP [11, 12].

Instead of tagging a transgene with the MS2 protein binding sequence, one can also tag an mRNA with multiple repeats of sequences that can bind to a fluorogenic ligand or a nucleic acid probe. In this chapter, we will report on our work to detect a transgene mRNA tagged with multiple repeats of an aptamer that can bind to the small molecule malachite green (MG). Aptamers are short oligonucleotides, which are selected from systematic evolution of ligands by exponential enrichment (SELEX) process and can be evolved to have strong binding affinity to specific proteins or small molecules [13]. One such RNA aptamer has been reported to have high binding affinity to malachite green (MG), which has very low fluorescence in the unbound state due to efficient vibrational de-excitation. However, upon binding to the aptamer, the vibrational modes of the molecule are restricted and its charge distribution and conformation are changed [14]. As a result, its fluorescence increases up to 2000 times, making it a good reporter to detect the RNA aptamer [15]. This MG aptamer has been adapted for the detection of nucleic acids [16]. Similar aptamers have also been studied to bind other ligands such as cocaine and ATP both *in vitro* [17, 18], and in living cells [19].

Our approach was to clone multiple repeats of the DNA sequence (cassette) coding for the MG aptamer into the 3'-end of an expression vector for the β2-adrenergic receptor fused with green fluorescence protein (Flag-mβ2AR-GFP). The expressed mRNA would thereby become fluorescent in the presence of Malachite Green, while the GFP would serve as an independent marker for expression of the transgene protein. This transgene

was constructed by a former lab member Dr. Huafeng Fang. He was able to show that the mRNA tagged with the repeating aptamer could be detected in a total cellular RNA extract in the presence of MG. I will demonstrate that such a transgene can also be used for fluorescence imaging of mRNA expression in living cells by confocal microscopy and flow cytometry.

EXPERIMENTAL PROCEDURES

Materials

All ODNs were purchased from Integrated DNA technologies Inc (Coralville, IA), and purified by 15% or 20% denaturing polyacrylamide gel electrophoresis, following extraction with phenol/chloroform and ethanol precipitation. The pET-28a vector was obtained from EMD Chemicals (Gibbstown, NJ). Flag-mβ2AR-GFP plasmid was a kindly gift from Dr. Factor, Columbia University. All restriction enzymes were obtained from New England Biolabs Inc (Ipswich, MA). RNA was isolated with the T7 RiboMAX^{TM} large RNA production system purchased from Promega (Madison, WI). All chemicals for buffers and media preparation were purchased from Sigma-Aldrich (St Louis, MO). The cell culture media was purchased from Invitrogen Inc (Carlsbad, CA). MDCK cells (CCL-34TM) were purchased from ATCC (Manassas, VA).

Cell culture

MDCK Cells were grown in Dulbecco's modified Eagle's medium (DMEM) supplemented with 10% fetal bovine serum (FBS) and penicillin/streptomycin (10 µg/mL). Cell cultures were maintained at 37°C, 5% CO2 incubator. G418 (200 µg/mL)

was added to select stable transfected MDCK cells.

Construction of the aptamer cassette-bearing vectors and transgene (Huafeng Fang)

An ODN identical to the aptamer sequence was annealed to its complementary ODN, digested by XbaI and HindIII and cloned into a pET-28a vector that had been cleaved by the same enzymes. Clones containing the insert were selected based on size and verified by plasmid sequencing. The single cassette could then be excised from the plasmid by restriction enzyme digestion with NheI and HindIII. To double the number of cassettes, the single cassette that had been excised by NheI and HindIII was cloned into the original plasmid that contained a single cassette that had been digested by XbaI and HindIII. By repeating this process it is possible to generate many repeating cassettes. To transfer a single or multiple cassette to the trans-gene vector, the appropriate pET-28a vector was excised by XbaI and NotI and the cassette bearing fragment was separated by polyacrylamide gel electrophoresis and ligated into Flag-mβ2AR-GFP that had been digested by BSrG1 and NotI. The ligation part contained a BSrG1/XbaI linker pd(GTACAAGTAAAAAAT)•pd(CTAGATTTTTTACTT). With this strategy, Flag-mβ2AR-GFP-MGIII (3 repeats of the MG aptamer sequence), Flag-mβ2AR-GFP-MGVI (6 repeats of the MG aptamer sequence), Flag-mβ2AR-GFP-24L (24 repeats of a liner sequence that is designed to bind molecular beacons and used as a negative control of MG aptamer in this study) were cloned.

Detection of *in vitro* transcribed aptamer cassettes in presence of cellular RNAs (Huafeng Fang)

A triple repeating aptamer sequence was prepared by *in vitro* transcription from pET-MGIII plasmid using T7 RiboMAXTM large RNA production systems (Promega Inc.). Different amounts of the *in vitro* transcribed aptamer were incubated with 100 nM MG and 1μg/ml total RNA extracted from MDCK cells for 30 min at 37 °C. The fluorescence was taken with excitation at 633 nm and emission at 650 nm. The buffer contained 40 U RNaseout Ribonuclease Inhibitor (Invitrogen), 0.1 M KCl, 5 mM $MgCl_2$, 10 mM Na-Hepes, pH 7.4.

Aptamer cassette expression in cells and detection of aptamer in total RNA by MG (Huafeng Fang)

Plasmids Flag-mβ2AR-GFP-MGVI and Flag-mβ2AR-GFP (no aptamer control) were transiently transfected into MDCK cells using Lipofectamine 2000. After 24 h, the cells were recovered and the total RNA was extracted by TRizol reagent (Invitrogen). Total RNA (1 μg/mL) of four different samples of cells (sample A, B were transfected with aptamer containing plasmid and C, D with control plasmid) was incubated with 1 μM Malachite green at 37 °C, 30 min with 40 U RNaseout Ribonuclease Inhibitor (Invitrogen), 0.1 M KCl, 5 mM $MgCl_2$, 10 mM Na-Hepes, pH 7.4. Fluorescence was quantified on a Varian Fluorimeter with an excitation wavelength at 630 nm and emission wavelength at 650 nm.

Slot blot hybridization was used to identify aptamer cassette expression in the transfected cells. Briefly, a Hybond-XL membrane (Amersham Bioscience) was placed

into the slot blot apparatus (Minifold I, Schleicher & Schnell). Then 20 μg of total RNA from each sample of cells was denatured for 5 min at 68 °C in 50% formamide, 7% formaldehyde, and $1 \times$ SSC (150 mM NaCl and 15 mM sodium citrate). The resulting RNA samples were applied to the slots of the manifold. After all of the samples had passed through the membrane, the membrane was dried and baked at 80°C for 2 h. The membrane was then pre-hybridized with ULTRhyb-Oligo (Ambion Inc.) for 1 h at 55 °C, then incubated with $[\gamma\text{-}^{32}\text{P}]$-ATP labeled ODN probe (dGATTCGTTACCTGGGTCTCCCCAGTCG) that was partially complementary to the aptmer sequence. The incubation was carried out over night at 55 °C. The blot was washed at 55 °C using $1 \times$ SSC with 0.5 % SDS twice, 30 min for each wash, followed by washing with $0.1 \times$ SSC and 0.5 % SDS twice, with 10 min each time. The blot was then exposed to a phosphorimager screen for 4 h, and scanned with a Bio-Rad Phosphorimager.

Transgene aptamer imaging in living cells

Flag-mβ2AR-GFP-MGVI transfected cells that showed the highest expression level of aptamers from slot blot hybridization results (sample B) were selected and were mixed with normal MDCK cells. About 5×10^5 of the mixed cells were plated in 35 mm MatTek glass bottom micro-well dishes and incubated with DMEM culture medium without G418 at 37°C overnight. MG was loaded into the semiconfluent cells by Influx^{TM} Pinocytic cell-Loading Reagent (Invitrogen, Inc.). The Hypotonic Lysis Medium and Recovery Medium were pre-warmed at 37 °C. After removing the medium from the plate, the cells were incubated in the Loading Medium containing 10 μM MG for 10 min

at 37°C. The Loading Medium was then removed and the cells were washed and incubated with lysis medium. After 2 min the lysis medium was removed and fresh medium (2 mL) was added, and the cells incubated at 37 °C, 5% CO_2 for another 2 h. Cells were then washed twice with PBS and the fluorescence images of the live cells were taken with a Zeiss confocal microscopy with excitation by a He-Ne (633 nm) laser.

Detection of MG aptamer in living cells by flow cytometry

In order to quantitatively compare the aptamer binding triggered fluorescence in cells, we used flow cytometry to collect the fluorescence of MG with excitation at 633 nm (Becton Dickinson FASCan) and the data were processed by FlowJo 8.84 software.

Two methods for delivering MG into living cells were used. One was the influx method as described previously. MDCK cells and cells transfected with Flag-mβ2AR-GFP-MGVI were grown in 6 well plates at 1×10^5 per well. When cells grew to 80% confluence after 48 h, they were treated with 300 μL loading buffer containing 10 μM MG for 10 min, followed by 2 min treatment with lysis buffer. The cells were then incubated in DMEM medium with serum for 2 h, digested by trypsin/EDTA, and filtered for flow cytometry.

In another set of experiments, MG was delivered into living cells by free diffusion. Wild type MDCK cells and cells that stably expressed Flag-mβ2AR-GFP-24L or Flag-mβ2AR-GFP-MGVI gene were seeded in a 6-well plate at 1×10^5 per well. When the cells grew to 80% confluence after 48 h, the media was changed to PBS solution containing 5 μM MG and the cells were incubated for an additional 2 h. The cells were then washed with PBS 3 times, and then incubated with fresh media for another 2 h or 24 h at 37° C

to let the excess MG molecules efflux from the cells. After the treatment, cells were digested with 0.05% Trypsin/EDTA, re-suspended in PBS buffer and filtered for flow cytometry.

RESULTS AND DISCUSSION

In the study herein we chose the MG binding aptamer (**Figure 2.1A**) as an mRNA because it has been reported previously to bind to MG with high affinity, and enhance its fluorescence by over 2000-fold [15]. Dr Huafeng Fang of our group had successfully constructed the Flag-mβ2AR-GFP-MGVI plasmid and transfected it into MDCK cells (**Figure 2.1B**). He also cloned a linear sequence that was devoid of secondary structure that could be used for antisense probes (Flag-mβ2AR-GFP-24L, **Figure 2.1B**). For the details of Flag-mβ2AR-GFP-24L transgene imaging using molecular beacons, please refer to the thesis of our former lab member Dr. Bereket Oquare.

Creation of multiple cassettes

Multiple repeats of the aptamer and antisense cassettes were created by an iterative cloning procedure [20] shown in **Figure 2.2**. First, a 61-mer DNA sequence containing MG aptamer coding gene, Xba I, Nhe I and Hind III restriction sites was prepared by automated DNA synthesis. Xba I and Nhe I were chosen because they can produce the same 5'-sticky end following cleavage while having different recognition sequences. In the first step of the cycle, the 61-mer was digested by Xba I and Hind III and cloned into a pET-28a vector that had been cleaved at the same sites. The presence of the insert was verified by sequencing. To add a second aptamer /cassette, the clone was

cleaved instead by Nhe I and Hind III followed by insertion of another aptamer sequence. Because the cleavage sites of Xba I and Nhe I share the same 5'-sticky end, they can be ligated together, rendering a sequence that is neither cleavable by Nhe I or Xba I. The double insert can then be excised by treatment with Xba I and Hind III and inserted back into the another clone that contains one insert to generate a 3-mer repeat, or back into the another clone with two inserts to generate a 4-mer repeat. This recycling strategy enables one to increase the number of the insert exponentially.

Cloning antisense repeats into the 3'-UTR of a transgene

As part of a research project to develop agents for monitoring the transcription of a therapeutic gene for the treatment of acute lung injury (ALI) *in vivo*, we cloned the multimeric antisense cassettes into the 3'-UTR of a flag-tagged β2-adrenergic receptor fused to EGFP (**Figure 2.2**). Transgenic overexpression of the β2-adrenergic receptor has been shown to increase the rate of alveolar fluid clearance in mouse [21] and improve the survival rate of mice with ALI [22]. The multiple repeating inserts were first excised from the pET28a vector by Xba I and Hind III. The repeats were then cloned into the Xba I site of the transgene following the EGFP coding region with a linker sequence (Figure 1B). We were able to produce and characterize the clones containing 6 repeating aptamer sites. These vectors could be used for transient expression of the aptamer, and to produce stably transformed MDCK cell lines for imaging studies by selection for G418 resistance. The presence of the aptamer cassette was confirmed by a dot blot experiment.

Detection of *in vitro* transcribed aptamer cassettes in the presence of cellular RNAs

First, we tested the ability of MG to detect different concentrations of *in vitro* transcribed aptamer in the presence of competing total RNA from cell extract (**Figure 2.3**). The three repeating aptamers were incubated with 100 nM MG and 1 μg/μl cellular total RNA extracted from MDCK cells at a final concentration of 100 nM, 10 nM and 1 nM respectively. The fluorescence was observed at an excitation wavelength of 630 nm and emission wavelength of 650 nm. We found that the fluorescence of 100 nM aptamer/MG complexes in the presence of 1 μg/μL of RNA was about 22 times higher than the MG alone in the absence of the aptamer. When the aptamer concentration decreased to 1 nM, we could still observe the signal to be 2 fold stronger than the control, indicating that MG is a sensitive probe to detect the presence of the aptamer *in vitro*.

Aptamer cassette expression in cells and detection of aptamer in total RNA by MG

We then examined the possibility of using MG to detect the aptamer labeled mRNA in total mRNA extracts isolated from various transformed cell lines (**Figure 2.4**). Four different colonies of cells were selected. Samples A and B were transfected cells and C and D were normal MDCK cells. Total RNA from each of the samples was extracted and was tested for the presence of the aptamer by dot blotting. The upper right panel in **Figure 2.4** shows the intensity of aptamer expression level measure by the dot blot. The fluorescence spectra of the MG in different RNA samples confirmed the difference in expression level of the aptamer in four samples. Sample E is a negative control which contains only buffer and MG. The fluorescence from the cell extracts expressing the aptamer (A and B) were 1.5 to 2.5 times greater than that of those not

expressing the aptamer (C and D), indicating that MG can be used to detect aptamer in the presence of competing RNA *in vitro*.

Fluorescence imaging studies of living cells

Malachite green is a small molecule and is much more cell membrane permeable than nucleic acids. MG can diffuse into cells without the assistance of other agents for delivery. The influx approach, on the other hand takes advantage of pinocytosis to introduce cargo into endosome within cells, and hypotonic shock to rupture the endosomes to release the encapsulated cargo into the cytoplasm [23]. The Influx system was used in this experiment because we wanted to use a universal method that could deliver MG into living cells as well as antisense nucleic acid probes which are otherwise membrane impermeable. Based on the above considerations, we used the Influx system to deliver MG into a mixture of MDCK and Flag-mβ2AR-GFP-MGVI transfected MDCK cells, which transiently express the six-repeating aptamer and the membrane associated AR-GFP. Confocal microscopy showed that blue fluorescence from the MG/aptamer co-localizes with cells expressing green fluorescence from the EGFP (**Figure 2.5**). This means that transfected cells expressing AR-GFP have the mRNA transcripts and aptamer binding sites, which will render stronger MG fluorescence. The co-localization pattern shows that MG can be used effectively to image the transfected cells expressing MG aptamer.

Fluorescence measurement by flow cytometry

To quantitatively measure the difference in aptamer expression for different types

59

of cells, we used flow cytometry to monitor the fluorescence of MG in living cells. We used two methods to deliver MG inside cells, one via influx and the other by free diffusion. In the influx delivery method, cells were treated in the same way as for the confocal microscopy study described above. For the Flag-mβ2AR-GFP-MGVI transgenic MDCK cells there are two populations: GFP positive cells and GFP negative cells. For cells expressing high level of GFP, the mean fluorescence was higher than those that didn't express GFP (**Figure 2.6** A, B). This confirms the results observed in the confocal microscopy study. The mean fluorescence for of MG for GFP positive cells, however, was only 1.33 fold higher than that of wild type MDCK cells under the same influx delivery conditions (**Figure 2.6** C, D).

To further confirm our findings, we also delivered MG into cells by free diffusion. Since MG has a certain level of toxicity [24], the concentration and incubation time needed to be carefully optimized in order to keep cells viable. We optimized the conditions and found that incubation with 5 μM MG for 2 h can results in the most efficient MG delivery with the minimum cytotoxicity. MDCK and Flag-mβ2AR-GFP-MG24L transfected MDCK cells were used as negative controls. All the cells were incubated until 80% confluence, treated with 5 μM MG for 2 h, washed to remove excess MG, and incubated in the media for an additional 2 h or 24 h after the removal of the MG. **Figure 2.7** A shows the mean fluorescence of cells that were not incubated with MG. **Figure 2.7** B shows the cell fluorescence after 2 h incubation post MG treatment. Each type of cells has almost the same amount of MG fluorescence. This may be because of overloading the MG molecules, which would then outnumber the aptamers that can bind to them. After 24 h of incubation, cells without the MG aptamer cannot trap MG

60

inside the cells and MG molecules could exit the cells. The Flag-mβ2AR-GFP-MGVI MDCK cells, on the other hand, have the aptamer that can bind to the MG molecules and show higher fluorescence. This was reflected clearly in **Figure 2.7** C showing that after 24 h of incubation post MG treatment, Flag-mβ2AR-GFP-MGVI transfected MDCK cells have higher mean fluorescence than the rest of the cell samples. **Figure 2.7** D shows the increase of fluorescence for each type of cell at 24 h incubation after removal of MG compared to cells not treated with MG. The mean fluorescence of the Flag-mβ2AR-GFP-MGVI MDCK cells is 1.27 fold higher than that of normal MDCK cells, which confirms our finding by influx method. Compared to free diffusion, the influx method used higher amount of MG (10 μM vs 5 μM), but for a less incubation time (10 min vs 2 h). Therefore the MG molecules delivered inside cells might be less. This could explain the fact that after 2 h of incubation post the influx delivery, the aptamer containing cells show higher fluorescence than the wild type MDCK cells, whereas cells undergoing free diffusion had to be incubated for a longer time (24 h) to show the similar difference in fluorescence.

Although the aptamer-MG binding shows a clear increase of fluorescence in vitro (around 22 times in our experiment), the difference in fluorescence between cells expressing and not expressing the aptamer is not very large (around 1.3 times). This may be attributed to a large excess of non-specifically bound MG remaining inside the cells. If one assumes that the ratio of unbound and bound MG molecules was 10:1 and the fluorescence of MG increases 22 times upon binding to the aptamer (as observed *in vitro*), then the signal to noise ratio would be predicted to be 2.2:1 for aptamer expressing cells. Thus, overloading of the MG probe may be a major problem that affects the signal

to noise ratio in mRNA imaging with the MG aptamer. Theoretically, a longer incubation time will allow more MG molecules to exit cells, which would improve the signal to noise ratio. However, MG is also toxic and can produce radicals that will damage DNA and the aptamer [25], which would not be desirable for imaging.

CONCLUSION

We have successfully constructed a transgene that is tagged with a multiple repeating MG binding aptamer. We have shown that this aptamer can be detected using MG in vitro and in total RNA extracted from transfected cells. We have also shown that MG can be used to detect the aptamer in living cells by confocal microscopy and flow cytometry.

Tagging the 3'-UTR of genes with a universal repeating target antisense cassette is potentially a useful approach to achieve sensitive detection of genes in *vitro* and *in vivo*. We have shown that a transgenic mRNA linked to an aptamer can be detected by a small molecule fluorescent probe. One of the advantages of the small molecule aptamer imaging system is that small molecules are much more membrane permeable than the antisense agents. Unfortunately, the fluorescence of transfected cells is only 1.3 times higher than that of wild type MDCK cells in the presence of MG. Malachite green may not be the best choice, however, as it is also known to generate free radicals that can damage DNA and aptamer [25]. Aptamers could be evolved to bind other desired probes with optimal membrane permeability and fluorescent properties.
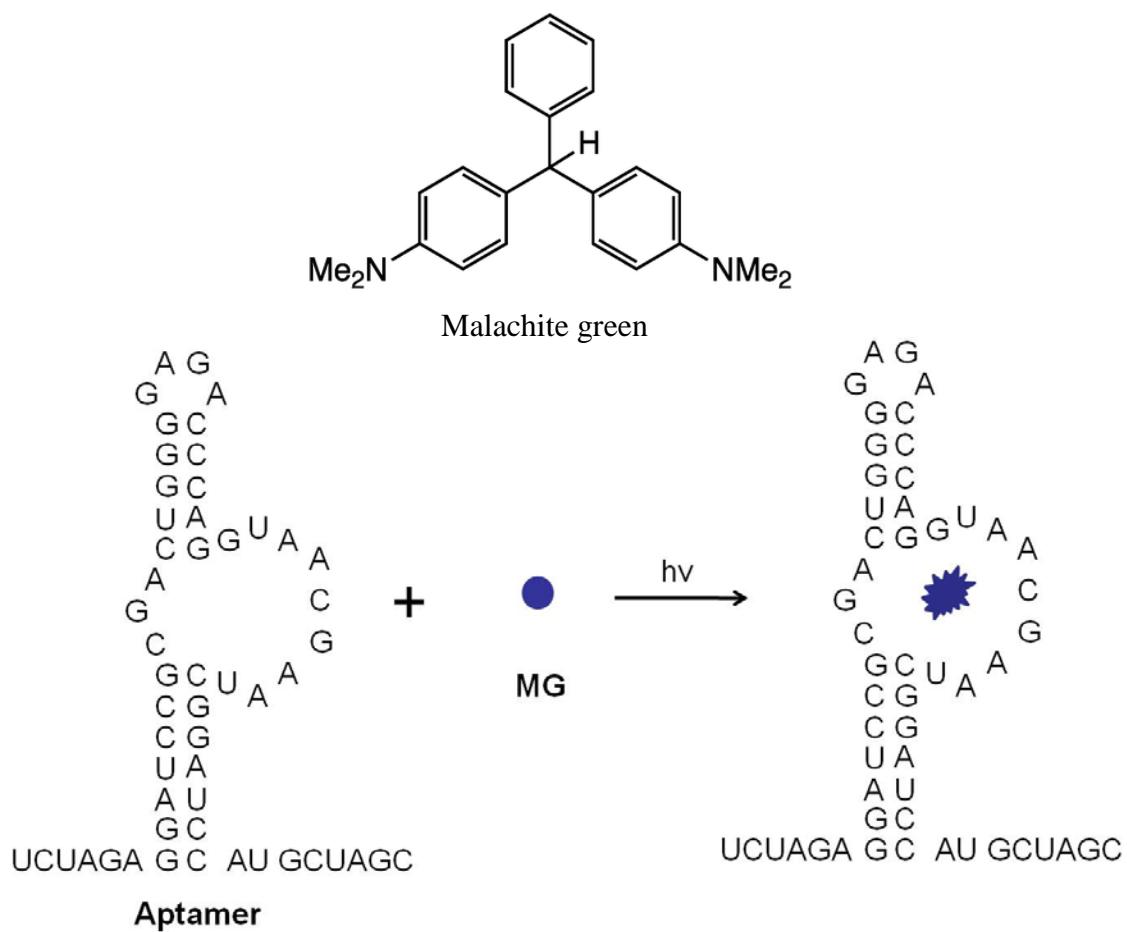
Figure 2.1A: Structure of MG, MG binding aptamer and the MG binding scheme

Aptamer

 XbaI
TCTAGAGGATCCGCGACTGGGGAGACCCAGGTAACG
AATCGGATCCATGCTAGCGTCAAGC
                    NheI   HindIII

Linear

         XbaI
CCGT|CTAGAAAGGAAGGGAGAAGAAAAAAGGAAGGGAGA
AGAG|CTAGCGTCA|AGCTTGGG
         NheI   HindIII

 Linker
 BSrG1
 GTACAAGTAAAAAAT
        TTCATTTTTTAGATC
                        Xba I

Figure 2.1B: Sequences used to generate the aptamer, the linear repeats, and the linker for insertion
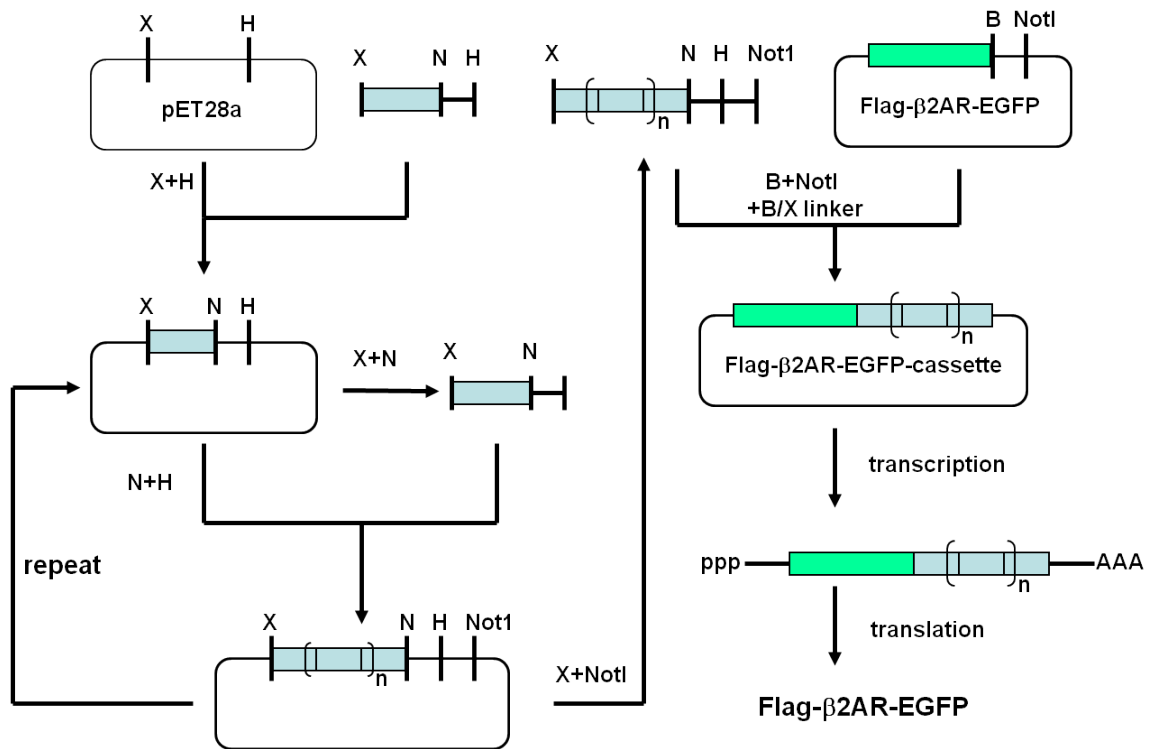
Figure 2.2: Repetitive cloning strategy used to generate multimeric aptamer cassettes
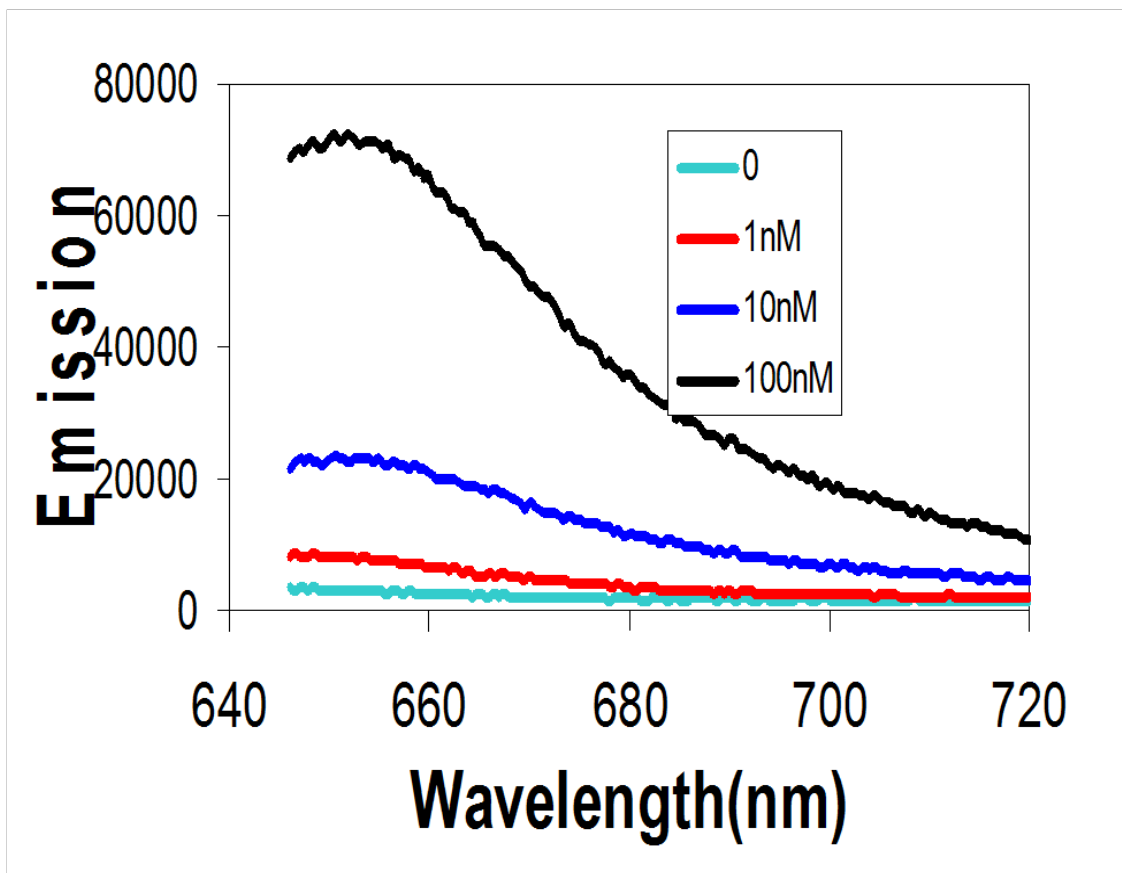
Figure 2.3: Aptamer-specific fluorescence in presence of total cellular RNA. Three different concentrations of *in vitro* transcribed three repeating aptamer RNA was incubated with 100 nM MG in presence of 1 μg/μL total RNA from MDCK cells at room temperature. Buffer: 0.1 M KCl, 5 mM $MgCl_2$, 10 mM Na-Hepes, pH 7.4. Excitation: 630 nm.
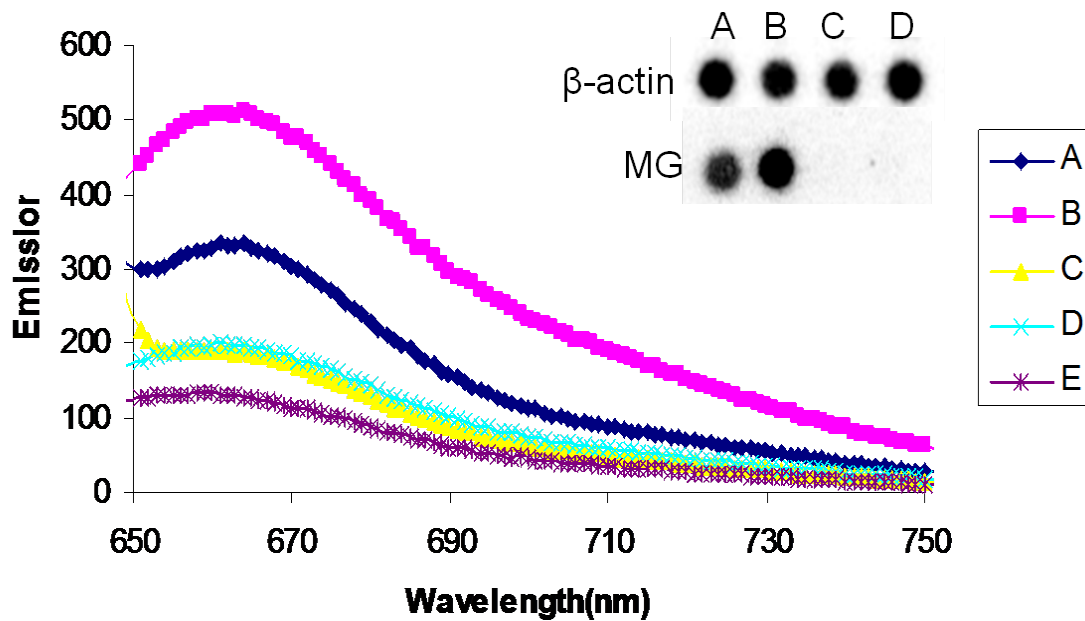
Figure 2.4: Detection of MG aptamer in cell extracts. MG: 1 μM, buffer: 0.1 M KCl, 5 mM $MgCl_2$, 10 mM Na-Hepes, pH 7.4, total RNA 1 μg/μl, extracted from cells expressing the Flag-mβ2AR-MGVI cassettes or Flag-mβ2AR. A: Flag-mβ2AR-MGVI-1, B: Flag-mβ2AR-MGVI-2, C: Flag-mβ2AR-1, D: Flag-mβ2AR-2, E: buffer without RNA. Excitation wavelength: 630 nm. RNA Slot blotting hybridization , $[\gamma^{32}P]$-ATP-labeled MG probe was hybridized with 20 μg A, B, C, D, E sample (same as above) overnight, aptamer expression is higher in sample B.
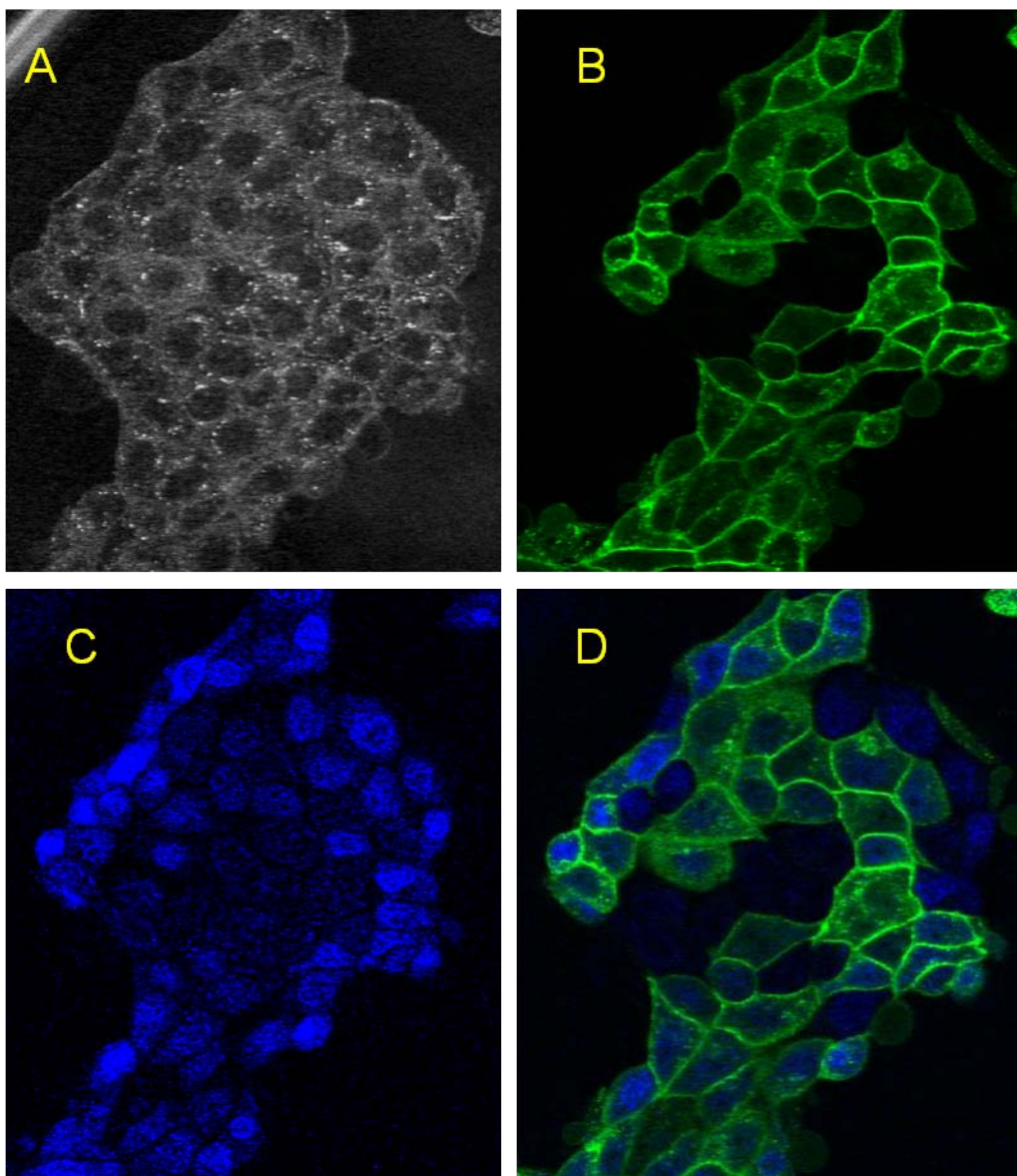
Figure 2.5: Aptamer cassette induced fluorescence of malachite green in cells. MG was loaded into cells using the Influx pinocytic reagent. Fluorescence was observed 2h later after loading. Mixture of MDCK & MDCK-Flag-mβ2AR-MGVI cells were cultured in the same plate. A: cell reflection photo, B: green, EGFP (ext: 488 nm), C: blue, aptamer/MG (ext: 633 nm) D: Superposition of B&C.
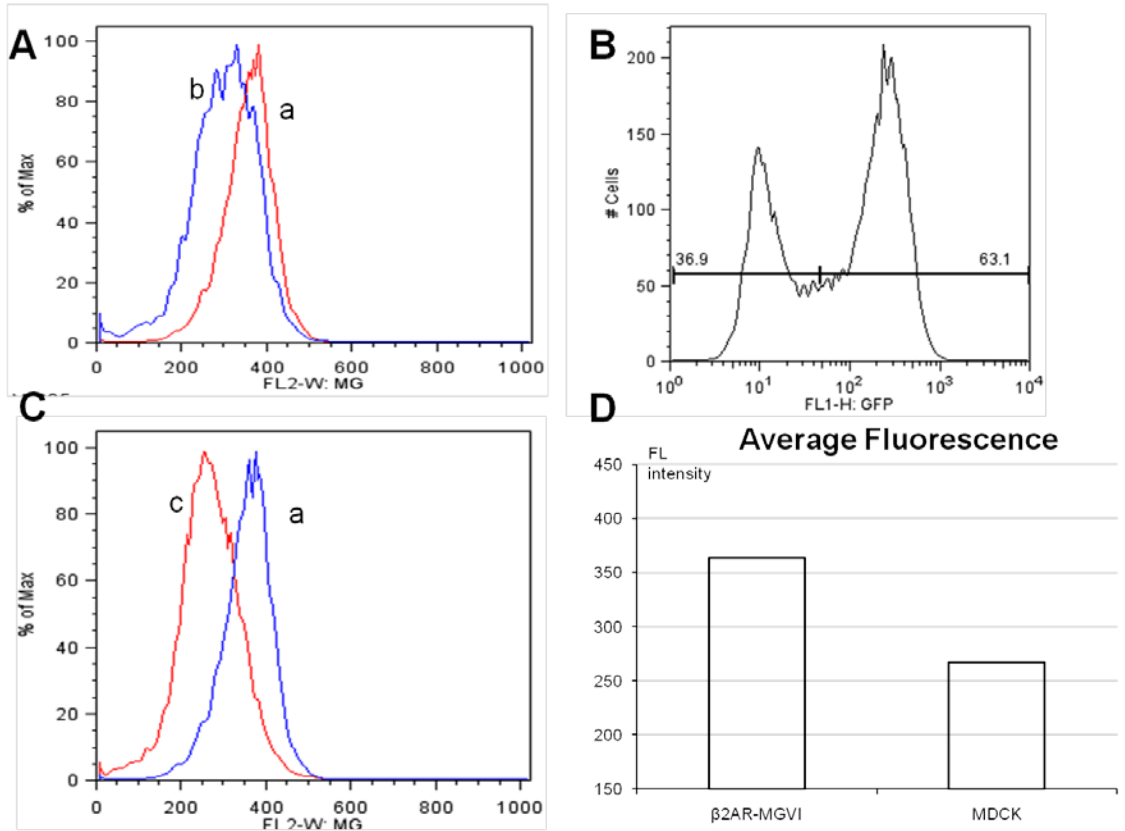
Figure2.6: Flow cytometric measurement of the MG fluorescence in transfected and wild type MDCK cells treated by influx. A. Mean MG fluorescence of (a) GFP positive transfected cells and (b) GFP negative transfected cells; B,GFP fluorescence of the MDCK-Flag-mβ2AR-MGVI transfected cells. The clear binominal distribution of GFP fluorescence indicating that some cells might have expressed the transgene while some might not; C, Mean MG fluorescence of (a) GFP positive transfected cells and (c) normal MDCK cells after influx delivery; D, Mean MG fluorescence of (a) and (c) cells.
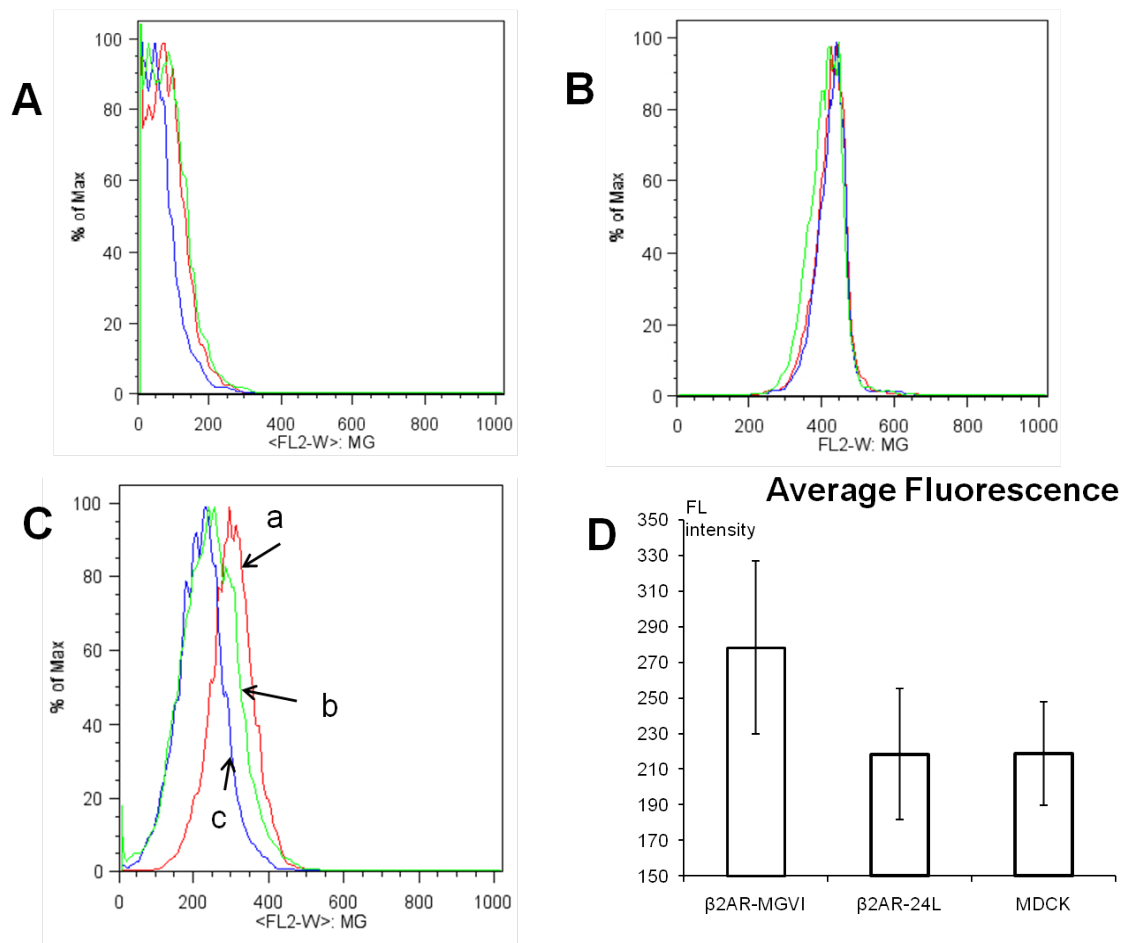
Figure 2.7: Flow cytometric measurement of MG fluorescence in transfected and wild type MDCK cells treated by free diffusion. (a). MDCK-Flag-mβ2AR-MGVI, (b)MDCK-Flag-mβ2AR-24L, (c) wild type MDCK,. Incubated with 5μM MG for 2 hours, washed, and added fresh media incubation for another 2 or 24 h respectively. A. Cells not treated with MG; B, 2 h incubation after MG delivery; C, 24 h incubation after MG delivery; D, Mean fluorescence increase of three type of cells after 24 h incubation post MG delivery. Fluorescence intensity was an average of three repeats for each type of cells.

References

1. Paroo, Z. and D.R. Corey, *Imaging gene expression using oligonucleotides and peptide nucleic acids.* J Cell Biochem, 2003. **90**(3): p. 437-42.

2. Lima, W.F., et al., *Implication of RNA structure on antisense oligonucleotide hybridization kinetics.* Biochemistry, 1992. **31**(48): p. 12055-61.

3. Lewis, M.R. and F. Jia, *Antisense imaging: and miles to go before we sleep?* J Cell Biochem, 2003. **90**(3): p. 464-72.

4. Nitin, N., W.J. Rhee, and G. Bao, *Translation inhibition reveals interaction of 2'-deoxy and 2'-O-methyl molecular beacons with mRNA targets in living cells.* Nucleic Acids Res, 2009. **37**(15): p. 4977-86.

5. Santangelo, P.J., N. Nitin, and G. Bao, *Direct visualization of mRNA colocalization with mitochondria in living cells using molecular beacons.* J Biomed Opt, 2005. **10**(4): p. 44025.

6. Santangelo, P.J., et al., *Dual FRET molecular beacons for mRNA detection in living cells.* Nucleic Acids Res, 2004. **32**(6): p. e57.

7. Bao, G., W.J. Rhee, and A. Tsourkas, *Fluorescent probes for live-cell RNA detection.* Annu Rev Biomed Eng, 2009. **11**: p. 25-47.

8. Hobbs, S.L., T.D. Warkentin, and C.M. DeLong, *Transgene copy number can be positively or negatively associated with transgene expression.* Plant Mol Biol, 1993. **21**(1): p. 17-26.

9. Sauer, B., *Manipulation of transgenes by site-specific recombination: use of Cre recombinase.* Methods Enzymol, 1993. **225**: p. 890-900.

10. Brem, G., et al., *Expression of synthetic cDNA sequences encoding human insulin-like growth factor-1 (IGF-1) in the mammary gland of transgenic rabbits.* Gene, 1994. **149**(2): p. 351-5.

11. Querido, E. and P. Chartrand, *Using fluorescent proteins to study mRNA trafficking in living cells.* Methods Cell Biol, 2008. **85**: p. 273-92.

12. Rodriguez, A.J., et al., *Imaging mRNA movement from transcription sites to translation sites.* Semin Cell Dev Biol, 2007. **18**(2): p. 202-8.

13. Ellington, A.D. and J.W. Szostak, *In vitro selection of RNA molecules that bind specific ligands.* Nature, 1990. **346**(6287): p. 818-22.

14. Nguyen, D.H., et al., *Binding to an RNA aptamer changes the charge distribution and conformation of malachite green.* J Am Chem Soc, 2002. **124**(50): p. 15081-4.

15. Babendure, J.R., S.R. Adams, and R.Y. Tsien, *Aptamers switch on fluorescence of triphenylmethane dyes.* J Am Chem Soc, 2003. **125**(48): p. 14716-7.

16. Kolpashchikov, D.M., *Binary malachite green aptamer for fluorescent detection of nucleic acids.* J Am Chem Soc, 2005. **127**(36): p. 12442-3.

17. Stojanovic, M.N., P. de Prada, and D.W. Landry, *Aptamer-based folding fluorescent sensor for cocaine.* J Am Chem Soc, 2001. **123**(21): p. 4928-31.

18. Nutiu, R. and Y. Li, *In vitro selection of structure-switching signaling aptamers.* Angew Chem Int Ed Engl, 2005. **44**(7): p. 1061-5.

19. Zheng, D., et al., *Aptamer nano-flares for molecular detection in living cells.* Nano Lett, 2009. **9**(9): p. 3258-61.

20.	Boe, F. and J.M. Masson, *Selective cloning of a defined number of tandem DNA repeats in Escherichia coli.* Nucleic Acids Res, 1996. **24**(12): p. 2450-1.

21.	McGraw, D.W., et al., *Targeted transgenic expression of beta(2)-adrenergic receptors to type II cells increases alveolar fluid clearance.* Am J Physiol Lung Cell Mol Physiol, 2001. **281**(4): p. L895-903.

22.	Liebler, J.M., et al., *Alveolar epithelial type I cells express beta2-adrenergic receptors and G-protein receptor kinase 2.* J Histochem Cytochem, 2004. **52**(6): p. 759-67.

23.	Park, R.D., P.C. Sullivan, and B. Storrie, *Hypertonic sucrose inhibition of endocytic transport suggests multiple early endocytic compartments.* J Cell Physiol, 1988. **135**(3): p. 443-50.

24.	Kraus, G.A., et al., *Fluorinated analogs of malachite green: synthesis and toxicity.* Molecules, 2008. **13**(4): p. 986-94.

25.	Panandiker, A., G.B. Maru, and K.V. Rao, *Dose-response effects of malachite green on free radical formation, lipid peroxidation and DNA damage in Syrian hamster embryo cells and their modulation by antioxidants.* Carcinogenesis, 1994. **15**(11): p. 2445-8.

Chapter Three

Strand-displacement activated Peptide Nucleic Acid (PNA) probes for imaging inducible nitric oxide synthase (iNOS) mRNA in living cells

ABSTRACT

Inducible nitric oxide synthase (iNOS) is an enzyme that catalyzes the production of nitric oxide in many eukaryotic species. iNOS expression is upregulated in inflammation, making it a good biomarker for monitoring injured tissue. We have investigated the use of strand-displacement activated fluorescent probes to image the expression of iNOS mRNA in living cells. The probes are constructed by annealing an antisense PNA bearing a fluorescein to a shorter DNA sequence bearing a Dabcyl^{plus} quencher, which quenches the fluorescence of the fluorescein. In the presence of the target mRNA, however, the mRNA will bind to the complementary PNA strand and displace the shorter DNA sequence, thereby restoring fluorescence of the fluorescein. We have designed and synthesized probes that are stable at 37 ^{o}C and undergo strand-displacement in the presence of a complementary DNA, and with *in vitro* transcribed iNOS mRNA in solution. We have also investigated the ability of the probes to detect the expression of iNOS mRNA in both fixed and living RAW 264.7 cells.

INTRODUCTION

Nitric oxide synthases (NOS) are a family of enzymes that catalyze the production of nitric oxide (NO) in many eukaryotic species. NO is a small molecule involved in signal transduction and immune responses. There are three types of nitric oxide synthases in most eukaryotic species: endothelial NOS (eNOS), neuronal NOS (nNOS) and inducible NOS (iNOS) [1, 2]. iNOS is involved in immune responses and is upregulated by environmental stimuli such as gamma interferon (γ-IFN) or lipopolysaccharide (LPS) [3-5]. The mechanism of γ-IFN and LPS triggered iNOS production has been well studied [6] and the inhibition of iNOS has been proved to be beneficial for curing inflammatory diseases [7]. Research has been conducted on lowering NO production by certain drugs that inhibit the protein [3, 4]. Another approach would be to inhibit mRNAs, such as the iNOS mRNA [8-10]. Meanwhile, iNOS mRNA can also be an important biomarker for cells or tissues in inflammatory conditions. It may therefore be worthwhile to be able to detect, quantify, and image iNOS mRNA *in vivo* for clinical applications.

One way to detect and quantify iNOS mRNA expression is by RT-PCR, which can detect mRNA at as low as a few copies per cell [11, 12]. However, this method requires lysis of cells or tissues, and would not be applicable for monitoring iNOS mRNA *in vivo*. Another way to monitor iNOS mRNA would be to use labeled antisense nucleic acid probes, which have been used to detect mRNAs both *in vitro* and *in vivo*. Antisense probes are complementary to the target mRNA and achieve their specificity by A-T and C-G Watson Crick base pairing. They can be radioactively or fluorescently labeled, and used for non-lethal, real time imaging of mRNA *in vivo* [13-16].

To reduce the background, nucleic acid probes have been designed to be fluorescent only in the presence of target mRNA. One class of such activatable probe designs is the quenched strand-displacement probe. In this design, an antisense probe is labeled with a fluorescent dye, whose fluorescence is quenched by a quencher attached to a shorter complementary oligonucleotide annealed to the antisense strand. The quenching mechanism can be by FRET, in which case the energy of the excited fluorophore is transferred to a quencher through space [17]; or by "contact quenching", in which a fluorophore and a quencher are close enough that they can form a non-fluorescent complex [18]. In the presence of the complementary target mRNA, which will form a more stable duplex, the shorter strand is displaced, and the fluorescence of the dye on the longer strand is no longer quenched, leading to the recovery of fluorescent signal. The rate of strand-displacement depends on the difference in length between the fluorescent and quenching probes. The larger the difference, the longer the un-paired section and the faster the rate for displacing the shorter strand by the target mRNA [19].

There are a few studies utilizing the strand-displacement probes. Hnatowich et al used a heterodimer consisting of a 25-mer phosphorodiamidatemorpholino (MORF) conjugated to a Cy5.5 and a complementary 18mer cDNA conjugated to a BHQ3 quencher to image a complementary 25mer biotinylated MORF oligomer immobilized on streptavidin polystyrene microspheres that had been planted intramuscularly into a mouse [20]. The same group have also utilized a probe consisting of a 25mer phosphorothioate DNA bearing Cy5.5 and a 10mer complementary phosphodiester DNA with BHQ3 quencher to image the multi drug resistance gene (mdr1) mRNA in mice bearing the KB-G2 tumor, which over-express the mdr1 mRNA, [21]. Meanwhile, Mirkin et al.

synthesized "nano flares" which consist of gold nanoparticles with single strand ODNs conjugated to the surface that are hybridized to a shorter strand of complementary ODN bearing a Cy5 quenched by the gold. In the presence of complementary mRNAs, the shorter strand was displaced, releasing the Cy5 bearing DNA, whose fluorescent signal could be detected. They reported that such "nano flares" can be used to detect specific mRNAs in living cells [22]. However, in this design, the fluorescent reporter was on the shorter reporter, which was displaced, and became free inside cells, so that the fluorescent image could not indicate the location of the mRNA. A better design would have been to place the fluorophore on the probe that will hybridize to the target mRNA so that the fluorescent signal will indicate the location and distribution of the mRNAs in inside cells.

Based on these reported studies, we utilized the strand-displacement activated probes to detect the iNOS mRNA *in vitro*, in situ, and in living cells. We have synthesized 23-mer peptide nucleic acid (PNA) probes bearing a fluorescein (FAM) at 5' end, whose fluorescence is quenched by a Dabcyl^plus, which is attached to the 3' end of a 17-mer complementary DNA probe. We have demonstrated that such strand-displacement activated probes can be used to detect both a complementary 21-mer target DNA and *in vitro* transcribed iNOS mRNA in solution. We have also employed such strand-displacement probes to image the iNOS mRNA in fixed RAW 264.7 cells by fluorescent in situ hybridization (FISH). We have investigated the possibility to deliver such probes into living RAW 264.7 cells by cationic shell-cross-linked knedel-like (cSCK) nanoparticles and image the iNOS mRNA in living cells (**Figure 3.1**). Analysis of the FISH image indicated that there was 3.6 (±1.8)-fold increase of fluorescence for

cells treated with LPS/γ-IFN compared to the non-treated cells, while the live cell imaging results showed 16.6 (±7.9) -fold increase in fluorescence for cells after LPS/γ-IFN stimulation.

EXPERIMENTAL PROCEDURES

Materials

Anhydrous N,N-dimethylformamide (DMF), diisopropylethylamine (DIPEA), trifluoroacetic acid (TFA), meta-cresol, dichloromethane (DCM)., N-methylpyrrolidone (NMP), dimethyl sulfoxide (DMSO), (5,6)-fluorescein-N-succinimidyl ester (FAM-NHS ester) were purchased from Sigma-Aldrich (St Louis, MO). Dbacyl[plus]-N-succinimidyl ester (Dabcyl[plus]-NHS) was purchased from Anaspec Inc (Fremont, CA). PNA monomers were purchased from PolyOrg Inc (Leominster, MA). Fmoc protected amino acids were purchased from EMD chemicals (Gibbstown, NJ). 2-(1H-7-Azabenzotriazol-1-yl)--1,1,3,3-tetramethyl uronium hexafluorophosphate (HATU) was purchased from GenScript (Piscataway, NJ). Fmoc-PAL-PEG-PS resin for the solid phase PNA synthesis was purchased from Applied Biosystems (Carlsbad, CA). The PNAs were synthesized by solid-phase Fmoc chemistry on an Expedite 8909 DNA/PNA synthesizer on a 2 µmol scale. All the oligodeoxynucleotides (ODN) and amino-modified ODNs were purchased from Intergrated DNA technologies (Coralville, IA). The crude PNA probes and the modified DNA probes were purified by a reversed phase high-performance liquid chromatography (HPLC) on a Beckman Gold System with a UV array detector and a Varian Microsorb-MV column (C-18, 5µm, 300Å pore size, 4.6×250 mm internal diameter and length). For the PNA probes, the running buffer A contains 0.1% TFA in

water and B contains 0.1% TFA in acetonitrile. For the DNA probes, the running buffer A contains 50 mM triethylammonium acetate (TEAA) in water and B contains 50 mM TEAA in water/acetonitrile (1:1) solution. The purified probes were verified by AppliedBiosystems 4700 MALDI-TOF mass spectrometry. The concentration of all the DNAs was determined from the absorbance at 260 nm taken on a Bausch and Lomb Spectronic 1001 spectrophotometer. To determine the PNAs' concentration, solutions were heated to 70 ^{o}C to eliminate the hypochromicity of the PNAs, after which the absorbance was measured at 260 nm on the same spectrophotometer. The concentration was then calculated based on Lambert-Beer Law $A = \varepsilon l c$, where A is the absorbance of the solution at 260 nm, l is the length of the light path (1 cm), and ε is the extinction coefficient of the probes. For each DNA oligo, ε was provided by the manufacturer. For the PNA probes, ε of each base was estimated at (A) 13.7 ml/μmol•cm, (G) 11.7 ml/μmol•cm, (C) 6.6 ml/ μmol•cm and (T) 8.6 ml/ μmol•cm.

PNA-Fluorescein synthesis and purification

A 23-mer PNA probe antisense to the bases starting at the 480 position of iNOS mRNA (480 PNA-FAM) and a control probe with the same length but targeting HeLa pLuc 705 cell's splicing correction site (pLuc PNA-FAM) were synthesized on an Expedite 8909 DNA/PNA synthesizer. After removal of the Fmoc protecting group at the 5' end of the PNA, the resin was dried by nitrogen gas and was mixed with 200 μL of 0.02 M FAM-NHS ester (2 eq) in DMSO, together with 2 eq DIPEA. The mixture was put on a shaker overnight at room temperature. The resin was then washed with DMF and then DCM, and dried under nitrogen. The resin was then cleaved in 250 μL TFA/m-

cresol (4:1) mixture for 2-4 h. The cleavage mixture was separated from the resin. PNAs were precipitated by adding 1 mL cold diethyl ether, and centrifuged down for 10 min. The product was dried on a hot block at 55 $^{\circ}$C and dissolved in water containing 0.1% TFA. The crude products were purified by HPLC and the masses of the purified products were confirmed by MALDI mass spectrometry.

DNA-Dabcyl plus synthesis and purification

Regular and 3'-end modified ODNs were purchased from IDT Inc. The 17-mer quencher ODNs were modified with a $(CH_2)_6-NH_2$ group at the 3'-end. They were complementary to the 23-mer 480 PNA-FAM and pLuc PNA-FAM probes. These modified ODNs were purified by HPLC. Each purified ODN (50 nmol) was reacted with 10 eq of Dabcyl plus-NHS ester in 10 mM $Na_2CO_3/NaHCO_3$ buffer, the pH of which was adjusted to 8.5 by adding drops of 1 M hydrogen chloride. The reaction was carried out overnight on a shaker. Then the reaction mixture was separated by gel electrophoresis on a 20% polyacrylamide gel. Bands containing DNA-Dabcyl[plus] were cut from the gel and eluted in diffusion buffer containing 0.5 M ammonia acetate, 10 mM $MgCl_2$, 1 mM EDTA and 0.1% SDS. The purified products were precipitated by adding 3 volumes of ethanol and spinning down in a centrifuge for 30 min after cooling to -20 $^{\circ}$C for 30 min. The Dabycl[plus]-DNA quencher probes were characterized by MALDI.

In vitro **mRNA transcription**

The PCMV-SPORT6 vector containing the iNOS mRNA gene was purchased from American Type Culture Collection (ATCC, Manassas, VA). LB media was

inoculated with E.coli containing the vector at 37 ^{o}C for 18 h. The plasmid was extracted from the E.coli by using HiPure Plasmid Maxprep kit (Invitrogen). The plasmid was then digested by Xhol (Promega) enzyme to form a linear DNA, which was purified by phenol extraction, ethanol precipitation and was characterized by electrophoresis on a 1% agarose gel stained with ethidium bromide. The linear DNA was then transcribed into iNOS mRNA by RiboMAX™ SP6 large scale RNA transcription kit (Promega) following the manufacturer's protocol. The integrity of iNOS mRNA was verified on the 1% w/v agarose gel. All the aqueous solution in this process was prepared by water treated with diethyl pyrocarbonate (DEPC) and the mRNA was stored at -80 ^{o}C in water with 2 µL (80 U) RNaseOUT™ recombinant RNase inhibitor (Invitrogen).

Displacement by complementary DNA in solution

PNA-FAM (0.5 µM) and complementary ODN or DNA-Dabcyl^{plus} (1µM) were heated at 95 ^{o}C for 3 min in a buffer containing 100 mM Tris, 5 mM MgCl$_2$, and annealed at room temperature.. Different amounts of the 21-mer complementary ODN were added to make the final concentration of 0.25, 0.5, 1, and 5 µM. The strand-displacement rate was monitored at 37 ^{o}C by measuring the fluorescence increase at 525 nm as a function of time on the fluorimeter with the excitation at 488 nm. After the fluorescent intensity reached its maximum value, each sample was then incubated at for another 15 min and the fluorescent emission spectrum was collected with excitation at 488 nm.

Displacement by *in vitro* transcribed mRNA

To test the ability of the probes to be displaced by mRNA without secondary structure, PNA-FAM and DNA-quencher probes (matched and mismatched) were annealed in 0.1 M KCl, 5 mM MgCl$_2$, 10 mM Na-Hepes buffer (pH=7.11) The final concentrations of the PNA-FAM and the DNA-Dabcyl [plus] probes were 0.2 and 0.4 μM respectively. *In vitro* transcribed iNOS mRNA was added to the solution to make the final concentration at 0.1, 0.2 and 0.4 μM respectively. Then the mixtures were heated at 65 ^{0}C for 1 min and incubated at 37 ^{0}C for 15 min. The fluorescence spectra of the samples were collected at 37 ^{0}C with excitation at 488 nm. All the solution in the experiment was prepared with DEPC treated water..

To study the kinetics of the strand-displacement with mRNA under physiological conditions, different amounts of mRNA were prepared in 10 mM Tris buffer (pH 7.15) to make final concentrations of 0.025, 0.05, 0.1 and 0.25 μM respectively. The mRNA solution was heated at 65 ^{o}C for 1.5 min and cooled at 37 ^{o}C, and then 1 μL RNaseOUT™ (40 U, Invitrogen) was added to each RNA sample. The pre-hybridized PNA-FAM/DNA-Dabcyl[plus] (1:2) solution (1 μM for PNA-FAM probe) was added to the mRNA solution to make the final concentration of the PNA-FAM probes at 0.05 μM. The fluorescence of the sample was monitored by Varian Eclipse Fluorimeter at 37 ^{o}C as a function of time. All the aqueous solution was prepared by water treated with DEPC.

q-RT PCR to quantify iNOS mRNA copy numbers in RAW 264.7 cells

RAW 264.7 cells were seeded on 10 mm Petri dish plates (Corning Inc, Lowell, MA) and grown until 70% confluence. Different sample plates were then treated with 1

µg/mL LPS and 300 ng/mL γ-IFN for 18, 6 and 0 h (without LPS and γ-IFN stimulation) respectively. Cells in each plate were counted by hemocytometer and spun down in a centrifuge. Total RNA of each sample was then extracted by TRizol reagent (Invitrogen, CA) following the manufacturer's protocol and quantified by measuring UV absorbance at 260 nm. After treatment with Turbo DNase (RNase free), 0.5 µg of each total RNA sample was reverse-transcribed into cDNA using SuperScript™ II reverse transcriptase (Invitrogen), following the manufacture's procedure. Briefly, 0.5 µg of each total RNA sample was mixed with 300 ng random primers and 1 µL dNTP (10 mM each) to make a solution of 12 µL. The mixture was incubated at 65 $^{\circ}$C for 5 min and quickly chilled on ice. Then 4 µL 5X first strand buffer, 2 µL 0.1 M DTT and 1 µL RNaseOUT™ were added and the mixture was incubated at 25 $^{\circ}$C for 2 min. Then 1 µL of the SuperScript™ II RT was added to the mixture, incubated at 25 $^{\circ}$C for 10 min and then at 42 $^{\circ}$C for another 50 min. The reaction was inactivated at 70 $^{\circ}$C for 15 min and the cDNA product was diluted 2500 fold for RT-PCR reaction. To generate the cDNA standard, 0.5 µg mRNA prepared previously was reverse transcribed into cDNA using the same kit with exactly the same procedure. The resulting cDNA product was diluted in tenfold series. The cDNAs and standards were then mixed with Power SYBR Green RT-PCR master mix (Invitrogen) and the RT-PCR was performed on a Steponeplus™ real-time PCR system with the following profile: 1 cycle of 50 $^{\circ}$C for 2 min, 95 $^{\circ}$C for 15 min, then 40 cycles of 95 $^{\circ}$C for 15 s, 60 $^{\circ}$C for 30 s, and 72 $^{\circ}$C for 45 s. The primer used to amplify iNOS cDNA were d(TGGTGGTGACAAGCACATTT) and d(AAGGCCAAACACAGCATACC), and for the GAPDH cDNA, the primers were d(TGGAGAAACCTGCCAAGTATG) and d(GTTGAAGTCGCAGGAGACAAC). Each

well contained 25 μL reaction mixtures including 2.5 μL forward primer, 2.5 μL reverse primer, 2.5 μL double distilled water, 5 μL cDNA template and 12.5 μL Power SYBR Green RT-PCR master mix. The threshold cycle C_T was automatically set by the machine. Standard curve method was used to determine the absolute copy number of the iNOS mRNA in cells. Comparative C_T ($\Delta\Delta C_T$) was used to calculate the relative increase of the iNOS mRNA level compared to the GAPDH mRNA.

Strand-displacement by iNOS mRNA using fluorescent in situ hybridization (FISH)

Raw 264.7 cells were seeded in glass bottom plate (14 mm) at 10^5 per well, and cultured overnight in DMEM (without phenol red) containing 10% FBS, streptomycin (100 μg/mL) and penicillin (100 units/mL) at 37°C in a humidified atmosphere with 5% CO_2. Samples were then divided into treatment group and control group. Cells in the treatment group were stimulated with 1 μg/ml LPS and 300 ng/ml γ-IFN, and cultured for another 18 h. Cells in the control group were incubated for 18 h without stimulation. Cells in both groups were washed with PBS twice and fixed in solution containing 4% formaldehyde, 5 % acetic acid 0.9 % sodium chloride at 37 °C for 10 min. The fixed cells were then washed with PBS and treated with 0.1 % triton X-100 in PBS for 5 min. The samples were then washed with PBS once, post fixed with 3% formaldehyde in PBS solution for 5 min, and washed with 2X SSC twice. After that, cells were dehydrated with series of ethanol (70%, 80%, 90%, and 100%) and air dried. Samples were then incubated with 150 μL Na-Hepes solution containing 0.2 μM matched or mismatched PNA-FAM/ DNA-Dabcyl^{plus} (1:2) probes for 60 min at 37 °C, washed with 2X SSC. The fluorescence of the samples was then observed by Nikon A1 confocal microscope. The fluorescent

images were processed by image J software. The mean fluorescence per cell is calculated by integrating the signal intensity of the regions of interest, then having it divided by the number of cells in the regions of interests.

Strand-displacement by mRNA in living cells

RAW 264.7 cells were seeded on 10 mm glass bottom dish (MatTek) at 5×10^4 per well and incubated overnight until they were 70% confluence. The cells were then washed with PBS and incubated in 1 mL media containing 1 µg/mL LPS, 0.3 µg/mL γ-IFN for 18 h at 37 °C in a humidified atmosphere with 5% CO_2. As for the control, cells were incubated under the same conditions without LPS and γ-IFN. Matched and mismatched PNA-FAM/DNA-Dabcyl^{plus} (1:1.25) probes were annealed in 25 µl OPTI-MEM for each sample and mixed with cSCK nanoparticles. The mixture was incubated at room temperature for 20 min to let the cSCK associate with PNA-FAM/DNA-Dabycl^{plus} and was added to 75 µl DMEM medium containing 10% FBS and without antibiotics. Cells were then washed with PBS and incubated with the 100 µl medium containing the cSCK complexes. To keep inducing the iNOS mRNA, LPS and γ-IFN were added at 1 µg/mL and 0.3 µg/mL concentration respectively. The final concentration of the PNA-FAM and the DNA-Dabcyl^{plus} in each sample solution was 0.4 µM and 0.5 µM. The concentration of cSCK was 9.7 µg/ml. The N/P ratio, which is the number of amines (positive charges) on the nanoparticles over the number of phosphate groups (negative charges) on the DNA backbone was 8:1. After 24 h of incubation, the fluorescent images of the cells were collected by Nikon A-1 confocal microscope. The fluorescent images were processed by image J software and were undertaken the same analysis as for the ones in the FISH experiment.

RESULTS AND DISCUSSION

Sequence design and synthesis of the PNA-FAM probes

PNA is a DNA analog that has a peptide backbone. Compared to regular DNA, it has many advantages, such as higher affinity to a complementary strand, greater resistance to many enzymes, and better specificity for targets [23]. Therefore, it is a good probe for antisense binding and imaging. Because PNA is a neutral molecule, it has poorer water solubility compared to DNA. We have designed a 23 base pair PNA which is antisense to iNOS mRNA position 473-494 (with one base at 5' end mismatched to the mRNA) (**Table 3.1**). The sequence was selected according to our lab's published results on mapping of the iNOS mRNA accessible sites [24]. We chose fluorescein as the fluorophore and Dabcyl^{plus} as the quencher on the complementary strand. We employed a 17-mer DNA strand as the quenching strand. The length of the quenching strand was determined by two factors: 1. The T_m of the duplex under physiological conditions is around 68 ^{o}C (Appendix **Figure A 3.1**), so it is stable under normal physiological conditions. 2. The specificity of the probe. We used the Basic Local Alignment Search Tool (BLAST) to verify the specificity of the PNA probe for iNOS mRNA, and found that 14 bases are antisense to the nucleoredoxin-like protein 1-like and myosin VA (Myo5a) mRNA (**Table 3.2**). Since the quencher strand is a 17-mer, it shouldn't be displaced by the non-targeting mRNA. We also knew that the fluorescence of fluorescein can be influenced by the oligodeoxynucleotide's primary and secondary structures [25, 26] and in particular that a G base opposite to fluorescein can quench up to 90% of its fluorescence [27]. To take the advantage of this quenching effect, we designed our PNA probe to have a C at the 5' end, to be complementary to a G in the quencher strand at the

3' end, which is mismatched to the mRNA sequence. When the PNA probe hybridizes to the quencher strand, the G base on the 3' end of the quencher strand enhances the quenching effect, but when the mRNA displaces the quencher strand, the C at the 5' end of the PNA would be opposite to an A base on the mRNA, which will not quench the fluorescence of the fluorescein. As for the control, we have synthesized a 23-mer PNA that is antisense to the pLuc 705 cell correct splicing site, which has been shown by BLAST not to specifically target any mouse mRNAs. The sequences of the probes and their MALDI results are shown in **Table 3.1.** For details about the characterizations of the probes, please refer to Appendix **Figures A3.2-A3.6.**

Displacement of the quencher probe by complementary DNA

We first tested the strand-displacement reaction by using complementary ODNs, which have 21 base pairs matched with the PNA probes, whereas the quencher ODNs only have 17 base pairs matched with the PNA probes. Noting that the PNA has strong secondary structure at 37 ^{o}C, the concentration of the PNA probe was measured by UV absorbance at 260 nm at 70 ^{o}C. As a positive control, the 21-mer ODNs were hybridized with PNA probes without the quencher strand. From **Figure 3.2**, we can see that the quencher ODN can quench 90% of the fluorescence of the PNA480-FAM. By adding the 21-mer cDNA to the quenched probe, 80% of the fluorescence could be recovered. In the mismatched control group, adding the complementary 21-mer ODN did not recover the fluorescence of the mismatched probe. All the measurements were done in triplicate and the average of the fluorescence emission is shown in **Figure 3.2** a and b. The reaction kinetics has also been measured and shown in **Figure 3.2** c. The results clearly indicate that the strand-displacement probe is able to effectively detect the target ODN in solution

Displacement by *in vitro* transcribed mRNA

Unlike the model target ODN, *in vitro* transcribed iNOS mRNA has around 4000 nucleotides (Appendix **Figure A3.7**), and a complicated secondary structure. Studies in our lab have shown previously that the iNOS mRNA is accessible to 480 PNA probe, and the probe has high binding affinity to the *in vitro* transcribed mRNA. Also, siRNA knockdown and PNA antisense inhibition experiments verified the accessibility of the 480 site [24]. We first tested whether the iNOS mRNA can displace the quencher strand in the absence of secondary structure. We mixed the probes together with the mRNA and heated the mixture to 65 ^{o}C for 1 min to disrupt the secondary structure of the mRNA. When heated, the mRNA will become unfolded and accessible to the probes in the solution. From **Figure 3.3** a and b, It is clear that after 15 min of incubation at 37 ^{o}C, the mRNA can displace the quencher DNA strand, restoring the fluorescence of the matched probe. For the mismatched probe, heating and cooling the mixture doesn't increase the fluorescence, which means the PNA480-FAM probe is specifically targeting the iNOS mRNA.

We then tested the ability of the probe to detect mRNA at 37 ^{o}C. Different concentrations of mRNA were heated at 65 ^{o}C for 1.5 min to unfold them and then annealed at 37 ^{o}C for 15 min in 10 mM Tris buffer to refold. Probes annealed at high concentration (1 µM) were then added (20 fold dilution) to the mRNA solution in order to cause minimal volume change of the solution. The fluorescence of the mixture was monitored as a function of time at 37 ^{o}C by the fluorimeter. **Figure 3.3** c shows the rate

of strand-displacement triggered by different concentrations of the mRNA. When the concentrations of iNOS mRNA increased from 25 nM to 250 nM, which correspond to 0.5 to 5 times the concentration of the probe, both the rates of displacement and the fluorescence intensity of the mixture increased, consistent with a bimolecular displacement reaction of the quencher probe. For the mismatched probe, even in the presence of 100 nM mRNA (2 times of the concentration of the mismatched probe), there was only a slight increase of fluorescence. However, the strand-displacement rates with the mRNA are much slower compared to the reactions with the ODN, and the increase of fluorescence is only around 2.5 fold even when the mRNA is in 5 times excess. This may be due to the complex secondary structures of the mRNA in solution, which make the binding sites not fully accessible to the probe. This may also restrict the detection limit and signal to noise of the probe in cellular experiments.

qRT-PCR and absolute copy numbers of iNOS mRNA inside cells

mRNAs are usually expressed at very low level inside cells, ranging from tens to thousands of copies per cell [28]. The low copy number of mRNAs can be a problem for *in vivo* mRNA imaging because the signal generated will be very low and hard to be distinguished from background noise. So far, antisense imaging by fluorescently labeled probes are still limited to relatively abundant transcripts [29]. Expression of iNOS mRNA, on the other hand, can be stimulated greatly by LPS and γ-IFN, making it a good target for antisense imaging. To our best knowledge, the actual copy number of iNOS mRNA inside cells following stimulation has never been reported. To determine the copy numbers for iNOS mRNA imaging in living cells, we performed a qRT-PCR for

stimulated and non-stimulated RAW 264.7 cells. The stimulated cells were treated by LPS/γ-IFN for 6 and 18 h. The *in vitro* transcribed iNOS mRNA was used to generate a standard curve, and the housekeeping gene glyceraldehyde 3-phosphate dehydrogenase (GAPDH) was used as an internal control to determine the relative increase of iNOS mRNA. **Figure 3.4** shows the average absolute copy numbers per cell in both stimulated and non-stimulated cells. The copy number for non-stimulated cells was 760 per cell, after 6 h of treatment, the mRNA copy number was as high as 53,000 per cell, and for cells stimulated for 18 h it was 76,000 per cell.. Thus the iNOS mRNA increased about 100 fold upon stimulation for 18 h. This large number of transcripts inside stimulated cells makes the iNOS mRNA an ideal target for antisense imaging. Meanwhile, the $\Delta\Delta C_T$ method using GAPDH control also showed 96 fold increase for the iNOS mRNA after cells being stimulated for 18 h. This confirms the reliability of the results obtained from the standard curve method.

Fluorescence in situ hybridization (FISH)

Nucleic acid probes are known to have little cell permeability and require extra effort to be delivered into the cytoplasm where they can hybridize to the target mRNA [30]. In order to test the ability of the probes to work independently of the delivery problem, we examined their ability to detect the iNOS mRNA under fluorescence in situ hybridization (FISH) conditions. FISH is a 30-year-old technique to detect DNA/RNA in cells or tissue samples, which are fixed onto glass slides with formaldehyde or methanol. Samples are then treated with enzymes such as pepsin or detergents such as triton X-100 to destroy the cell membrane to increase their permeability. FISH has been widely

utilized to image mRNAs and to detect mRNA at the single molecule level [31]. In order to achieve the best sensitivity, fixation protocols and hybridization buffers have to be optimized.

Herein we modified a protocol reported by Van de Corput et al [32] and employed by many researchers to detect mRNA using nucleic acid probes [33, 34]. In FISH experiments, blocking reagents such as sheared salmon sperm DNA are usually added to the hybridization buffer to block the nonspecific binding sites. However, we did not use a blocking reagent because the strand-displacement should only "switch-on" when bound to the target mRNA. Raw 264.7 cells were fixed and hybridized to the PNA/DNA probes as described in experimental section. Each sample of cells was scanned in xyz mode, and the picture of each layer was integrated to determine the fluorescence of the cells. From **Figure 3.5** we can see that cells treated with LPS/γ-IFN show bright green fluorescence in the cytoplasm of cells. The mismatch probe shows no significant green fluorescence, indicating that the strand-displacement probe is specific to target mRNA in fixed cells. The punctate pattern indicates that the iNOS mRNA is dispersed inside cytoplasm. Non-stimulated cells, however, are also fluorescent. This fluorescence may be caused by fluorescent compounds produced in the fixation process, or from the basal level of iNOS mRNA in the non-stimulated cells.

Figure 3.5 shows the difference in fluorescence per cell for stimulated and non-stimulated cells using PNA480-FAM probe. The measured difference is 3.6 (±1.8)-fold which is 25-fold less than expected based on the RT-PCR assay for iNOS expression under stimulated and non-stimulated conditions. The lower than expected ratio for the strand-displacement probe may be attributed to both nonspecific binding of the probe and

the loss of mRNA or probe during the washing steps in the FISH protocol. Although all of the solutions used were treated with DEPC before use, it is quite possible that some RNA molecules were not fixed on to the glass surface and were washed off during the washing steps. The different results between RT-PCR and FISH reflect the pros and cons of the two methods. FISH can be used to image the mRNA in fixed cells, and show the location and distribution of the mRNA. However, the high detection limit and low signal to noise ratio restricts its usefulness for quantitative determination of mRNA copy number. Real-time PCR on the other hand, has the advantage of quantitatively determining mRNA copy numbers at very low levels. It is also more reliable and reproducible, but does not give any information on the spatial location of the mRNA and is time consuming. These two methods are complementary to each other and may be used as a combination to study mRNA concentration and distribution in cells.

Strand-displacement imaging of mRNA in living cells

Cellular delivery of nucleic acid probes has always been a major problem for antisense imaging. One way to deliver PNA into cells is to hybridize the PNA with negatively charged DNA and complex them with cationic nanoparticles [35]. The PNA/DNA duplex will associate with nanoparticles via electrostatic interactions and enter cells via endocytosis. Here we used cationic shell-cross-linked knedel-like (cSCK) nanoparticles to deliver the PNA/DNA probes into the cells. The cSCK nanoparticles were developed by our collaborator Professor Karen Wooley, and have been shown to be able to deliver PNA/DNA and siRNA into cells effectively [36]. We expected that the probes would remain quenched until the quencher strand on the matched probe was

displaced by the iNOS mRNA inside cells. **Figure 3.6** shows the results of our living cells imaging following optimization of the concentrations of both the probes and cSCK nanoparticles. For cells treated with LPS/γ-IFN, and matched probes, there was bright fluorescence inside the cytoplasm, indicating hybridization of the probes to the mRNA. For cells not treated with LPS/γ-IFN and cells treated with LPS/γ-IFN but with mismatched probes, there is little observable fluorescence. Quantification of the fluorescence indicates that there was a 16.6 ($\pm$ 7.9)-fold increase in fluorescence of the cells treated with LPS/γ-IFN than in cells without treatment. Stimulated cells treated with mismatched probes however, also showed 4.1 ($\pm$ 2.3)-fold increase in fluorescence compared to nonstimulated cells. The difference of fluorescence between stimulated and nonstimulated cells presumably indicated the different expression level of iNOS mRNA in living cells, however, the LPS/γ-IFN treatment might also affect the delivery efficiency of cSCK nanoparticles in two groups of cells. **Figure 3.6** shows that cells treated with stimuli are larger than cells not stimulated (about twice in diameter). Such change of morphology may also be companied with an enhance internalization of the cSCK nanoparticles, which can bring more probes into cells. To further study the difference of cSCK uptake in cells under various conditions, fluorescently labeled cSCK nanoparticles that emit at different wavelengths from the probes need to be used. This dual labeling strategy will also enable us to study the endosomal trapping and release of the nanoparticles and PNA probes. Another concern is the degradation of the ODN quenchers which might cause false positive fluorescent signal. However, it has been reported that PNA/DNA chimeras are resistant to enzymatic degradations in cell extract and serum [37]. We believe that hybridizing a DNA to a PNA, and forming complexes

94

with cSCK nanoparticles will protect the DNA from enzymatic degradation. Our lab's unpublished data have shown that mixing siRNA with cSCK nanoparticles can protect the siRNA from degradation in serum. The difference of fluorescence between stimulated cells treated with matched and mismatched probes (around 4-fold) indicates that after 24 hours of incubation, probes can still be protected from total degradation, however, a small proportion of mismatched probes had opened up, presumably because of probe degradation or nonspecific binding. Compared to the RT-PCR method, the strand-displacement activated probes delivered by cSCK nanoparticles can be used to image the mRNA in living cells, but further optimization will be needed to quantify the iNOS mRNA, mainly because of the undetermined efficiency of cellular delivery of cSCK nanoparticles and the stability of the probes in cellular environment.

CONCLUSIONS

We have investigated the use of strand-displacement activated PNA probe to image iNOS mRNA in solution, in situ, and in living cells. A 23-mer PNA antisense to the iNOS mRNA was conjugated to a fluorescein, whose fluorescence was quenched by a Dabcyl^{plus} quencher on the 17-mer complementary DNA. We investigated the displacement reaction *in vitro* with a short DNA target and with transcribed mRNA and shown that such displacement probes can be used to image the iNOS mRNA by fluorescence in situ hybridization. We used qRT-PCR to determine the copy number of the iNOS mRNA under stimulation and found that after 18 h of stimulation, the mRNA can increase up to 100 fold and the absolute copy number can reach as high as 75,000 copies per cell. However, the FISH experiment only detected a 3.6 ($\pm$1.8)-fold increase in the iNOS mRNA. This difference may be due to the nonspecific binding of the strand-

displacement probes, as well as the loss of target mRNA during the washing steps in FISH experiment. We also investigated live cell imaging of iNOS expression using cSCK nanoparticles as delivery agents. We have showed that the strand-displacement activated PNA probes delivered by cSCK nanoparticles can be used to image iNOS mRNAs. We observed a 16.6 ($\pm$ 7.9)-fold increase in iNOS expression for the stimulated cells. However, compared to the RT-PCR method, the strand-displacement probes appear to be less accurate in quantifying the mRNAs inside living cells, possibly because of the lack of efficient delivery, entrapment in endosomes, and nonspecific binding due to the complex cellular environment.
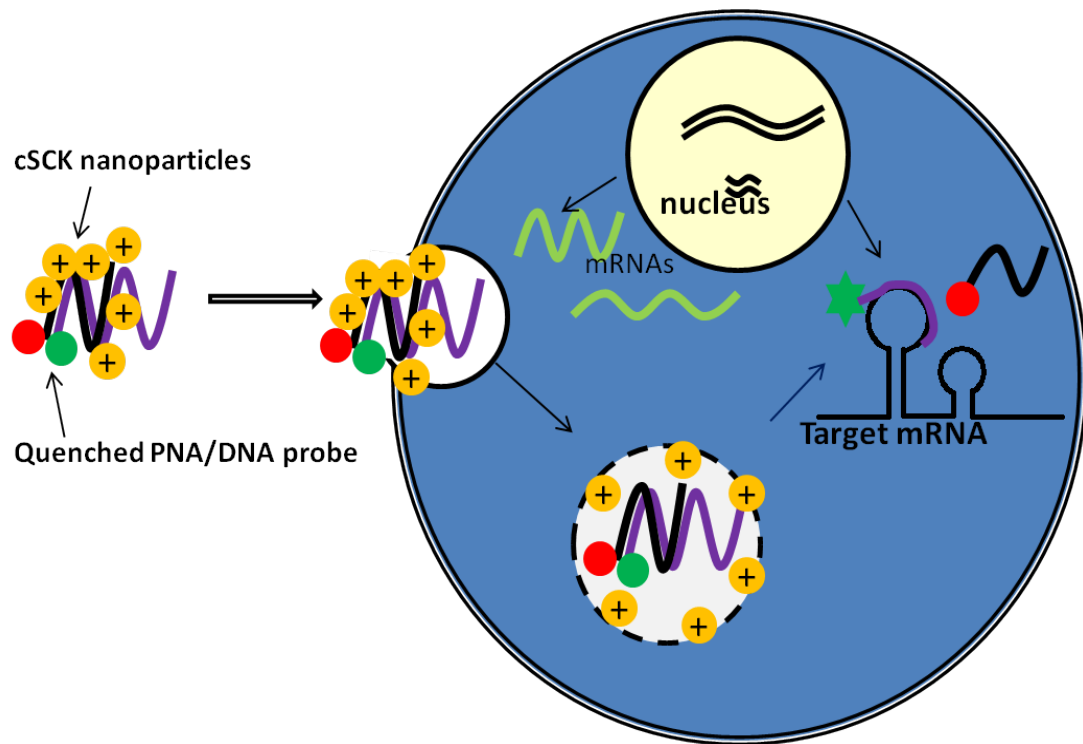
Figure 3.1: Schematic representation of cSCK mediated strand-displacement activated PNA probes to image mRNA in living cells.

a. Matched probe

b. Mis-matched probe

c. Strand-displacement kinetic with 480 cDNA.
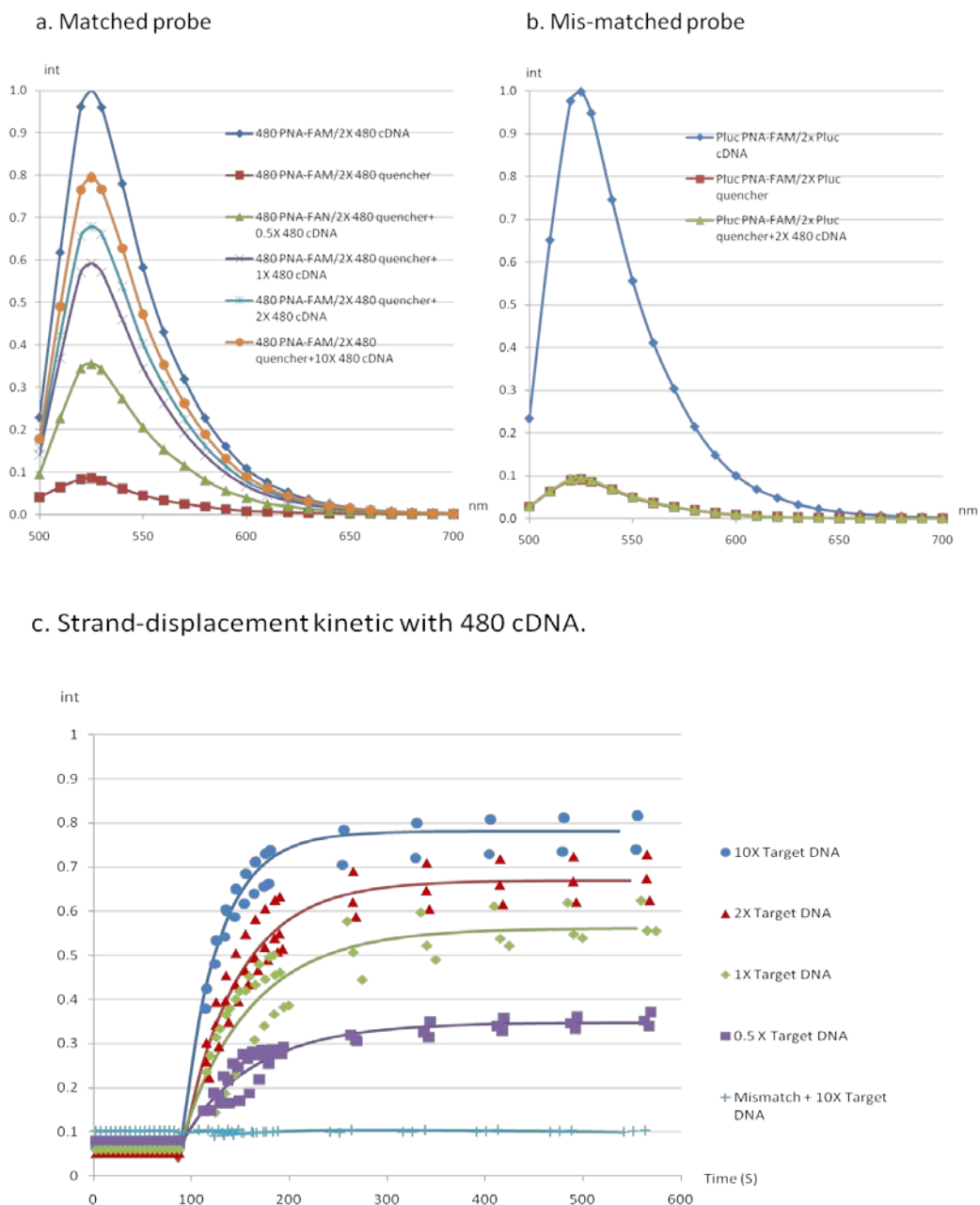
Figure 3.2: Strand-displacement by DNA target in solution. (a) 0.2 μM 480 PNA-FAM (matched) annealed to 0.4 μM 480 quencher DNA. The 480 cDNA were added at 0.1, 0.2, 0.4 and 2 μM concentrations. Positive control: 0.2 μM 480 PNA-FAM annealed to 0.4 μM 480 cDNA. (b) 0.2 μM pLuc PNA-FAM (mismatched) annealed to 0.4 μM pLuc quencher DNA. The 480 cDNA was added at 0.4 μM. Positive control: 0.2 μM pLuc PNA-FAM annealed to 0.4 μM pLuc cDNA. (c) Reaction kinetics. Buffer: 100 mM Tris-HCl, 5mM $MgCl_2$, pH=7.10. Excitation wavelength: 488 nm. Temperature: 37 ^{o}C.
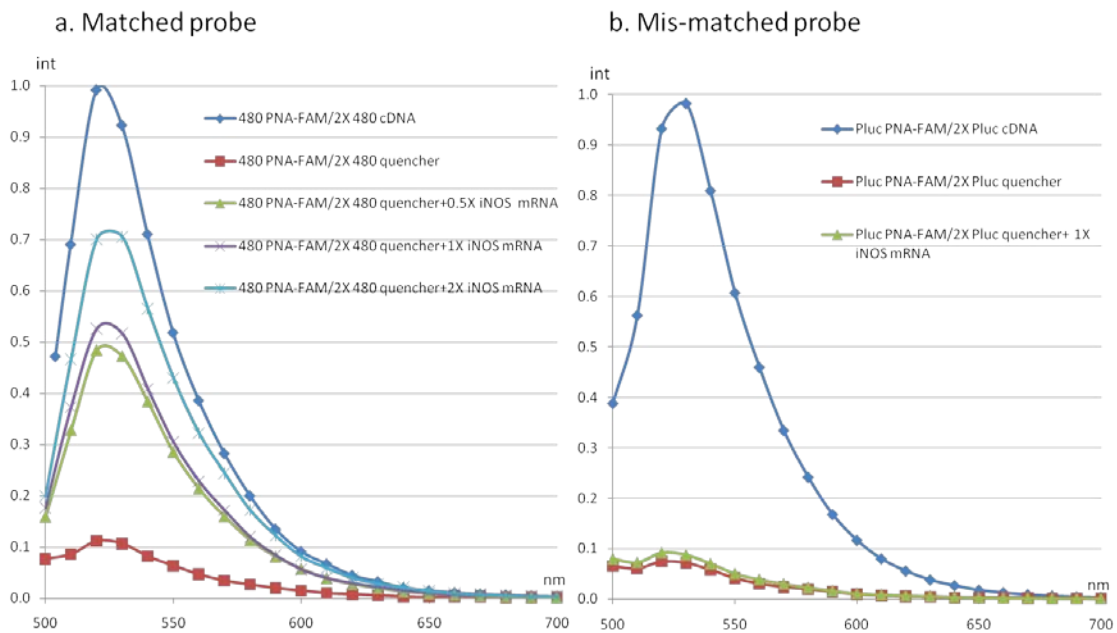
Figure 3.3: Strand-displacement by in vitro transcribed iNOS mRNA in solution. (a) 0.2 μM 480 PNA-FAM (matched) annealed to 0.4 μM 480 quencher DNA. The iNOS mRNA was added at 0.1, 0.2, and 0.4 μM respectively. Positive control: 0.2 μM 480 PNA-FAM annealed to 0.4 μM iNOS mRNA. (b) 0.2 μM pLuc PNA-FAM (mismatched) annealed to 0.4 μM pLuc quencher DNA. The iNOS mRNA was added at 0.4 μM. Buffer solution: 0.1 M KCl, 5 mM $MgCl_2$, 10 mM Na-Hepes. pH=7.11. Solutions were heated at 65 ^{o}C for 1 min and incubated at 37 ^{o}C for 15 min.

c. Strand-displacement kinetics with iNOS mRNA
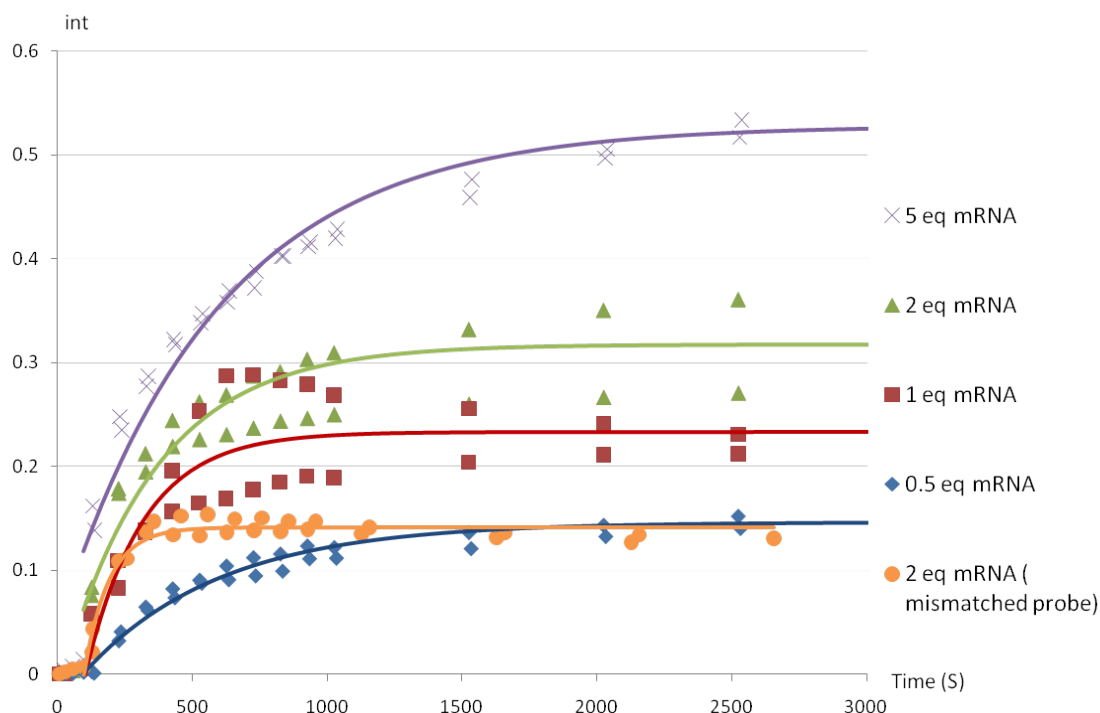
Figure 3.3: Strand-displacement by *in vitro* transcribed iNOS mRNA in solution. (c) Reaction kinetics. 0.05 μM 480 PNA-FAM (matched) or pLuc PNA-FAM (mismatched) was annealed to 0.1 μM 480 quencher DNA or pLuc quencher DNA. The iNOS mRNA was added at 0.025, 0.5, 0.1 and 0.25 μM for different samples. Buffer: 10 mM Tris-HCl, pH=7.15. Excitation wavelength: 488 nm, emission at 525 nm. Temperature: 37 °C. All the curves were normalized and zeroed at their starting fluorescence.

a.

Standard Curve

$y = -3.5447x + 22.946$
$R^2 = 0.9983$
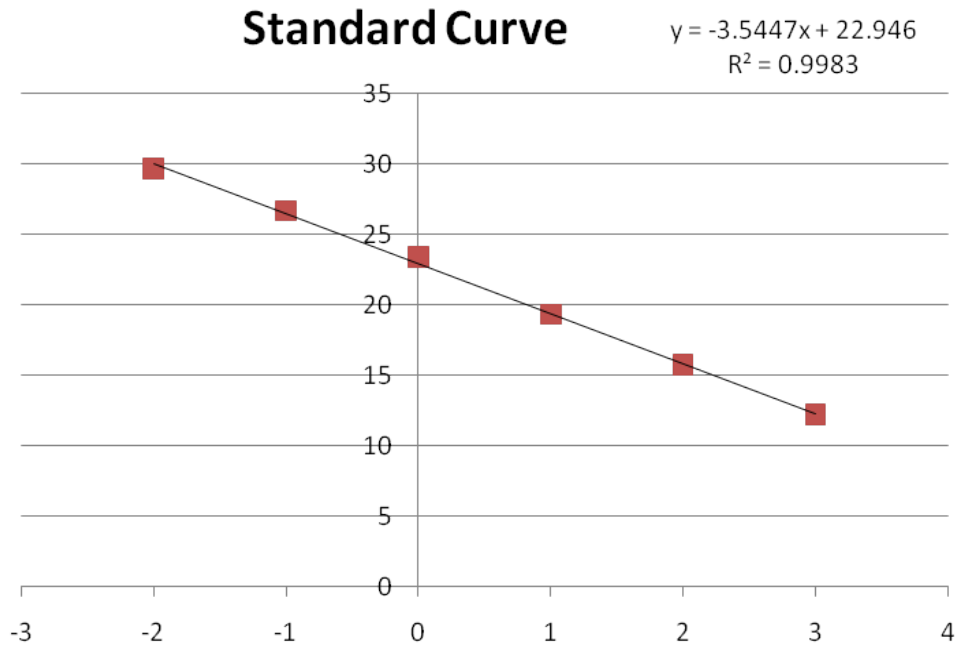
mRNA amount	1ng	0.1ng	0.01ng	1pg	0.1pg	0.01pg
Log n	3	2	1	0	-1	-2

b.

	Ct	Copy/Cell
Stimulated for 18 hrs	23.491 (±0.113)	**7.6×10^4** ($7.1 - 8.2 \times 10^4$)
Stimulated for 6 hrs	23.833 (±0.073)	**5.3×10^4** ($5.1 - 5.6 \times 10^4$)
Untreated	29.545 (±0.146)	**7.59×10^2** ($6.77 - 8.31 \times 10^2$)

c.

	Absolute RT-PCR (standard curve)	Relative RT-PCR ($\Delta\Delta C_T$)
Fold of increase after 18h	100	96
Fold of increase after 6 h	70	45

Figure 3.4: RT-PCR to determine the absolute copy numbers of iNOS mRNA in RAW 264.7 cells. Cells were treated with LPS and γ-IFN for 6 h or 18 h. Untreated cells were incubated under the same condition without stimuli. (a). Standard curve generated from known amount of *in vitro* transcribed mRNA. (b). Absolute copy number of iNOS mRNA in cells obtained from the standard curve. (c). Comparison of standard curve method and $\Delta\Delta C_T$ method to determine the relative increase of iNOS mRNA in cells.

Transmitted light   mRNA (Green, 488 nm)   Overlay

Stimulated cells matched probe

Stimulated cells mismatched probe

Nonstimulated cells matched probe

Stimulated

Nonstimulated

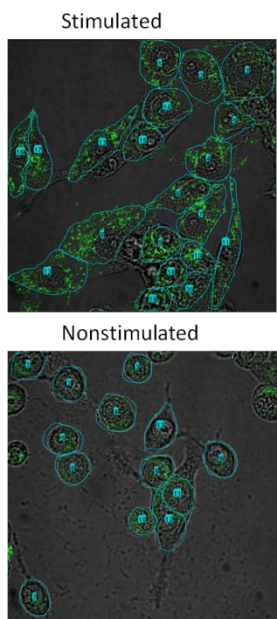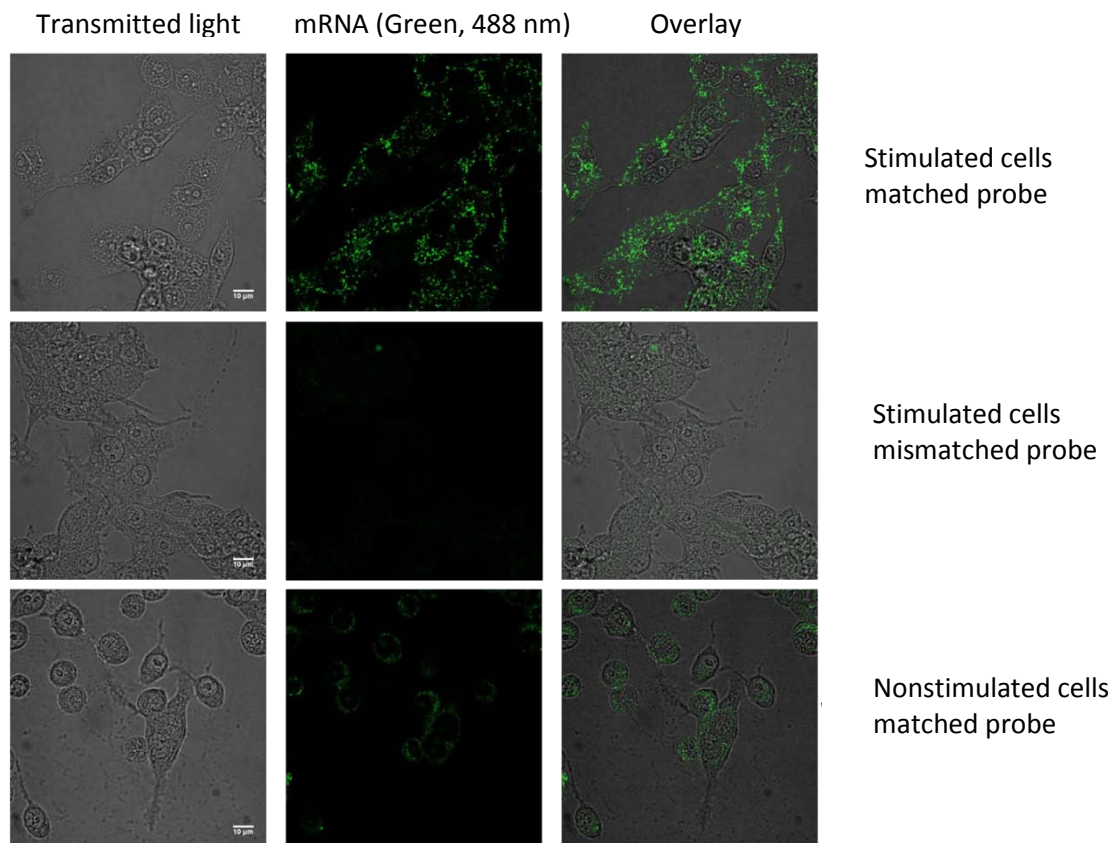Average Fluorescence (per cell)
increase: 3.6 ± 1.8 fold
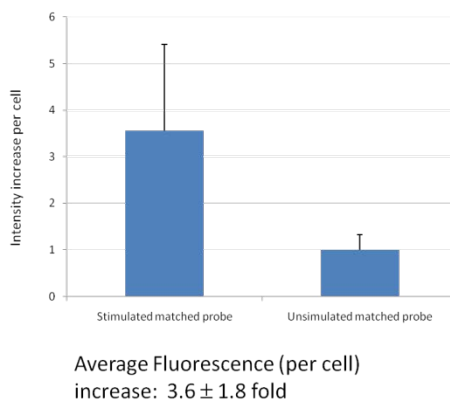
Figure 3.5: Fluorescence in situ hybridization (FISH) images of iNOS mRNA in RAW 264.7 cells and the quantitative analysis of fluorescence in selected regions of interests (ROIs).
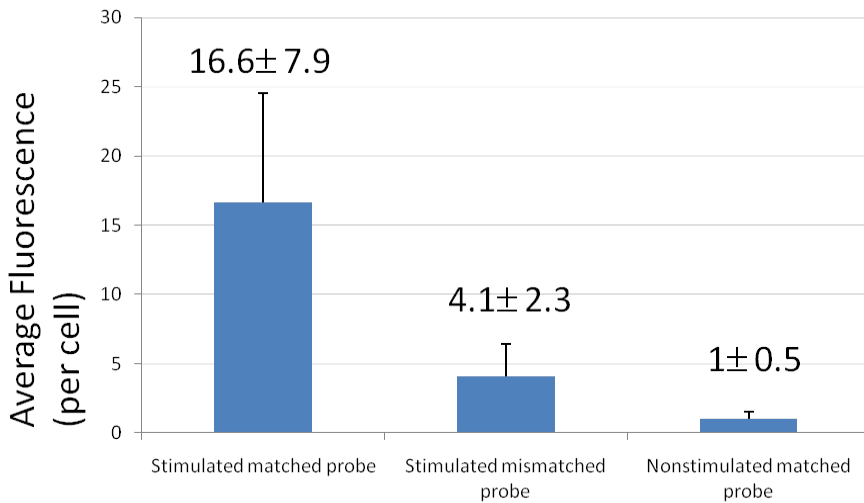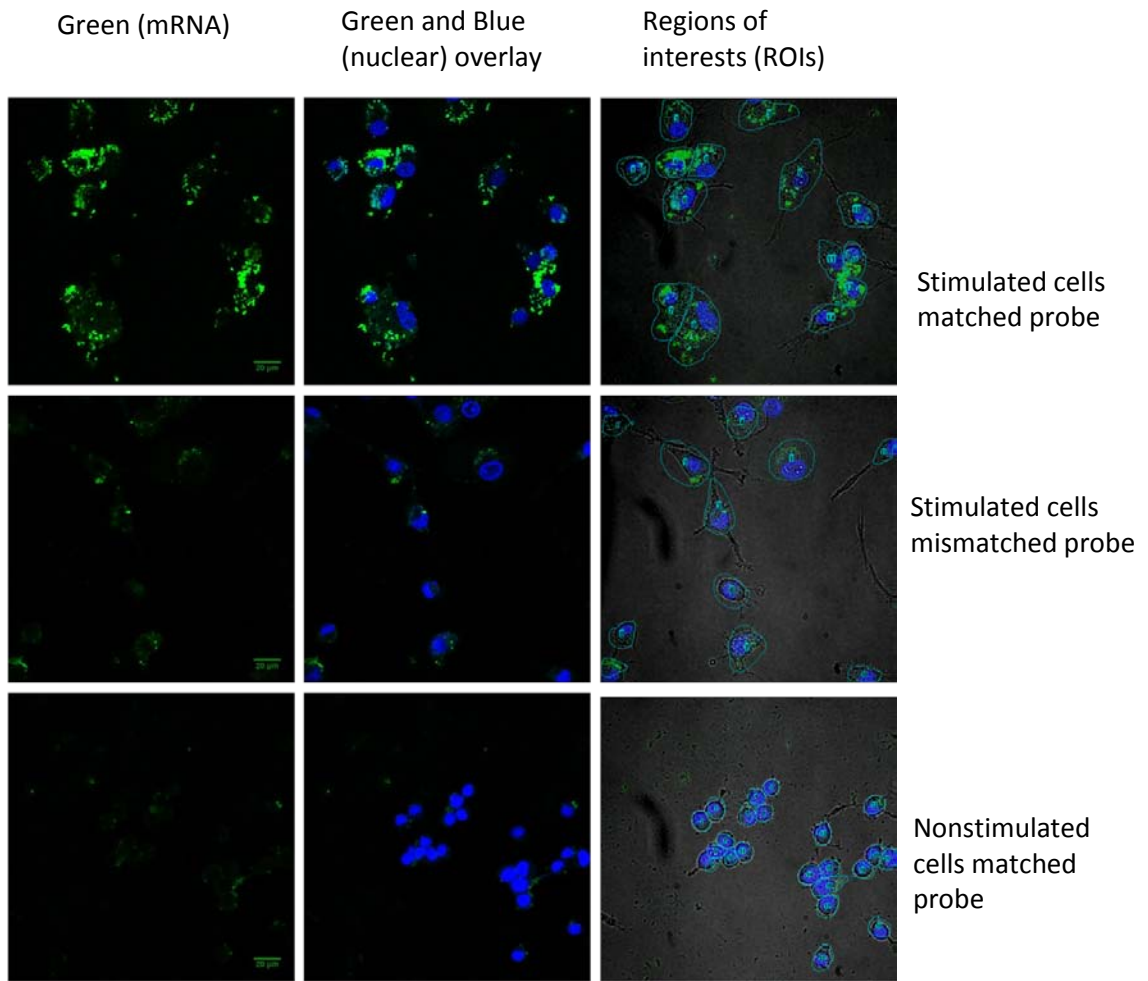
Figure 3.6: Confocal fluorescent images of iNOS mRNA in RAW 264.7 cells and the quantitative analysis of fluorescence in selected regions of interests (ROIs). For each sample, 0.4 μM PNA probe was delivered with 9.7 μg/mL cSCK nanoparticles. N/P=8:1. Green: FAM signal. Blue: Hoechst nuclear stain.

Probe name	Sequence	Calculated mass	Observed mass
480 PNA-FAM	5'-**FAM**-CCAAGTGAAATCCGATGTGGCCT-3'	6615.7	6620.5
480 DNA-Dabcyl^{plus}	5'-CATCGGATTTCACTTGG-**Dabcyl**^{**plus**}-3'	5748.1	5748.5
480 cDNA	5'-AGGCCACATCGGATTTCACTT-3'	6381.2	N/A
Pluc PNA-FAM	5'-**FAM**-CCACCTCTTACCTCAGTTACAAT-3'	6445.2	6444.5
Pluc DNA-Dabcyl^{plus}	5'-ACTGAGGTAAGAGGTGG-**Dabcyl**^{**plus**}3'	5886.2	5887.4
Pluc cDNA	5'-ATTGTAACTGAGGTAAGAGGT-3'	6549.3	N/A
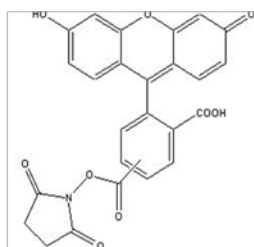
Fluorescein（5，6）(FAM)
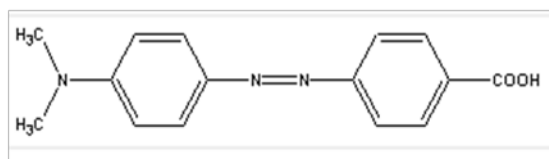
DABCYL (quencher)

Table 3.1: Sequence design, dye structures and MALDI results of the probes

Sequence name	Sequence complementary to 480 PNA-FAM probe	Number of matched base pairs
Mus musculus nitric oxide synthase 2 (iNOS) mRNA	PNA 2 CAAGTGAAATCCGATGTGGCCT 23 |||||||||||||||||||||| mRNA 494 CAAGTGAAATCCGATGTGGCCT 473	22
Mus musculus nucleoredoxin-like protein 1-like mRNA	PNA 10 ATCCGATGTGGCCT 23 |||||||||||||| mRNA 27 ATCCGATGTGGCCT 14	14
Mus musculus myosin VA (Myo5a), mRNA	PNA 3 AAGTGAAATCCGAT 16 |||||||||||||| mRNA 4645 AAGTGAAATCCGAT 4632	14

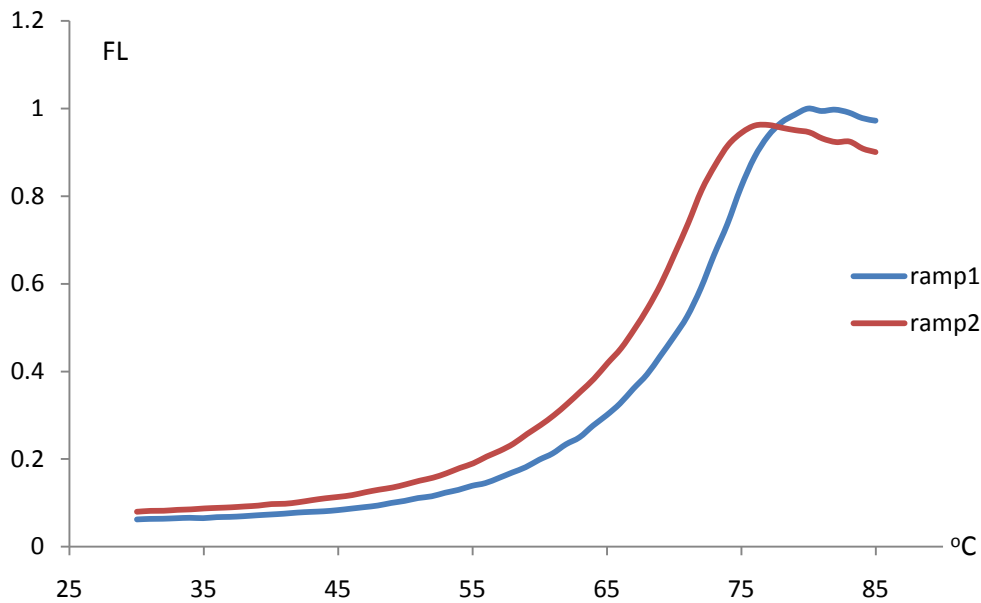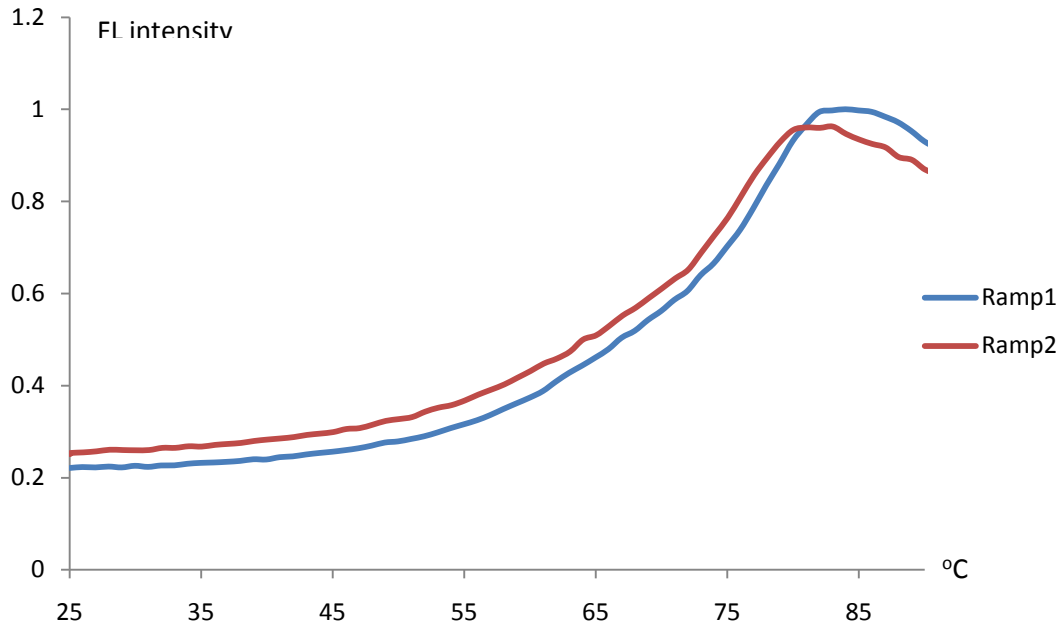**Table 3.2: BLAST results for 480 PNA-FAM probe**

Figure A 3.1: Tm measurement of 480 PNA-FAM/DNA-Dabcyl^{plus} (top) and pLuc PNA-FAM/DNA-Dabcyl^{plus} (bottom). 0.2 µM of probes were annealed in 100 mM Tris, 5mM MgCl$_2$ buffer. Fluorescence intensity of the probes was measured at excitation at 488 nm and emission at 525 nm.
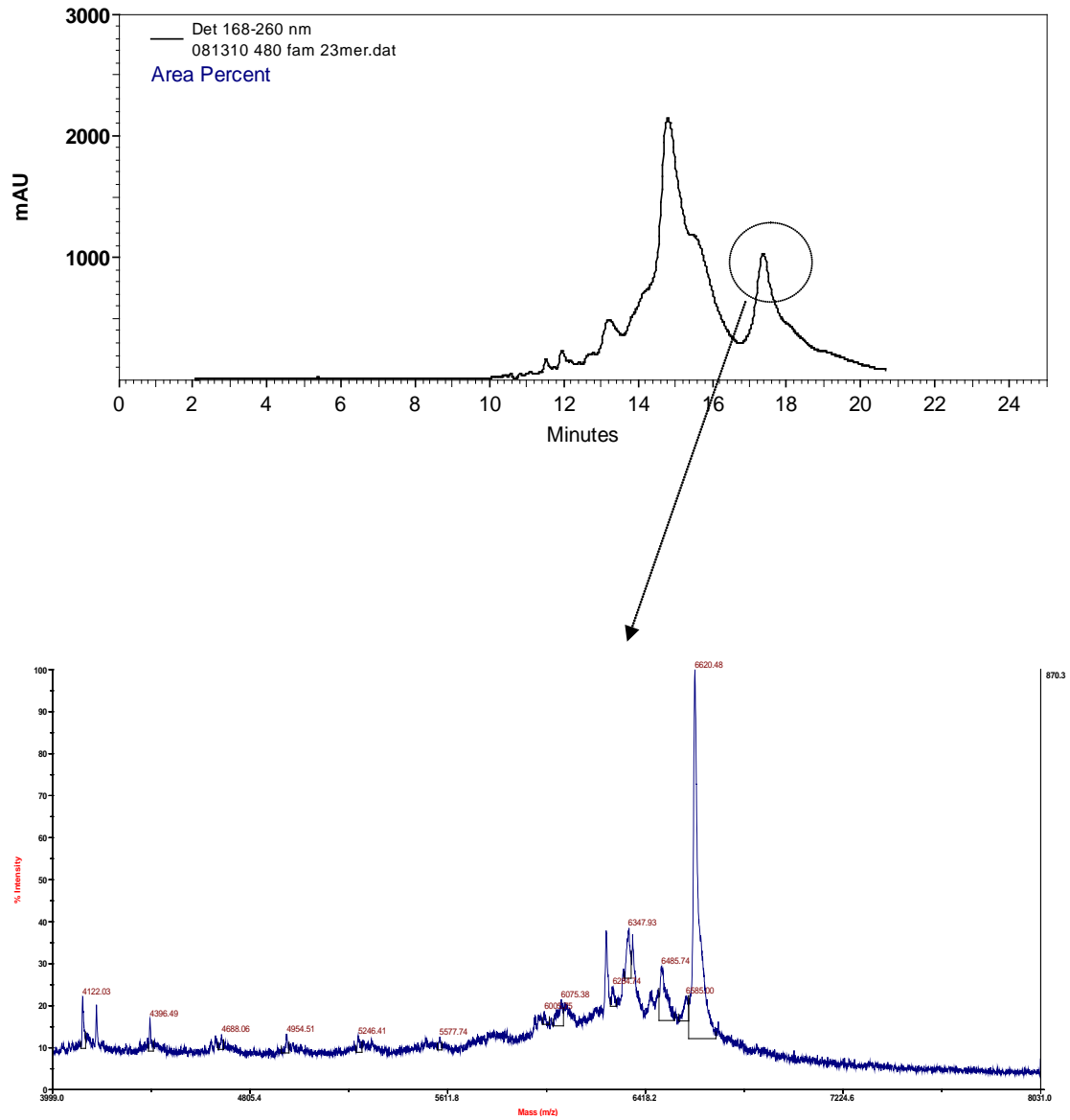
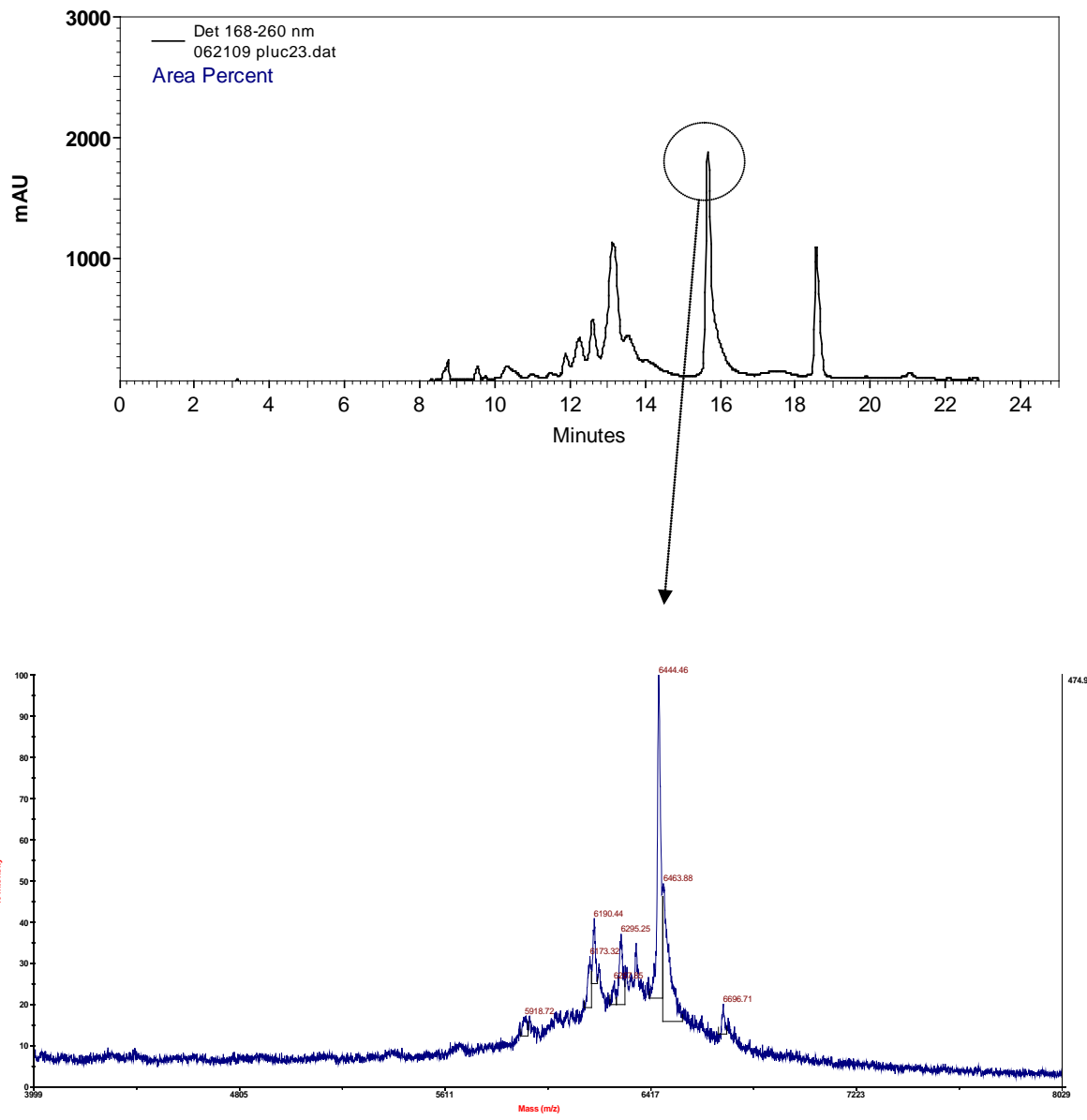**Figure A 3.2: HPLC trace and MALDI-TOF mass spectrum of 480 PNA-FAM.**

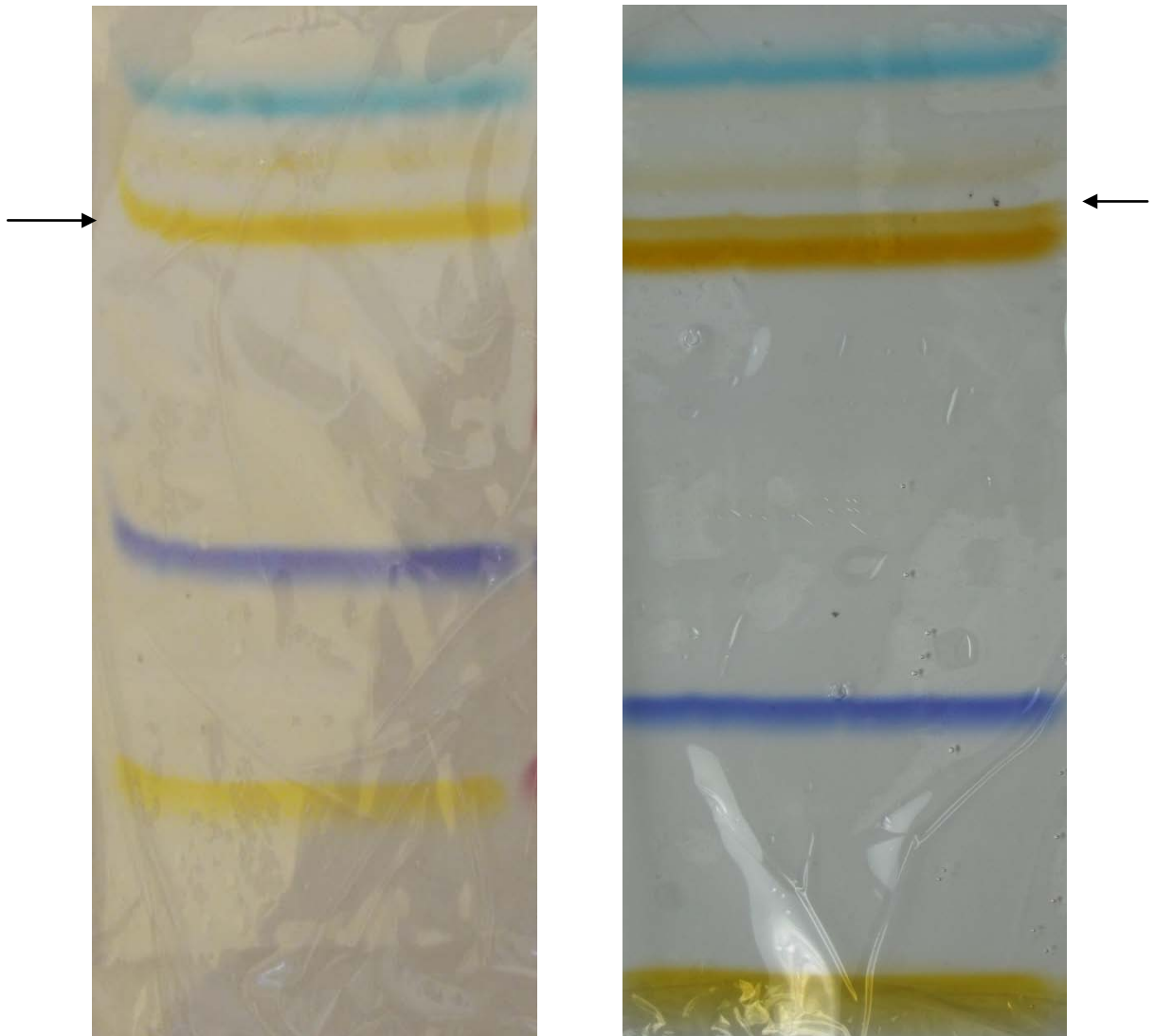**Figure A 3.3: HPLC trace and MALDI-TOF mass spectrum of pLuc PNA-FAM.**

Figure A 3.4: Separation of DNA-Dabcyl^plus by PAGE. Left arrow: 480 DNA-Dabcyl^plus. Right arrow: pLuc DNA-Dabcyl^plus.
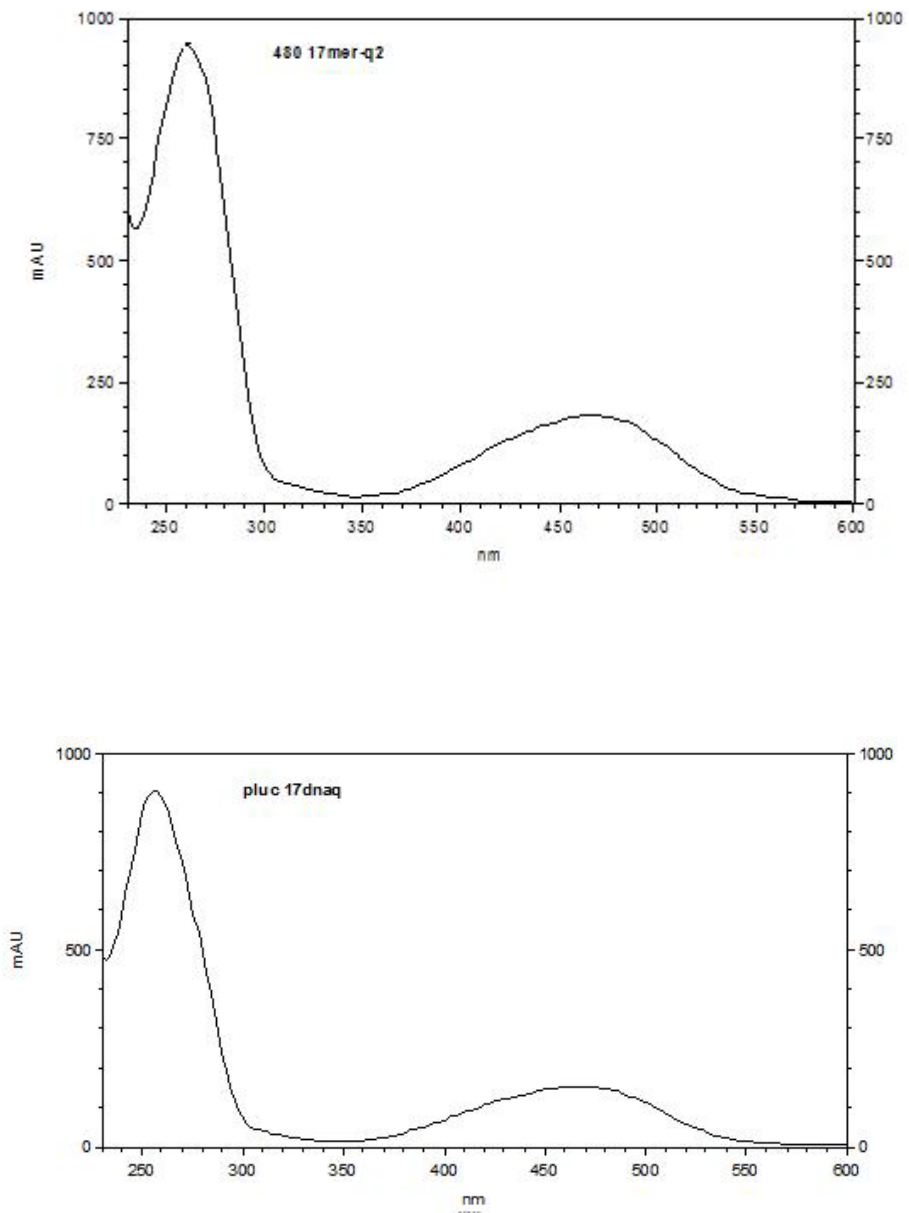
Figure A 3.5: Uv-Vis spectra of 480 DNA-Dabcyl[plus] (top) and pLuc DNA-Dabcyl[plus] (bottom).
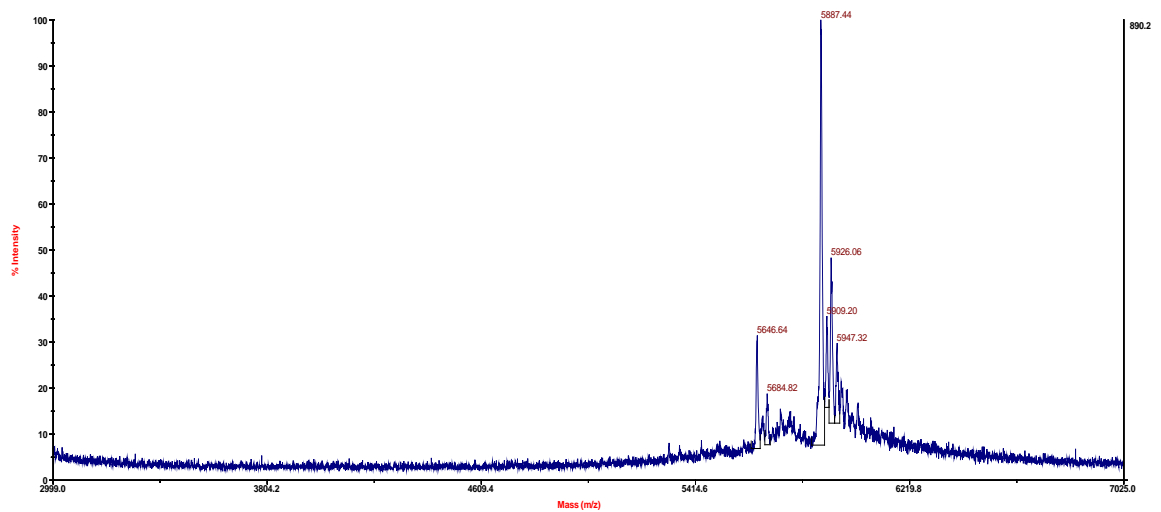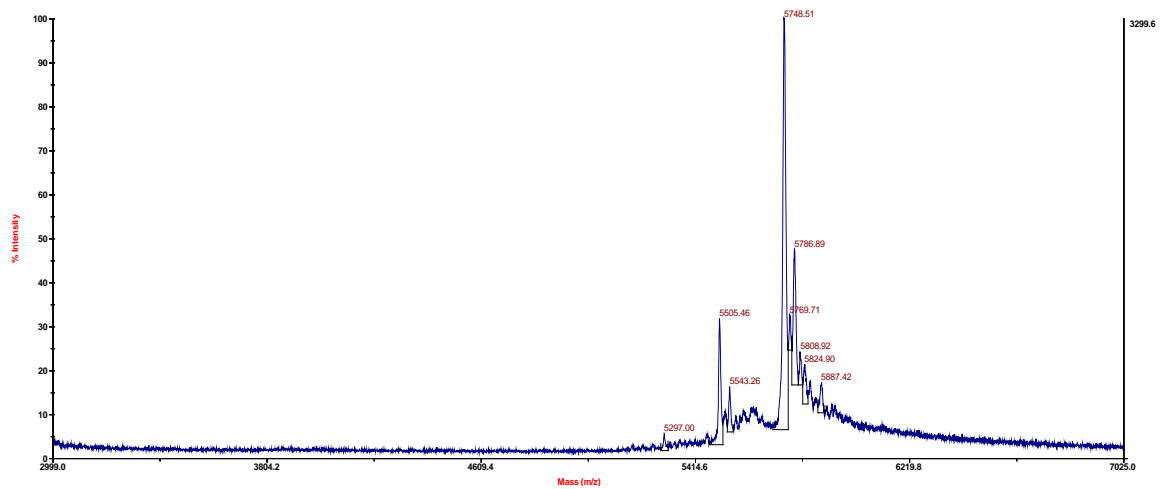
Figure A 3.6: MALDI-TOF spectra of 480 DNA-Dabcyl[plus] (top) and pLuc DNA-Dabcyl[plus] (bottom).
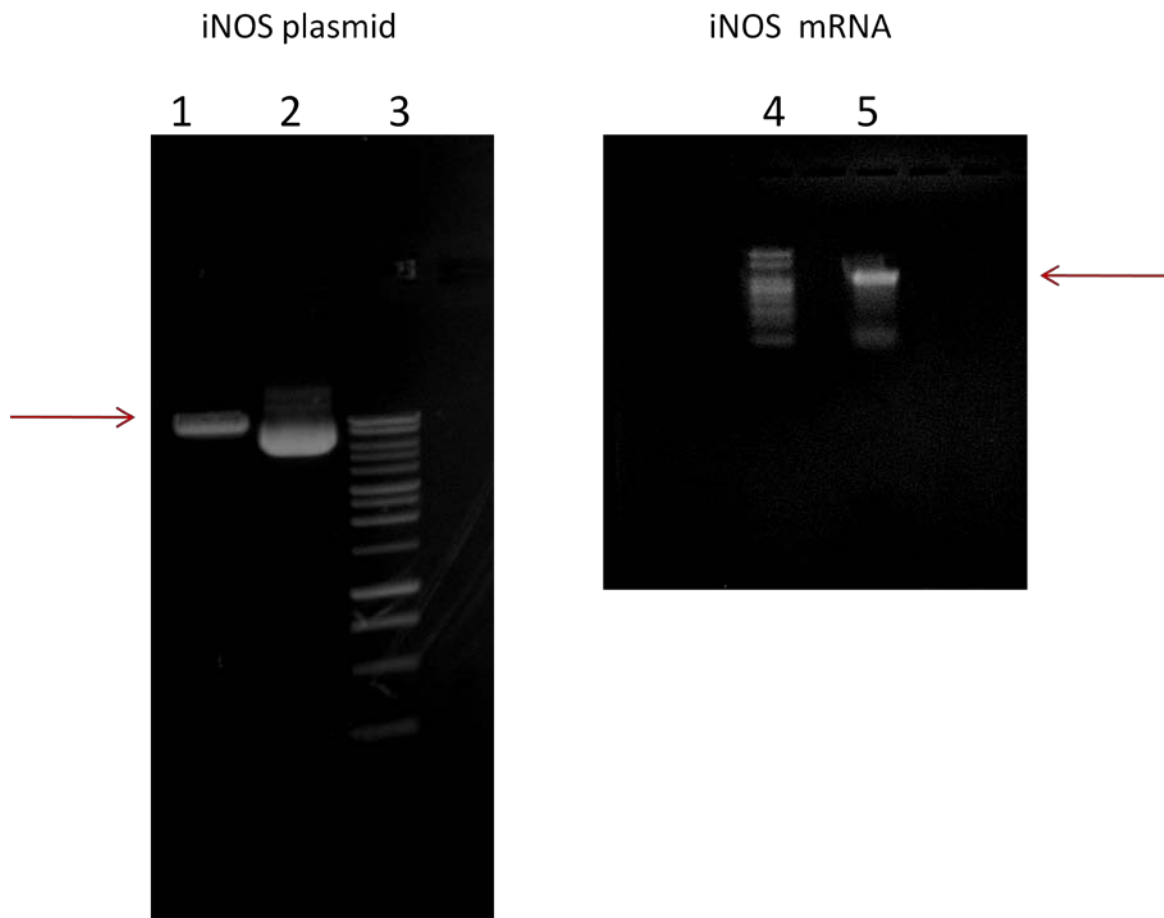
**Figure A 3.7: Gel electrophoresis image of iNOS plasmid and mRNA on
1% agarose gel.** Stained with ethidium bromide. Lane 1.iNOS plasmid after
enzyme digestion. 2. iNOS plasmid before enzyme digestion. 3. DNA
ladder. 4. RNA ladder. 5. *In vitro* transcribed iNOS mRNA.

References

1. Knowles, R.G. and S. Moncada, *Nitric oxide synthases in mammals.* Biochem J, 1994. **298 (Pt 2)**: p. 249-58.

2. Menshikova, E.B., N.K. Zenkov, and V.P. Reutov, *Nitric oxide and NO-synthases in mammals in different functional states.* Biochemistry (Mosc), 2000. **65**(4): p. 409-26.

3. Chiou, W.F., C.F. Chen, and J.J. Lin, *Mechanisms of suppression of inducible nitric oxide synthase (iNOS) expression in RAW 264.7 cells by andrographolide.* Br J Pharmacol, 2000. **129**(8): p. 1553-60.

4. Walker, G., J. Pfeilschifter, and D. Kunz, *Mechanisms of suppression of inducible nitric-oxide synthase (iNOS) expression in interferon (IFN)-gamma-stimulated RAW 264.7 cells by dexamethasone. Evidence for glucocorticoid-induced degradation of iNOS protein by calpain as a key step in post-transcriptional regulation.* J Biol Chem, 1997. **272**(26): p. 16679-87.

5. Sharma, K., et al., *Enhanced expression of inducible nitric oxide synthase in murine macrophages and glomerular mesangial cells by elevated glucose levels: possible mediation via protein kinase C.* Biochem Biophys Res Commun, 1995. **207**(1): p. 80-8.

6. Aktan, F., *iNOS-mediated nitric oxide production and its regulation.* Life Sci, 2004. **75**(6): p. 639-53.

7. Kroncke, K.D., K. Fehsel, and V. Kolb-Bachofen, *Inducible nitric oxide synthase in human diseases.* Clin Exp Immunol, 1998. **113**(2): p. 147-56.

8. Eskra, L., A. Mathison, and G. Splitter, *Microarray analysis of mRNA levels from RAW264.7 macrophages infected with Brucella abortus.* Infect Immun, 2003. **71**(3): p. 1125-33.

9. Farber, J.M., *A collection of mRNA species that are inducible in the RAW 264.7 mouse macrophage cell line by gamma interferon and other agents.* Mol Cell Biol, 1992. **12**(4): p. 1535-45.

10. Nahrevanian, H. and M.J. Dascombe, *Expression of inducible nitric oxide synthase (iNOS) mRNA in target organs of lethal and non-lethal strains of murine malaria.* Parasite Immunol, 2002. **24**(9-10): p. 471-8.

11. Sonoki, T., et al., *Detection of inducible nitric oxide synthase (iNOS) mRNA by RT-PCR in ATL patients and HTLV-I infected cell lines: clinical features and apoptosis by NOS inhibitor.* Leukemia, 1999. **13**(5): p. 713-8.

12. Han, B., et al., *Quantification of iNOS mRNA with reverse transcription polymerase chain reaction directly from cell lysates.* Nitric Oxide, 1999. **3**(4): p. 281-91.

13. Zhang, Y.M., et al., *In vitro investigations of tumor targeting with (99m)Tc-labeled antisense DNA.* J Nucl Med, 2001. **42**(11): p. 1660-9.

14. Shi, N., R.J. Boado, and W.M. Pardridge, *Antisense imaging of gene expression in the brain in vivo.* Proc Natl Acad Sci U S A, 2000. **97**(26): p. 14709-14.

15. Suzuki, T., et al., *Imaging endogenous gene expression in brain cancer in vivo with 111In-peptide nucleic acid antisense radiopharmaceuticals and brain drug-targeting technology.* J Nucl Med, 2004. **45**(10): p. 1766-75.

16.   Medarova, Z., et al., *In vivo imaging of siRNA delivery and silencing in tumors.* Nat Med, 2007. **13**(3): p. 372-7.

17.   Livak, K.J., et al., *Oligonucleotides with fluorescent dyes at opposite ends provide a quenched probe system useful for detecting PCR product and nucleic acid hybridization.* PCR Methods Appl, 1995. **4**(6): p. 357-62.

18.   Johansson, M.K., et al., *Intramolecular dimers: a new strategy to fluorescence quenching in dual-labeled oligonucleotide probes.* J Am Chem Soc, 2002. **124**(24): p. 6950-6.

19.   Li, Q., et al., *A new class of homogeneous nucleic acid probes based on specific displacement hybridization.* Nucleic Acids Res, 2002. **30**(2): p. E5.

20.   He, J., et al., *Optical pretargeting of tumor with fluorescent MORF oligomers.* Mol Imaging Biol, 2007. **9**(1): p. 17-23.

21.   Liang, M., et al., *Optical antisense tumor targeting in vivo with an improved fluorescent DNA duplex probe.* Bioconjug Chem, 2009. **20**(6): p. 1223-7.

22.   Seferos, D.S., et al., *Nano-flares: probes for transfection and mRNA detection in living cells.* J Am Chem Soc, 2007. **129**(50): p. 15477-9.

23.   Shakeel, S., S. Karim, and A. Ali, *Peptide nucleic acid (PNA) — a review.* Journal of Chemical Technology & Biotechnology, 2006. **81**(6): p. 892-899.

24.   Fang, H., Y. Shen, and J.S. Taylor, *Native mRNA antisense-accessible sites library for the selection of antisense oligonucleotides, PNAs, and siRNAs.* RNA. **16**(7): p. 1429-35.

25.   Nazarenko, I., et al., *Multiplex quantitative PCR using self-quenched primers labeled with a single fluorophore.* Nucleic Acids Res, 2002. **30**(9): p. e37.

26.   Nazarenko, I., et al., *Effect of primary and secondary structure of oligodeoxyribonucleotides on the fluorescent properties of conjugated dyes.* Nucleic Acids Res, 2002. **30**(9): p. 2089-195.

27.   Nazarenko, I., *Homogeneous detection of nucleic acids using self-quenched polymerase chain reaction primers labeled with a single fluorophore (LUX primers).* Methods Mol Biol, 2006. **335**: p. 95-114.

28.   Lewis, M.R. and F. Jia, *Antisense imaging: and miles to go before we sleep?* J Cell Biochem, 2003. **90**(3): p. 464-72.

29.   Bao, G., W.J. Rhee, and A. Tsourkas, *Fluorescent probes for live-cell RNA detection.* Annu Rev Biomed Eng, 2009. **11**: p. 25-47.

30.   Wittung, P., et al., *Phospholipid membrane permeability of peptide nucleic acid.* FEBS Lett, 1995. **375**(3): p. 27-9.

31.   Femino, A.M., et al., *Visualization of single RNA transcripts in situ.* Science, 1998. **280**(5363): p. 585-90.

32.   van de Corput, M.P. and F.G. Grosveld, *Fluorescence in situ hybridization analysis of transcript dynamics in cells.* Methods, 2001. **25**(1): p. 111-8.

33.   Choi, Y., et al., *In situ visualization of gene expression using polymer-coated quantum-dot-DNA conjugates.* Small, 2009. **5**(18): p. 2085-91.

34.   Blanco, A.M., et al., *A FRET-based assay for characterization of alternative splicing events using peptide nucleic acid fluorescence in situ hybridization.* Nucleic Acids Res, 2009. **37**(17): p. e116.

35.   Koppelhus, U. and P.E. Nielsen, *Cellular delivery of peptide nucleic acid (PNA).* Adv Drug Deliv Rev, 2003. **55**(2): p. 267-80.

36.   Zhang, K., et al., *Well-defined cationic shell crosslinked nanoparticles for efficient delivery of DNA or peptide nucleic acids.* Proc Am Thorac Soc, 2009. **6**(5): p. 450-7.

37.   Borgatti, M., et al., *Resistance of decoy PNA-DNA chimeras to enzymatic degradation in cellular extracts and serum.* Oncol Res, 2003. **13**(5): p. 279-87.

Chapter Four

FRET PNA probes for imaging inducible nitric oxide synthase (iNOS) mRNA in living cells

ABSTRACT

Förster resonance energy transfer (FRET) has been widely used to study the interactions between macromolecules in biological systems, such as proteins and nucleic acids. One application of the FRET is to detect mRNAs using fluorescently labeled nucleic acid probes. In this study, we explored the FRET technology to image iNOS mRNA, whose transcription is induced upon environmental stimulation. Peptide nucleic acids (PNA) bearing donor dyes (Fluorescein or Cy3) or receptor dye (Cy5) were synthesized and were designed to target adjacent sites on the iNOS mRNA. We were able to detect the FRET signal of Cy5 dye at 670 nm by exciting the donor dye at 488 nm (Fluorescein) or 535 nm (Cy3) when the FRET probes bind to the complementary DNA in solution. FRET pairs with FAM and Cy5 were chosen to detect *in vitro* transcribed iNOS mRNA. The PNA FRET probes were first annealed to partially complementary oligodeoxynucleotides (ODNs) so that they would bind to cationic cSCK nanoparticles which delivered the probes into RAW 264.7 cells. We were able to show that these PNA FRET probes could be used to image iNOS mRNA in living RAW 264.7 cells.

INTRODUCTION

Förster resonance energy transfer (FRET) is an energy transfer mechanism that can take place between nearby fluorescent molecules [1]. The energy transfer takes place through nonradiative dipole-dipole coupling interaction, in which the energy of one molecule (the donor) at electronic excited state is transferred to the other molecule (the acceptor), resulting in emission of the acceptor. One of the most important factors that determine the efficiency of FRET is the distance between the donor and the acceptor. The effective range for FRET is from 10 to 100 Å [2]. Therefore, researchers often use FRET to study the interactions between molecules, such as nucleic acid hybridization [3], protein-protein interactions [4, 5], and protein-nucleic acid interactions [6, 7]. One application of FRET is to image mRNA in living cells using fluorescently labeled nucleic acid probes. Compared with other methods that detect mRNA, such as RT-PCR [8], which requires the lysis of the cells or tissue, nucleic acid hybridization probes can be used to monitor the mRNA *in vivo* in real time [9, 10].

A typical FRET design for nucleic acid probes is the "binary probes", which utilizes two single strand nucleic acid probes bearing two different dyes. Upon hybridizing to a target at neighboring sites, FRET can occur between the donor and the acceptor dye [11]. This design depends on the successful hybridization of the probes, and can eliminate signal from unbound probes because the excitation wavelength of the donor is usually chosen so that it does not overlap that of the acceptor.

Because traditional DNA probes are susceptible to enzymatic degradation and can trigger RNase H degradation of the mRNA target, many DNA mimics have been developed that have higher biological stability and won't trigger RNase H activity.

Peptide Nucleic Acid (PNA) is a DNA analogue with N-aminoethylglycine-based polyamide backbone. It can hybridize to DNA or mRNA with high specificity and binding affinity [12-14]. PNA probes are more resistant to nuclease degradation and will not induce RNase H activity upon hybridizing to the mRNA [15]. Researchers have successfully used PNA FRET probes to investigate mRNA splicing both in solution and in fixed cells [16, 17], by targeting two exons to be spliced with a donor and acceptor probe. In the pre-mRNA, the exons are separated by an intron which prevents FRET from occurring, but after splicing, FRET will occur because the two exons become linked to each together.

FRET probes have also been used to image mRNA in living cells, although the intracellular delivery of the probes remains to be one of the biggest challenges for mRNA imaging in living cells. For example, Tsuji and coworkers have used labeled DNA FRET pairs to visualize specific mRNA inside living cells by directly injecting the probes into cells [18, 19]. Other methods for intracellular delivery of FRET probes include electroporation [20] and reversible pore-forming agents such as Streptolysin-O (SLO) [21, 22]. Although these methods have been shown to enable the delivery of nucleic acid probes into cytoplasm, they are time consuming, cause damage to the cells, and cannot be used for *in vivo* studies. Another method for delivering nucleic acid probes is to use synthetic agents such as nanoparticles [23, 24]. These particles are usually positively charged so that they can associate with cell membranes and enter cells via endocytosis. Nucleic acid probes can associate with cationic nanoparticles via electrostatic interactions, or via covalent bonds. Because the PNA probes are uncharged, they have to be first hybridized to a negatively charged ODN to form complexes with cationic lipids or

nanoparticles [25]. The advantage of using nanoparticles for delivery is that they can be modified with other functional groups, such as polyethylene glycol (PEG) to increase their retention time in the blood stream, or specific targeting ligands to achieve high efficiency for *in vivo* delivery [24]. Recently, the Wooley group has developed a cationic shell-cross-linked (cSCK) nanoparticle. Through collaborative work between our two labs, Huafeng Fang and Ke Zhang have shown that cSCK nanoparticles can effectively deliver DNA plasmid and PNA/DNA hybrids into HeLa and pLuc 705 cells. They have also conjugated the PNAs onto cSCK nanoparticles via disulfide bonds and shown that the disulfide bond can be cleaved inside cells to release the PNA [26-28].

In this chapter, we will report on the design and synthesis of peptide nucleic acid (PNA) FRET probes and their use for detecting iNOS mRNA, whose transcription is up-regulated in inflammation or by environmental stimuli such as lipopolysaccharide (LPS) or γ-interferon (γ-IFN) [29]. We will demonstrate the ability of the FRET probes to detect a complementary DNA target and *in vitro* transcribed iNOS mRNA. We will also demonstrate the ability of cSCK nanoparticles to deliver the PNA probes annealed to partially complementary ODNs into living cells **(Figure 4.1)**. We will show that this nanoparticle-based FRET probe system can be used to image iNOS mRNA in living RAW 264.7 cells.

EXPERIMENTAL PROCEDURES

Materials:

Anhydrous N,N-dimethylformamide (DMF), diisopropylethylamine (DIPEA), trifluoroacetic acid (TFA), meta-cresol, dichloromethane (DCM), N-methylpyrrolidone (NMP) were purchased from Sigma-Aldrich (St Louis, MO). PNA monomers were purchased from PolyOrg, Inc (Leominster, MA). Fmoc protected amino acids were purchased from EMD chemicals (Gibbstown, NJ). 2-(1H-7-Azabenzotriazol-1-yl)-1,1,3,3-tetramethyl uronium hexafluorophosphate (HATU) was purchased from GenScript (Piscataway, NJ). (5,6)-fluorescein-N-succinimidyl ester (FAM-NHS ester) were purchased from Sigma-Aldrich (St Louis, MO). Cy3-N-hydroxysuccinimidyl ester (Cy3-NHS ester) was purchased from Lumiprobe, LLC (Hallandale Beach, FL). Cy5-N-hydroxysuccinimidyl ester (Cy5-NHS ester) was synthesized and provided by Jillian Smith from our lab. Fmoc-PAL-PEG-PS resin for the solid phase PNA synthesis was purchased from Applied Biosystems (Carlsbad, CA). The PNAs were synthesized by solid-phase Fmoc chemistry on an Expedite 8909 DNA/PNA synthesizer at 2 µmol scale. All the DNA oligonucleotides were purchased from Integrated DNA technologies (Coralville, IA). The crude PNA probes were purified by reversed phase high-performance liquid chromatography (HPLC) on a Beckman Gold System with a UV array detector and a Varian Microsorb-MV column (C-18, 5µm, 300 Å pore size, 4.6×250 mm internal diameter and length). Running buffer A contains 0.1% TFA in water, and B contains 0.1% TFA in acetonitrile. The purified probes were characterized by MALDI-TOF mass spectrometry on an Applied Biosystems 4700 MALDI-TOF mass spectrometer. The concentration of the DNAs was determined from the absorbance at 260

nm on a Bausch and Lomb Spectronic 1001 spectrophotometer. PNA concentrations were determined from the absorbance at 260 nm at 70 ^{o}C.

Synthesis of the FRET probes

PNAs were synthesized on the Expedite 8909 PNA synthesizer. Fmoc-Lys (Mtt)-OH was attached to the N terminus on the donor PNA and to the C terminus on the acceptor PNA. After the PNA synthesis was completed, the column was taken out from the synthesizer and the N-terminal NH_2 of the PNA was capped with capping solution (5% acetic anhydride, 6% 2,6-lutidine in DMF) using double syringes for 10 min. Then the Mtt group on the lysine was then removed by washing the column with 1% TFA in DCM until the yellow color of the deprotection mixture faded away. The column was then washed twice by DCM followed by 5% DIPEA in DCM for 5 min. The column was dried by nitrogen gas and infused overnight with FAM-NHS ester (4 μmol, 2 eq), Cy3-NHS (4 μmol, 2 eq) or Cy5-NHS (4 μmol, 2 eq) ester in dry DMSO with DIPEA (4 μmol, 2 eq). The excess dyes were then washed off column by DMF and DCM. The dried resin was taken out from column and cleaved by cleavage cocktail (20% m-cresol in TFA, 250 μL) for 2 to 4 h. Crude PNA products were precipitated by cold ether, dried, dissolved in 0.1% TFA water and filtered through an Xpertek syringe filter (13 mm, 0.45 μm) before HPLC purification. The purified PNA-FRET probes were dried in a SC110A Thermo Savant speed vacuum system and re-dissolved in de-ionized water to make stock solutions. The concentration of the solutions was determined from the absorbance at 260 nm at 70 ^{o}C. All probes were characterized by MALDI-TOF mass spectrometry.

FRET studies with DNA templates in solution

FRET probes were hybridized to the DNA template in 100 mM Tris 5 mM $MgCl_2$ buffer. The concentrations of PNA1-FAM or PNA2-FAM and the DNA target were 0.5 µM. PNA3-Cy5 was added at different concentrations (0 µM, 0.3 µM and 0.6 µM). For negative controls, one sample contained 0.6 µM PNA3-Cy5 and 0.6 µM DNA template and others included 0.5 µM PNA1-FAM or PNA2-FAM mixed with an excess amount of PNA3-Cy5 (2.4 µM) without the DNA template. The probes and targets were mixed in solution and excited at 488 nm. To compare FAM and Cy3 as donors, 0.5 µM PNA2-FAM or PNA2-Cy3 was mixed with 0.5 µM PNA3-Cy5 and 0.5 µM target DNA. All the solutions were heated at 95 ^{o}C for 2 min and allowed to anneal at 37 ^{o}C. Each sample solution was excited at the donors' absorption maximum (488 nm for FAM or 535 nm for Cy3) and the fluorescence spectra were collected on a Varian Eclipse Fluorimeter.

FRET probes to detect *in vitro* transcribed iNOS mRNA

PCMV-SPORT6 vector containing the iNOS mRNA gene was purchased from American Type Culture Collection (ATCC, Manassas, VA). *E. col*i containing the vector was inoculated in LB media at 37 ^{o}C for 18 h. The plasmid was extracted from the *E. coli* by using HiPure Plasmid Maxprep kit (Invitrogen) following the manufacturer's protocol. The plasmid was then digested by restriction enzyme Xbal (Promega, WA). The resulting linear plasmid was characterized by electrophoresis on a 1% agarose gel in TAE buffer. The linearized plasmid was then transcribed with MEGAtranscript® SP6 (Ambion) kit to produce an mRNA of around 3.9 K bases that was verified by gel electrophoresis on a 1% agarose gel using DEPC treated TAE buffer. The mRNA was quantified by its

126

absorbance at 260 nM and its estimated molecular weight of 1284 µg/nmol. The mRNA was dissolved in OPTI-MEM® solution to make a 0.2 µM solution, together with equal molar amounts of PNA2-FAM or PNA3-Cy5 or both. Samples were incubated at 37 °C for 30 min. The fluorescence spectrum of each sample was collected at excitation wavelength of 488 nm. For a negative control, 0.2 µM PNA2-FAM and a mismatched PNA-Cy5 sequence (pLuc sequence that targeting the splicing correction site of pLuc 705 cells) were mixed with 0.2 µM iNOS mRNA. The fluorescence of the control sample was taken under the same conditions as other samples. For the positive control, equal molar FRET probes and mRNA were mixed and heated at 65 °C for 2 min before incubation at 37 °C for 30 min.

To test the strand-displacement of the PNA/DNA probes delivered into live cells, the 15mer PNA FRET probes and control probes were hybridized to 13mer ODNs, which have 9 bases complementary to the PNA probes with a 4 base overhang. The mixed probes (0.2 µM) were then incubated with 0.2 µM iNOS mRNA in OPTI-MEM® solution for 30 min at 37 °C. Fluorescence spectra were taken with excitation at 488 nm.

FRET imaging of iNOS mRNA in living cells

Mouse macrophage RAW 264.7 cells were seeded on 14 mm glass-bottom dish (MatTek, MA) at 1×10^5 cells/well and incubated overnight until reaching about 70% confluence. Some samples were then treated with 1 µg/mL LPS and 300 ng/mL γ-IFN for 18 h. Cells were then treated with cSCK/PNA-DNA for 6 h or 24 h respectively.

For cells treated for 6 h, PNA2-FAM and PNA3-Cy5 were first annealed to their complementary ODNs, and mixed with cSCK at an N/P ratio of 10:1 in Opti-MEM®

127

medium. The mixture was incubated at room temperature for 20 min to let the cSCK fully complex with the PNA/DNA duplexes electrostatically. Then the solution containing the donor/acceptor/cSCK was mixed with DMEM medium containing 10% FBS and added to the cells. The final volume was 150 µL and the final concentration of the probes and the cSCK were 0.5 µM and 18.1 µg/mL respectively. LPS (1 µg/mL) and γ-IFN (0.3 µg/mL) were added to the delivery media to keep inducing the iNOS mRNA. Samples were incubated at 37 ^{o}C in a wet chamber with 5% CO_2 for 6 h.

For cells treated for 24 h, PNA2-FAM, PNA3-Cy5 or pLuc-Cy5 was first annealed to their complementary ODNs separately in 25 µL Opti-MEM$^{®}$. For each solution, cSCK nanoparticles were added at the N/P ratio of 8:1 and the mixture was incubated at room temperature for 20 min. Solutions containing donor/cSCK and acceptor/cSCK (or mismatched probes) were then mixed together with 100 µL DMEM medium containing 10% FBS to make a final volume of 150 µL and were added to the cells. The final concentration of each probe was 0.5 µM, and the cSCK concentration was 14.5 µg/ml. For stimulated samples, LPS (1 µg/ml) and γ-IFN (0.3 µg/ml) were added to the media to keep inducing the iNOS mRNA. Cells were incubated at 37 ^{o}C in a wet chamber with 5% CO_2 for 24 h and then washed and observed by confocal microscope. Cells incubated with probes for 6 h were observed with a Nikon A1 confocal microscope and cells incubated with probes for 24 h were observed with an Olympus Fluoview FV1000 confocal microscope with a lambda scan function. The FRET spectra of the cells treated with the probes for 24 h were collected by performing the lambda scan. Images were analyzed using the image J software.

RESULTS AND DISCUSSION

Design and synthesis of the PNA FRET probes

PNAs were selected to construct the FRET probes for their high binding affinity to RNAs and resistance to enzymatic degradation [30]. A former lab member, Bereket Oquare, had previously shown that FRET pairs based on fluorescein and Cy5 could be used to detect a DNA sequence in solution [31] and so we chose this pair for initial studies. The sequences of the PNAs for our study were chosen to target iNOS mRNA from position 236 to 272 (**Table 4.1**). This site is one of the accessible sites according to our lab's published results [32]. A binding affinity assay conducted by our lab member Yuefei Shen showed that two PNA probes targeting this sites (probes 240 and 261) have high binding affinity to the iNOS mRNA with K_ds of 101 and 68 pM respectively (**Table 4.2**). This is also a purine rich region, which means the antisense PNAs are pyrimidine rich and won't have complex secondary structures and solubility problems.

One key consideration in designing the FRET probes was the length. Probes need to be long enough to be specific for the target mRNA, but not so long that they will bind with mismatched sequences under physiological conditions. Because of their higher affinity to the target mRNA than the DNA probes, PNA probes are usually shorter, with around 13 to 15 base pairs [16, 17]. The PNAs used in this study are 15-mers and the specificity of the probes was verified by searching through Basic Local Alignment Search Tool (BLAST) data base. While PNAs 2 is highly specific for iNOS mRNA, PNA 1 and PNA3 may also target other mRNAs with 14 or more 15 base pairs. However, since the FRET signal can only be detected upon successful hybridization of the two probes to adjacent sites on the target mRNA, even if one probe can bind non-specifically to other sequences, it won't cause significant background signal as long as the other probe does

not bind close to it. The PNAs were modified with a lysine group on their 3' or 5' end, and the ε-amino group of the lysine was used to conjugate the donor and acceptor dyes. **Table 4.1** shows the sequences of each probes and their observed mass by MALDI mass spectrometry. The detailed characterization of the probes were shown in the appendix **Figures A 4.1-A4.5**.

FRET study with DNA template in solution

In order to find an optimal FRET probe pair for imaging iNOS mRNA, we synthesized PNAs separated by 2 or 6 bases when hybridized to the target. We also tested different fluorescent dyes to achieve the optimal FRET efficiency and the lowest background. **Figure 4.2 A** and **B** compare the FRET efficiency of different pairs of probes with the same template ODN. When the amount of acceptor probe increased, the FRET signal also increased. However, mixing the acceptor PNA alone with the DNA template did not result in any FRET signal. This indicates that the emission of Cy5 can only come from FRET and not from direct excitation of the acceptor with 488 nm light. As a general trend, sequences 2 and 3 yield higher FRET signals than sequences 1 and 3. This may be because sequences 2 and 3, which are 2 bases apart, are closer to each other than sequences 1 and 3, which are 6 bases apart. Another reason could be that the FAM on PNA1 is next to a C base, which would be paired to a G base on the DNA template that might quench the fluorescence of the FAM, thereby weakening the FRET signal of Cy5 [33].

We also compared the FRET observed from FAM with the FRET from Cy3 using Cy5 as the acceptor (**Figure 4.3 A** and **B**). While the excitation maximum for FAM is

488 nm, it is 535 nm for Cy3. Although Cy3 and Cy5 pairs show a higher FRET efficiency and stronger signal, the emission spectrum of Cy3 also overlaps slightly with Cy5's emission spectrum, which results in a background signal. On the other hand, the emission spectrum of FAM doesn't show any overlap with the emission of Cy5. Based on these results, we chose PNA2-FAM as the donor and PNA3-Cy5 as the acceptor for our in vivo experiments. Similar DNA-based FRET pairs have been utilized by Tsuji et al [19] to image RNA in living cells.

FRET study with *in vitro* transcribed mRNA in solution

In order to see if our FRET probes would be suitable for imaging iNOS mRNA *in vivo*, we first tested their ability to detect *in vitro* transcribed iNOS mRNA in solution. After mixing PNA2-FAM and PNA3-Cy5 with equal amounts of iNOS mRNA at 0.2 µM in Opti-MEM® medium a significant FRET signal was detected at 670 nm. However, when the donor sequence and a mismatched Cy5 bearing sequence were mixed with the mRNA, there was no observable FRET signal (**Figure 4.4 A**). This means that FRET occurred because of the successful hybridization of the probes with the iNOS mRNA. Heating the mRNA to 65 $^{\circ}$C, further increased the FRET signal presumably because the mRNA unfolded making the target site more accessible. It is worthwhile to note that mRNA may have different secondary structures under different conditions and that the mRNA may adopt a different structure in living cells.

To deliver the probes inside the cells, the PNA probes would have to be annealed to complementary DNAs so that they can be electrostatically bound to the cSCK nanoparticles. When the nanoparticles deliver probes into cytoplasm, the DNA strand will be displaced by the iNOS mRNA. We have utilized such a strand-displacement

strategy in the previous chapter. We therefore first tested the strand-displacement of such PNA-DNA hybrids by iNOS mRNA in solution. **Figure 4.4 B** shows that the iNOS mRNA can displace the short DNAs on the PNA probe and a FRET signal can be detected in solution. This observation demonstrates the viability of the system for imaging in living cells.

FRET imaging of iNOS mRNA in living cells

For live cell imaging studies the FRET PNA probes were first hybridized to partially complementary ODNs so that they could be delivered into living RAW 264.7 cells via cSCK nanoparticles. cSCK nanoparticles are positively charged nanoparticles that can bind PNA/DNA duplexes via electrostatic forces. The ability of the PNA/DNA duplexes to bind cSCKs depends on the N/P ratio which refers to the number of amines on the particle (number of positive charges) over the number of phosphates (negative charges) on the DNA backbone. Gel retardation assay conducted by our lab member Yuefei Shen (Appendix **Figure A 4.6**) has shown that for the cSCK to form complexes with PNA/DNA duplexes and thereby retard the migration of the duplexes on polyacrylamide gel electrophoresis (PAGE), the N/P ratio needs to be 4 or higher. As N increases, more PNA/DNA duplex will associate with cSCK nanoparticles, which will be taken up by the cells via endocytosis. It is hypothesized that once trapped in the endosomes, the cSCK will help release the probes via the "proton sponge" effect, in which the amino groups will buffer against the increase of protons as the endosomes acidify, bring more protons and counter ions inside the endosomes. The accumulation of counter ions will increase the osmotic pressure that leads to the disruption of the

endosomes [28]. However, cSCKs are also toxic to cells at higher concentrations [28]. Therefore, the concentrations of the cSCK and probes need to be optimized to most efficiently deliver the probes into the cells with minimum cytotoxicity. In our study, we have used an N/P ratio of 10 for cells treated for 6 h and decreased the N/P ratio to 8 for cells treated for 24 h while maintaining the same probe concentration of 0.5 µM to minimize the toxicity at longer times. Cells were treated with LPS and γ-IFN for 18 h to induce iNOS mRNA expression and then incubated with cSCK/PNA/DNA polyplexes. LPS and γ-IFN were added again during the cSCK transfection period to keep the expression level of the mRNA high. We have found that after 6 h, most of the probes were associated with cell membranes, and did not penetrate deeply into the cytoplasm (**Figure 4.5**). There was also no observable FRET signal detected, consistent with most of the probes being trapped in the membrane or endosomes and not reaching the mRNA in the cytoplasm. After 24 h of incubation, however, the probes appeared to be inside the cytoplasm, and the fluorescence was more diffuse, indicating the release of the probes from endosomes and hybridization to the iNOS mRNA. The confocal images in **Figure 4.6A** shows that when excited at 488 nm, cells treated with FRET probes emitted detectable FRET signal at 650-700 nm. For the non-stimulated cells (**Figure 4.6 B**) and stimulated cells treated with mismatch Cy5 probes (**Figure 4.6 C**), there was very little FRET signal detected.

To better quantify the FRET signal, a wavelength scan was performed to show the FRET spectrum of different regions of interest (ROI). Cells were excited at 488 nm and fluorescence images of the cells were collected at 10 nm intervals. The spectra of ROIs clearly show that antisense FRET PNA probes were giving strong FRET signals inside

the cells. Changing the acceptor probe to a control sequence showed no FRET signal in the stimulated cells, indicating that the FRET signal was produced by hybridization of FRET probes to the iNOS mRNA, rather than through proximity effects in the polyplexes with the cSCK, which might bring the two probes close to each other. For the non-stimulated cells, the FRET signal could also be detected, but was significantly weaker than the FRET signal in the stimulated cells. The difference in FRET signal intensity for selected regions of interests (ROI) of stimulated and non-stimulated cells was 3.8 ($\pm$ 0.9)-fold (**Figure 4.7**).

CONCLUSION

We have synthesized fluorescently labeled PNA FRET probes that can hybridize to adjacent positions on iNOS mRNA. We have optimized targeting positions of the probes and fluorescent molecule pairs for this study. We have shown that the 15mer PNA labeled with FAM or Cy3 (donor) and the PNA labeled with Cy5 (acceptor) can hybridize to the target DNA and mRNA *in vitro* and produce FRET signals that can be detected by a fluorimeter. We then showed that these probes could be delivered into living cells by hybridizing them with partially complementary DNAs and complexing them with cSCK nanoparticles and that After 24 hours of incubation, FRET signals could be observed in iNOS stimulated living cells. Control probes showed no FRET signal and non-stimulated RAW cells showed a weaker FRET signal, which confirmed that the FRET image observed in stimulated living cells was due to hybridization of the probes to the iNOS mRNA. By using the FAM and Cy5 FRET pairs, we were able to avoid overlapping of the emission spectra of the two dyes, though perhaps at the expense of a

lower FRET efficiency. The Cy3 and Cy5 FRET pairs, while having much higher FRET efficiency, also have slightly overlapping emission. Therefore, unbound Cy3 probes, if in large excess, could interfere with detection of the FRET signal from the bound probes. Nonetheless, a design that combines the strand-displacement probes and FRET probes may solve this problem. Instead of using unmodified DNAs to hybridize with the PNA, DNA bearing fluorescent quenchers could be used to quench the signals of fluorophores. Only when both quencher strands are displaced by the iNOS mRNA will the FRET signal be detected. This design will be more likely to give higher signal/noise ratio in living cells by having lower background noise of the unbound probes. It will also eliminate the possible unwanted FRET signal from the interaction of cSCK associating with two FRET probes.
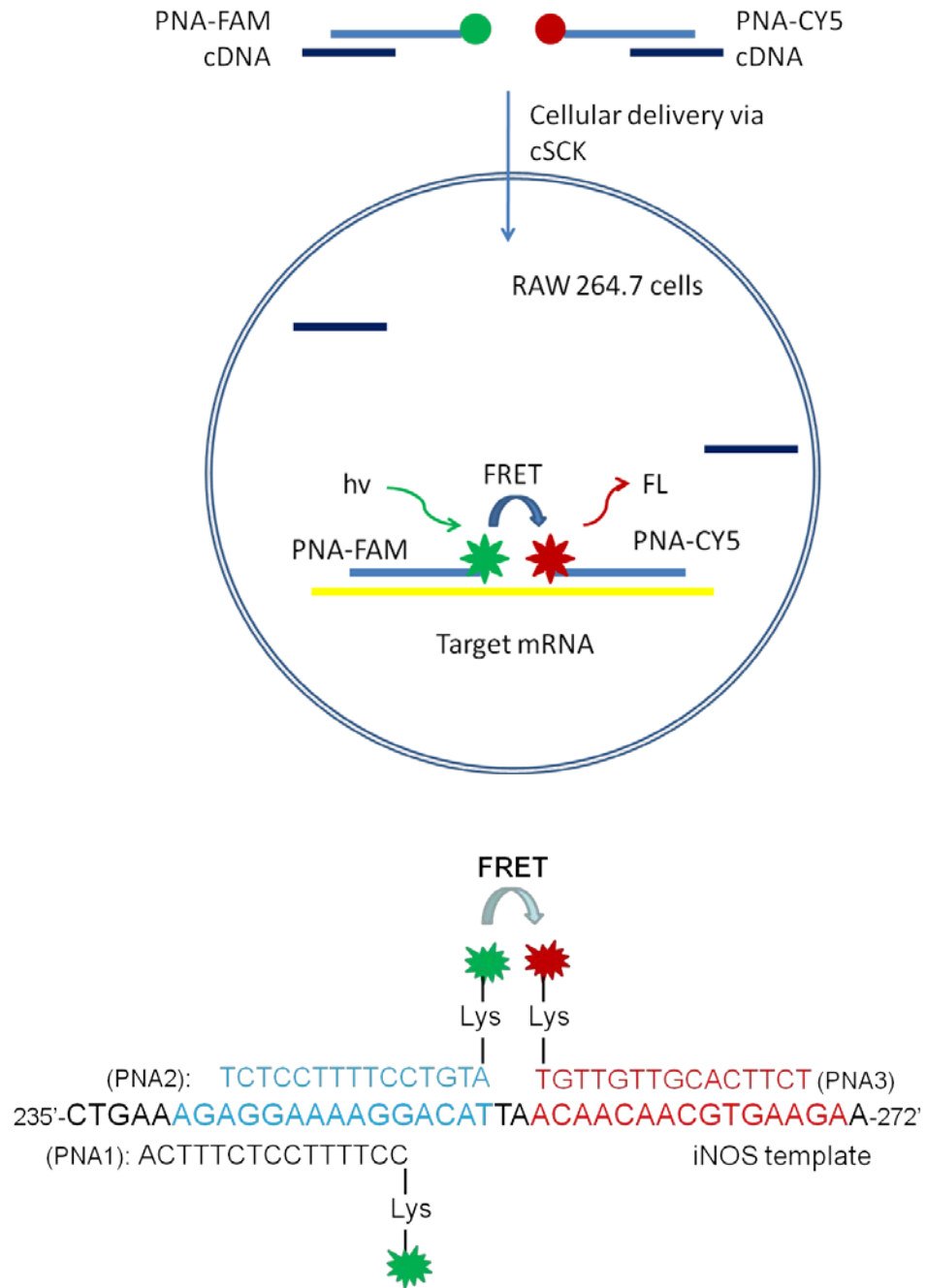
Figure 4.1: Schematic representation of FRET PNA probes for imaging iNOS mRNA in living cells.
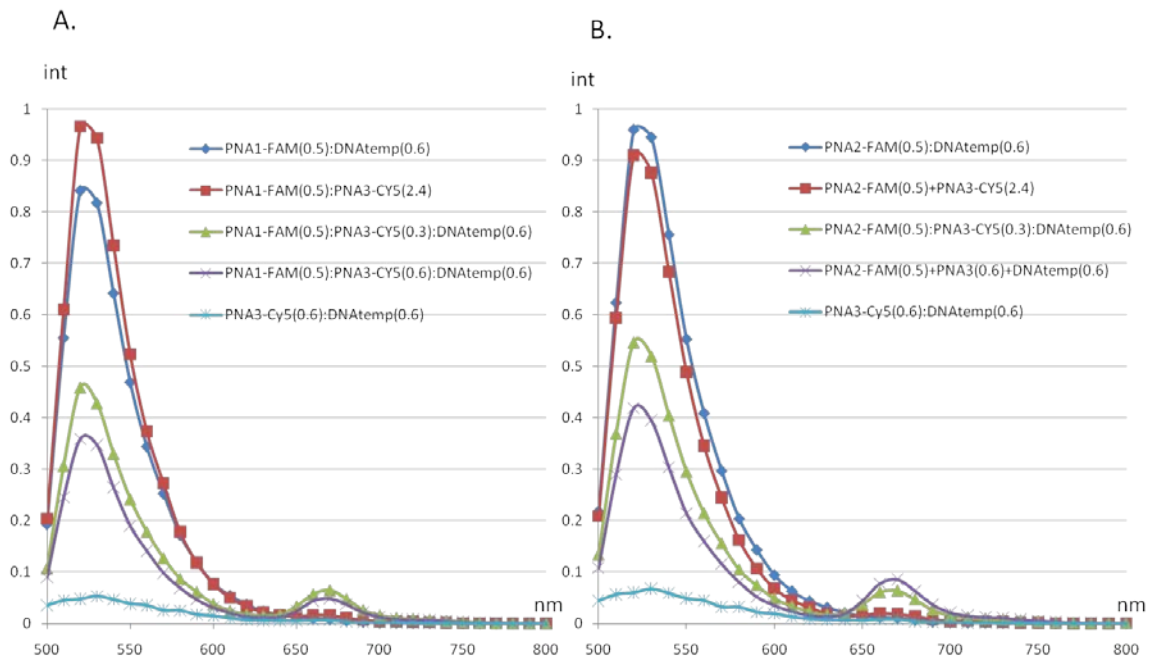
Figure 4.2: FRET probes hybridizing with DNA template. A. PNA1-FAM and PNA3-Cy5 probes. B. PNA2-FAM and PNA3-Cy5 probes. PNA1-FAM and PNA2-FAM concentration: 0.5 µM. DNA template concentration: 0.6 µM. PNA3-Cy5 was added in different amount (0, 0.3, 0.6 µM). For a negative control, 0.5 µM PNA1-FAM or PNA2-FAM was mixed with excessive amount of PNA3-Cy5 (2.4 µM) without DNA template. Buffer: 100 mM Tris 5 mM $MgCl_2$, pH=7.1. Excitation wavelength: 488 nm.
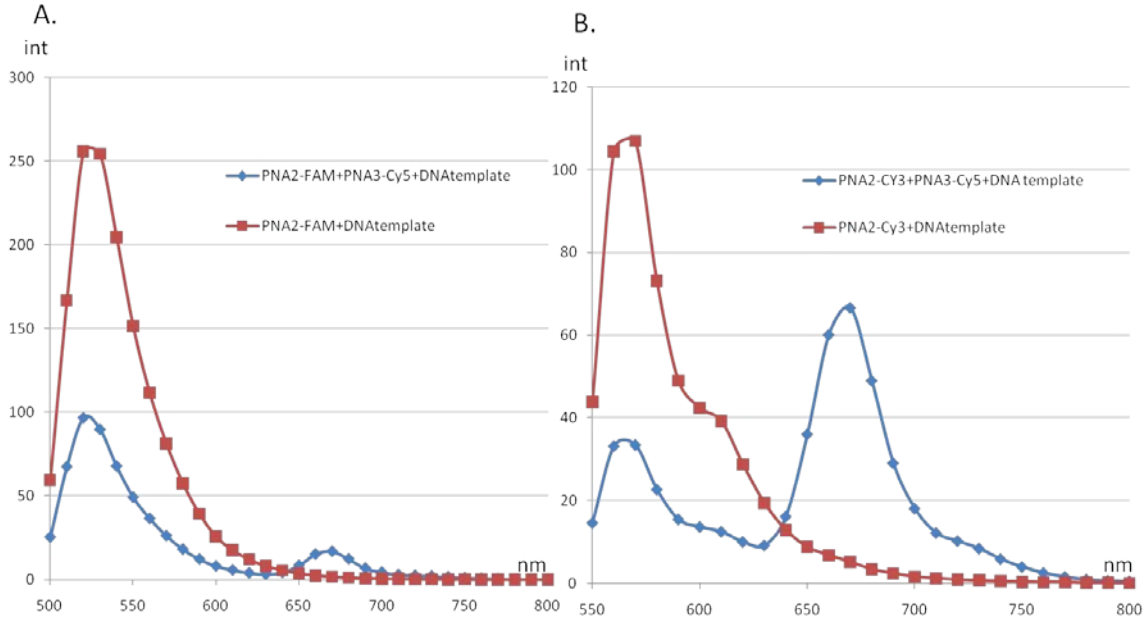
Figure 4.3: Comparison of FAM and Cy3 as FRET donors. 0.5 μM PNA2-FAM (A.) or PNA2-Cy3 (B.) was mixed with 0.5 μM PNA3-Cy3 and DNA template in buffer containing 100 mM Tris 5 mM MgCl$_2$. For the positive control, no PNA3-Cy5 was added. Excitation wavelength: 488 nm for FAM and 535 nm for Cy3.
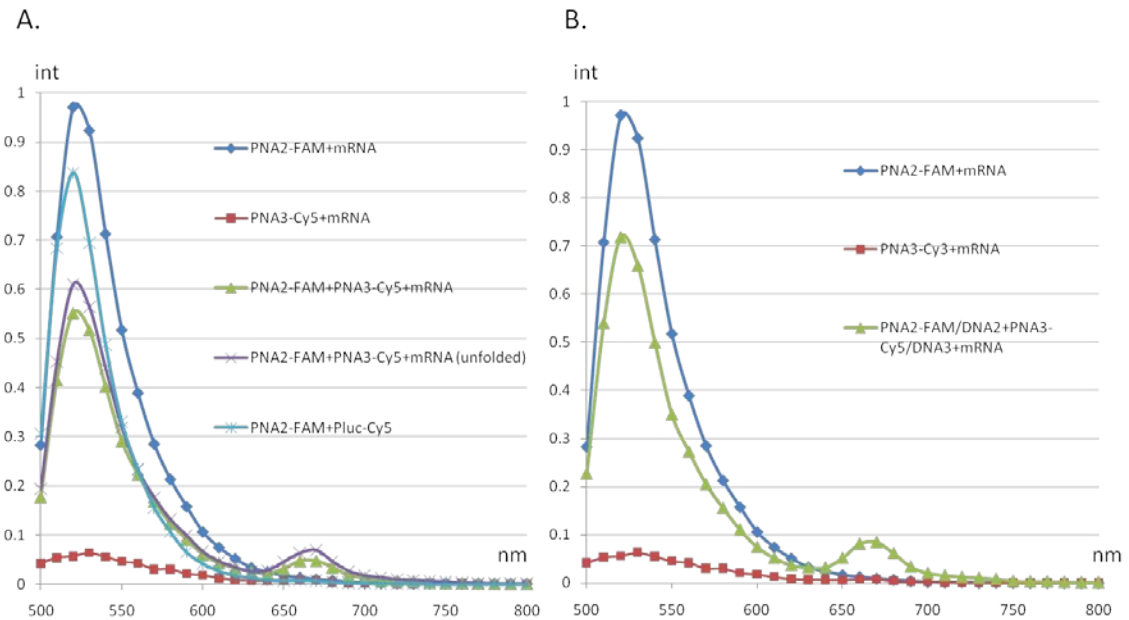
Figure 4.4: FRET PNA probes to detect *in vitro* transcribed iNOS mRNA. A. 0.2 μM PNA2-FAM and PNA3-Cy5 or pLuc-Cy5 (mismatch) were incubated with 0.2 μM in vitro transcribed iNOS mRNA at 37 ^{o}C for 30 min. Positive control including 0.2 μM PNA2-FAM, PNA3-Cy5 and iNOS mRNA was heated at 65 ^{o}C for 1 min to unfold the mRNA before incubation at 37 ^{o}C for 30 min. B. 0.2 μM PNA2-FAM and PNA3-Cy5 were annealed to their partially complementary ODNs and incubated with the iNOS mRNA at 37 ^{o}C for 30 min. Controls are 0.2 μM PNA2-FAM or PNA3-Cy5 incubated with the iNOS mRNA under the same conditions. Buffer solution: Opti-MEM$^®$ medium. Excitation wavelength 488 nm.
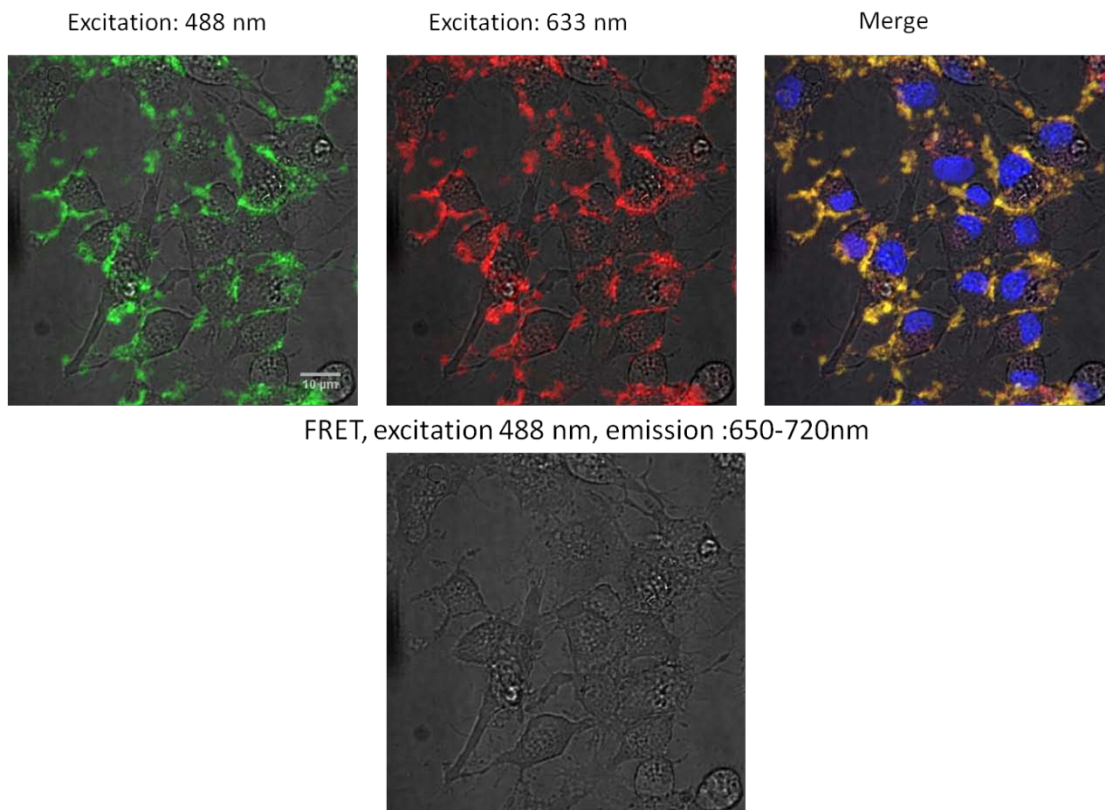
Figure 4.5: Confocal images of stimulated RAW 264.7 cells treated with cSCK and FRET probes for 6 h. Cells were treated with 0.5 µM PNA2-FAM /DNA2, 0.5 µM PNA3-FAM /DNA3 and 18.3 µg/ml cSCK. N/P ratio is 10:1. Cells were incubated for 6 hours and stained with Hoechst 33258 nuclear staining dye for 1 h. Green: excitation at 488 nm, FAM signal. Red: excitation at 633 nm, Cy5 signal. Blue: excitation at 405 nm, hoechst signal.
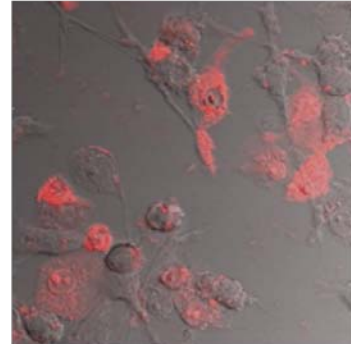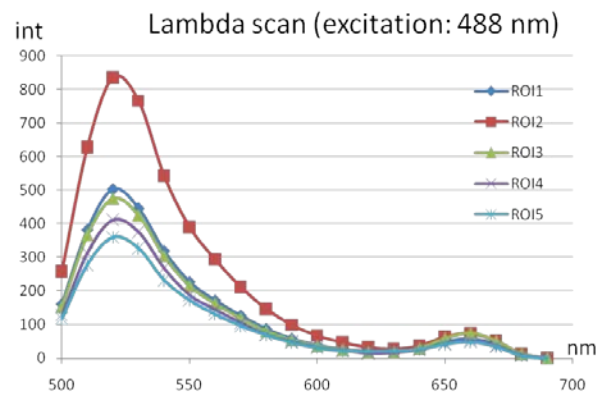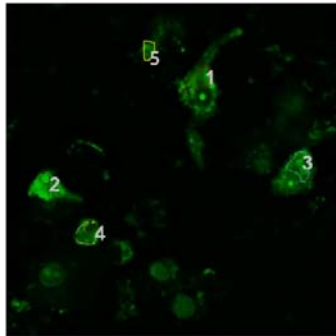
A: Stimulated cells. FRET probes.
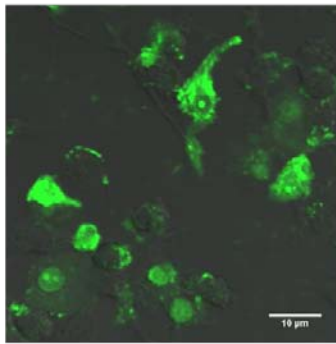
Excitation: Donor
Emission: Donor

Excitation: Donor
Emission: Acceptor
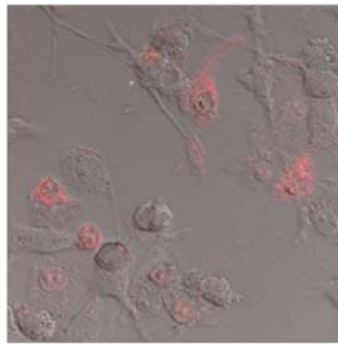
Excitation: Acceptor
Emission: Acceptor

Selected ROIs
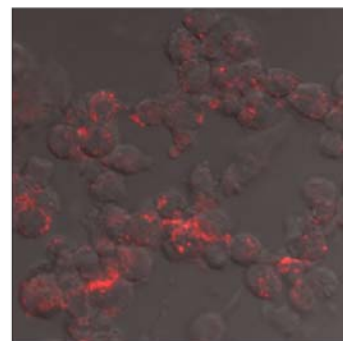

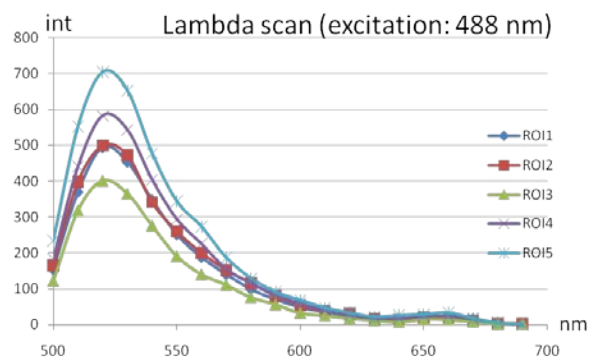B: Nonstimulated cells, FRET probes.
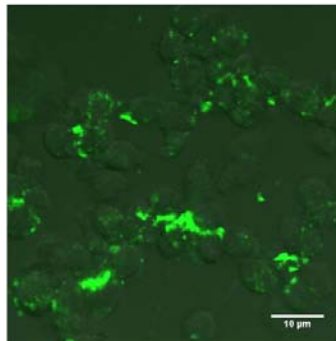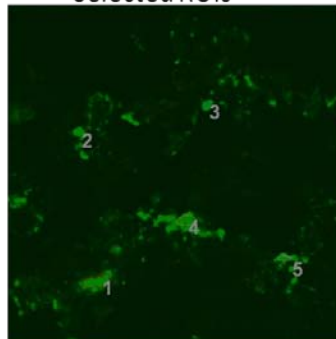
Excitation: Donor
Emission: Donor

Excitation: Donor
Emission: Acceptor

Excitation: Acceptor
Emission: Acceptor

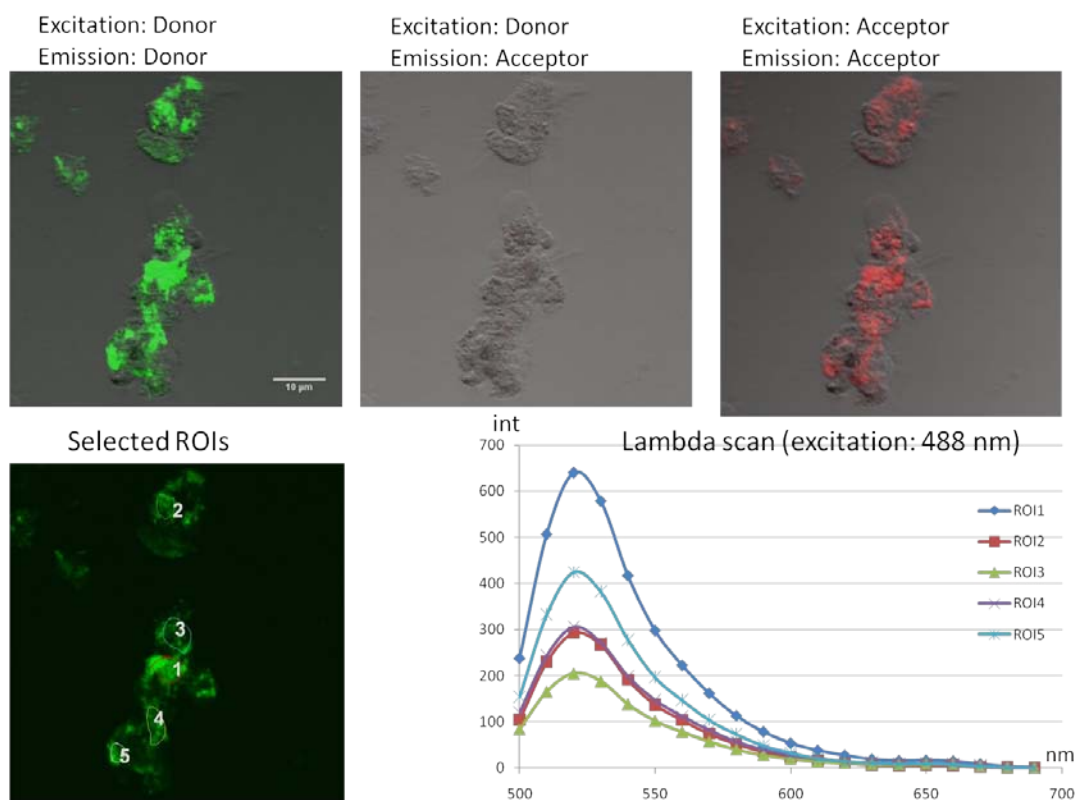Selected ROIs

C: Stimulated cells, mismatched acceptor probe.

Figure 4.6: Confocal images of cells treated with cSCK and FRET probes for 24 h.
PNA2-FAM and PNA3-FAM or pLuc-Cy5 were annealed to the partially complementary
ODNs and mixed with cSCK nanoparticles. The concentration for each probe was
0.5 µM and the cSCK concentration was 14.5 μg/ml. N/P: 8. A. Stimulated RAW 264.7
cells treated with PNA2-FAM and PNA3-Cy5. B. Nonstimulated RAW 264.7 cells
treated with PNA2-FAM and PNA3-Cy5. C. Stimulated RAW 264.7 cells treated with
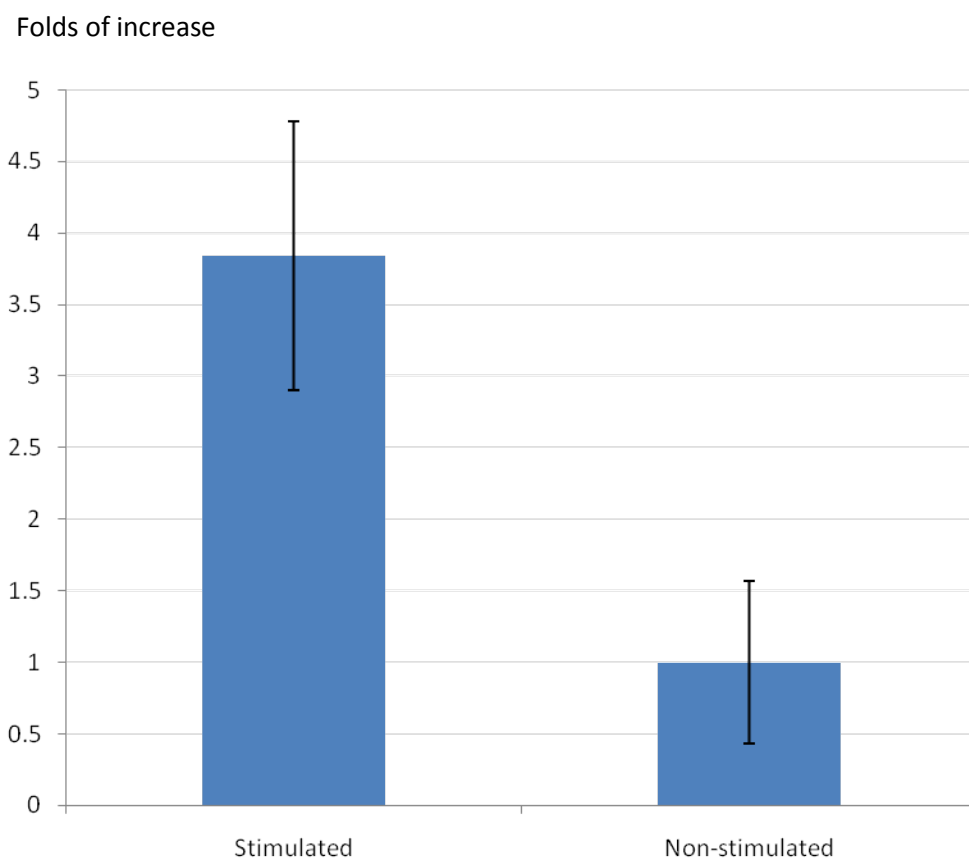PNA2-FAM and pLuc -Cy5.

Folds of increase

Figure 4.7: Average FRET intensity for cells in selected ROI in Figure 4.6A and B.

Probe name	Sequence	Calculated mass	Observed mass
PNA1-FAM	5'-lys- (ε)-FAM-CCTTTTCCTCTTTCA-3'	4461.2	4463.5
PNA2-FAM	5'-lys- (ε)-FAM-ATGTCCTTTTCCTCT-3'	4500.3	4505.5
PNA2-Cy3	5'-lys- (ε)-FAM-ATGTCCTTTTCCTCT-3'	4580.6	4585.6
PNA3-Cy5	5'-TCTTCACGTTGTTGT-lys-(ε)-Cy5-3'	4686.6	4689.4
pLuc-Cy5 (control)	5'-lys- (ε)-Cy5-CTTACCTCAGTTACA-3'	4634.6	4639.3

DNA temp (inos): 235'-CTGAAAGAGGAAAAGGACATTAACAACAACGTGAAGAA-272'
DNA1: 5'-ATAATGAAAGAGG-3'
DNA2: 5'-ATAAAGAGGAAAA-3'
DNA3: 5'-ACGTGaaGAATAA-3'
DNA(pLuc): 5'-ATAATGTAACTGA-3'

Table 4.1: Sequences and MALDI results of the probes.

	sequence	Kd (pM)
iNOS-240 PNA	5'- TGT CCT TTT CCT CTT TCA -3'	101±52
iNOS-261 PNA	5'- GTT TTC TTC ACG TTG TTG -3'	68±21
iNOS-299 PNA	5'- GTC ATC TTG TAT TGT TGG - 3'	15±3
iNOS-480 PNA	5'- TGA AAT CCG ATG TGG CCT-3'	86±26
iNOS-240mm PNA	5'- TGT CCT CCT TTT CTT TCA -3'	>10000
iNOS-480mm PNA	5'-TAG AAT CCA GTG GTG CCT- 3'	>10000

Table 4.2: Binding affinity of PNAs for iNOS mRNA (Yuefei Shen).
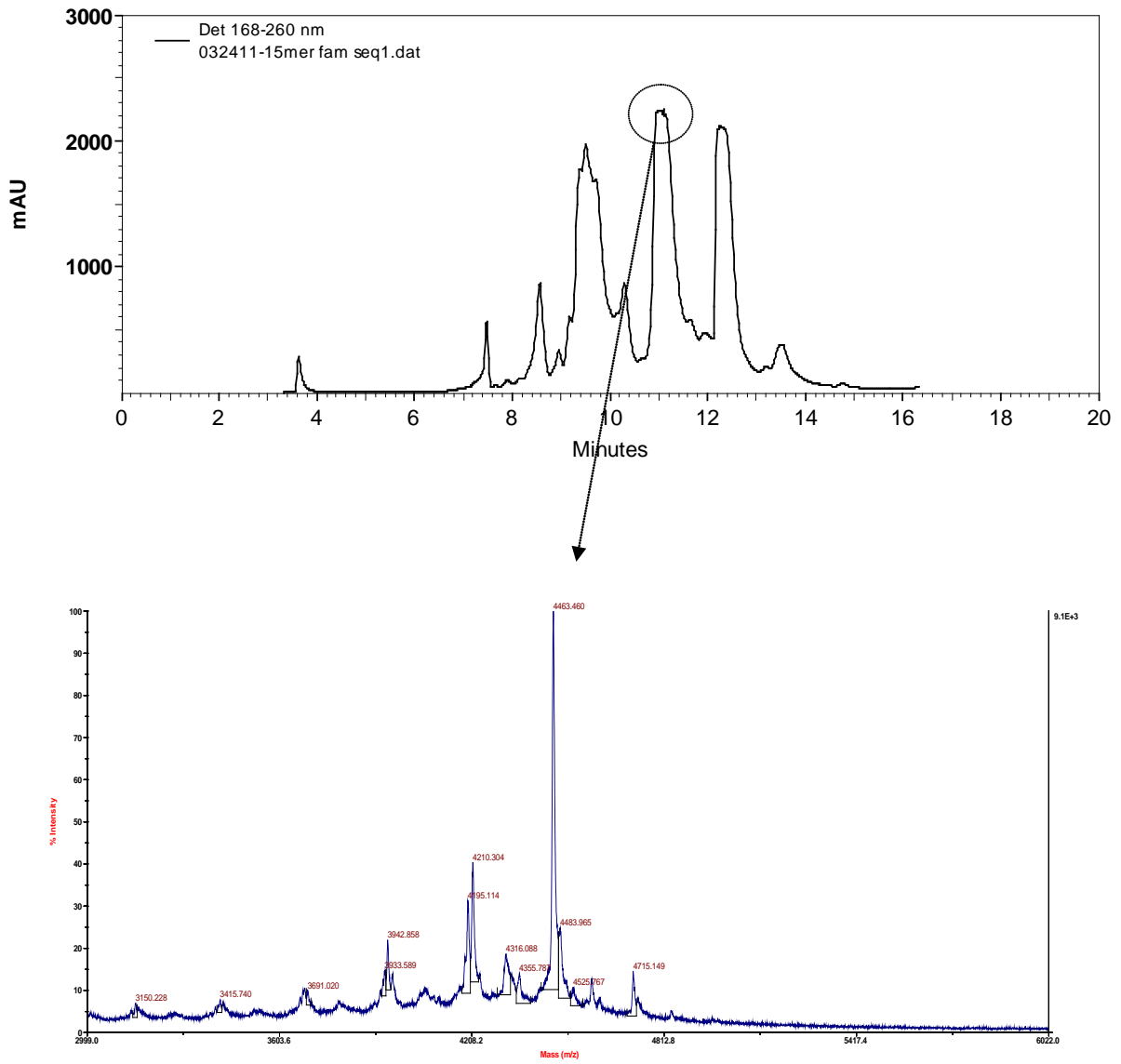
Appendix

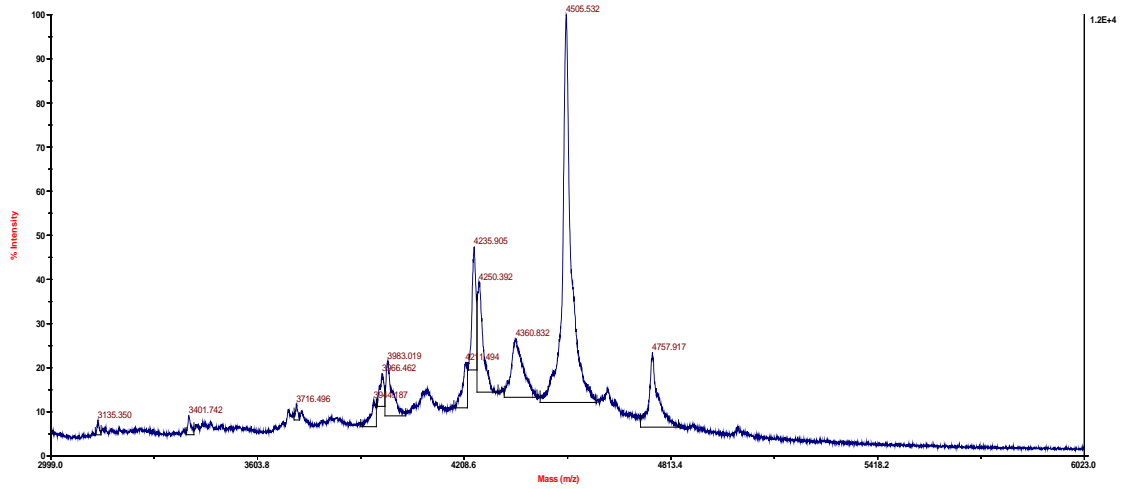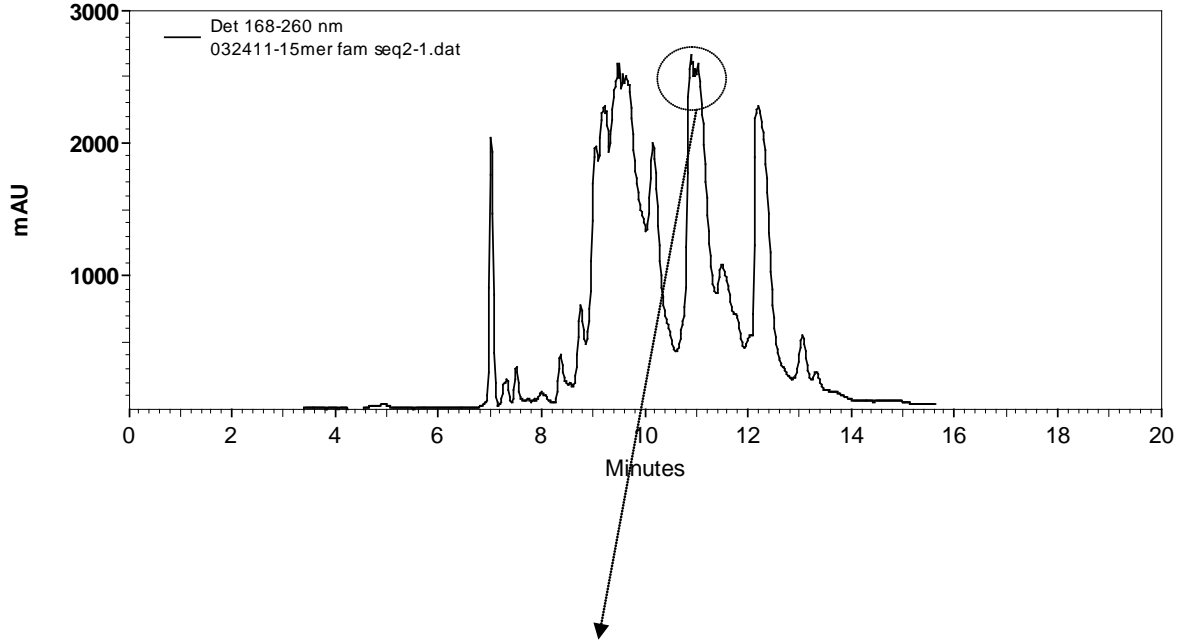**Figure A 4.1: HPLC trace and MALDI-TOF mass spectrum of PNA1-FAM.**

Figure A 4.2: HPLC trace and MALDI-TOF mass spectrum of PNA2-FAM.

Figure A 4.3: HPLC trace and MALDI-TOF mass spectrum of PNA2-Cy3.
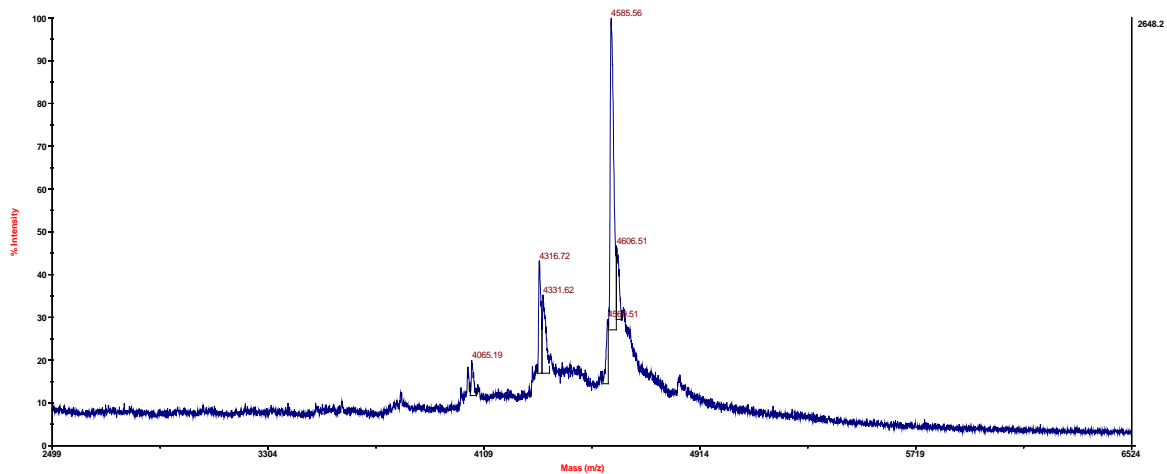
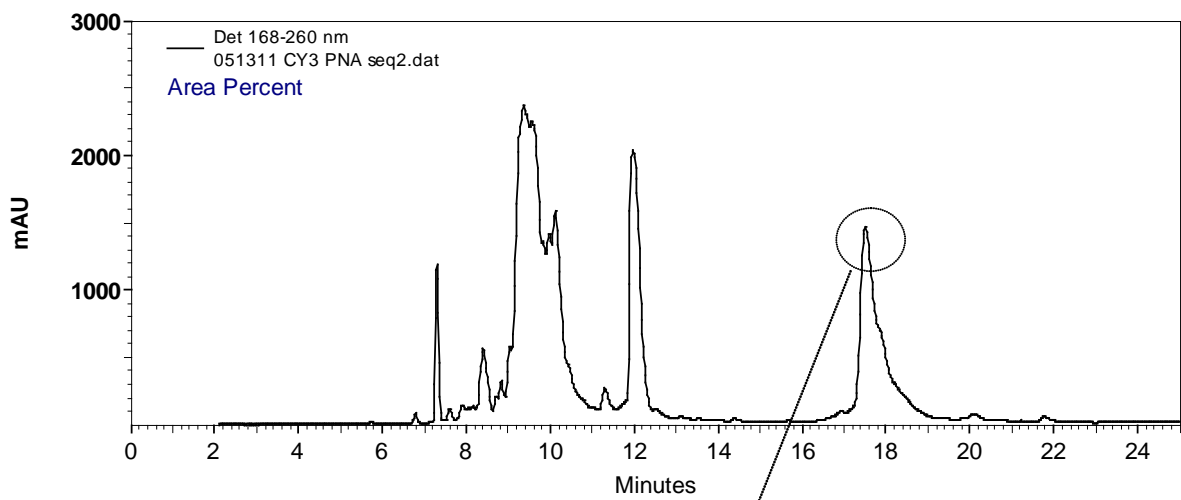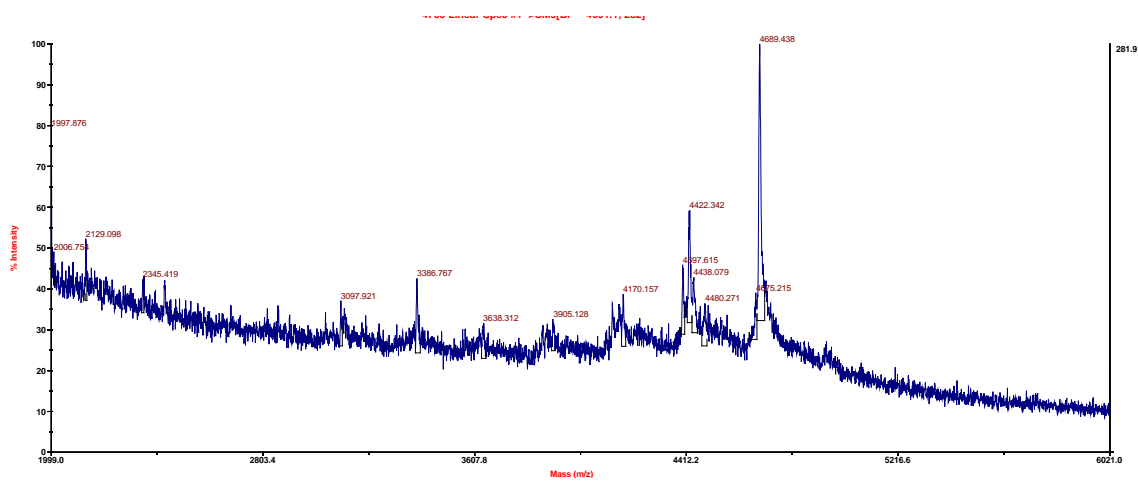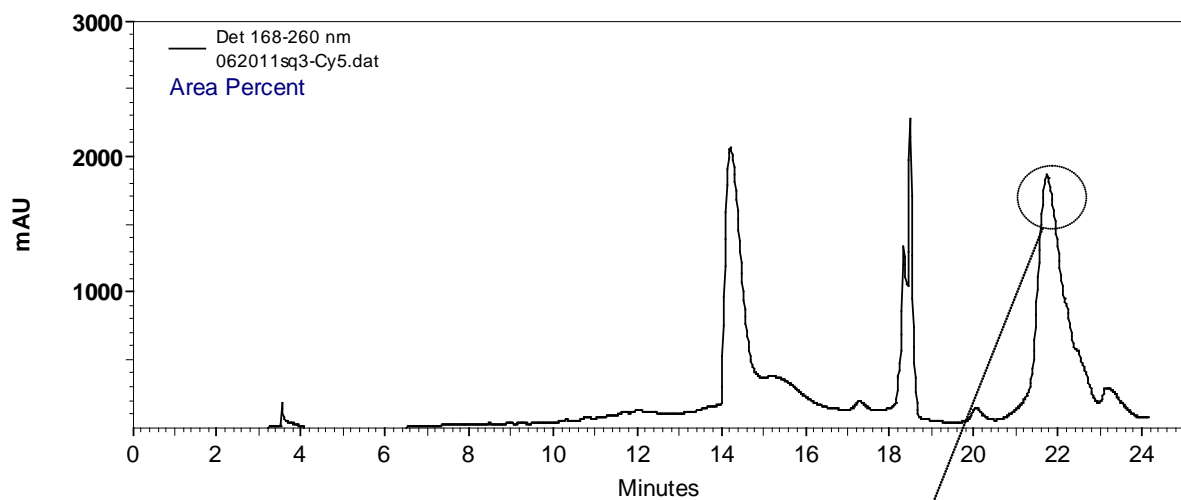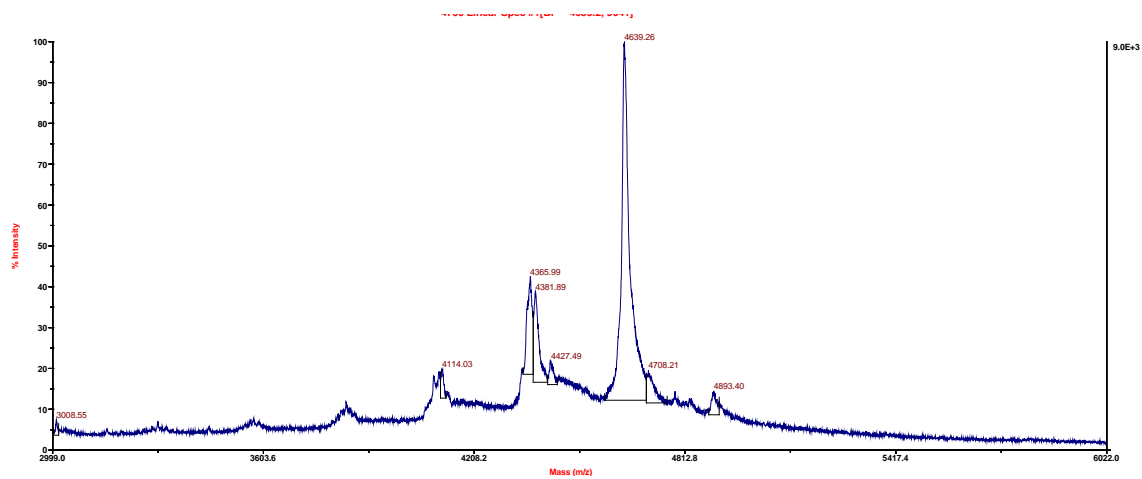**Figure A 4.4: HPLC trace and MALDI-TOF mass spectrum of PNA3-Cy5.**
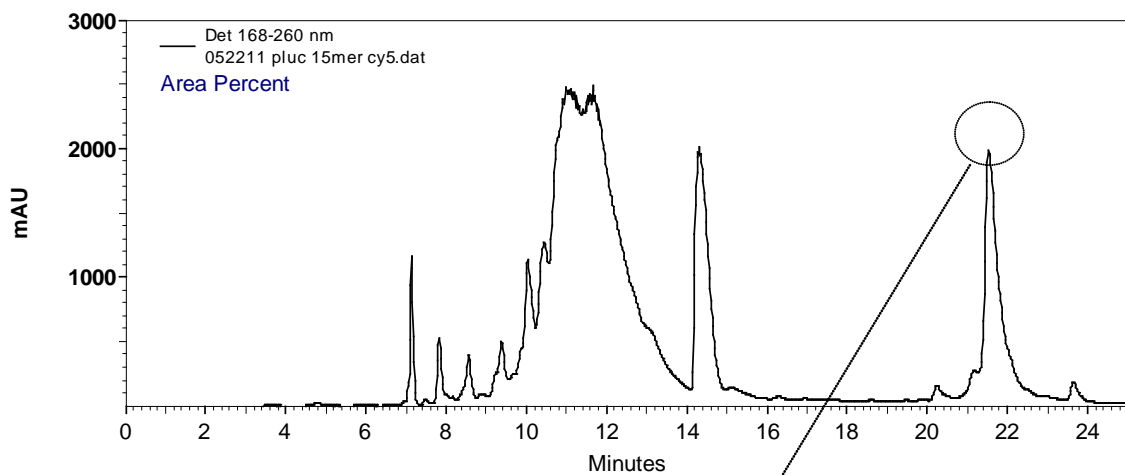
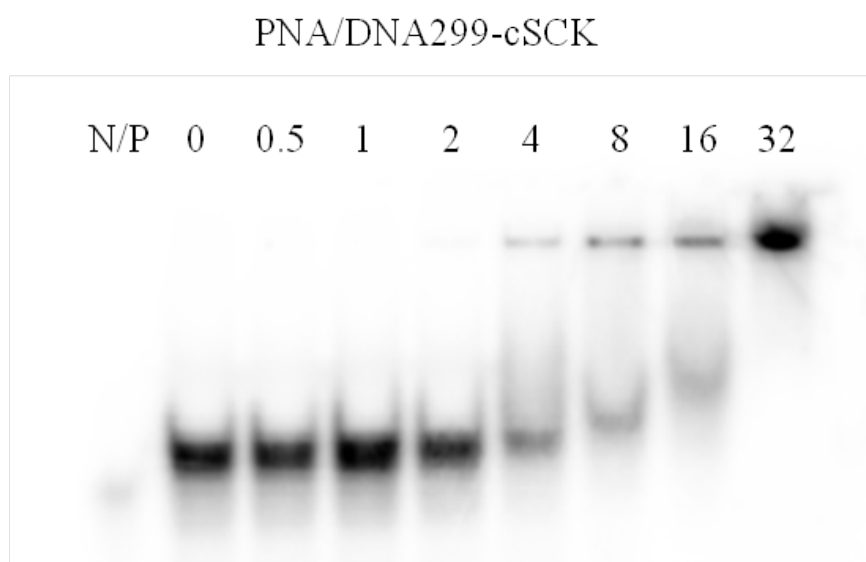**Figure A 4.5: HPLC trace and MALDI-TOF mass spectrum of pLuc-Cy5.**

Figure A 4.6: Gel retardation assay of PNA/DNA hybrid mixed with cSCK nanoparticles (Yuefei Shen). 0.5 uM of PNA/DNA (2:1) hybrids mixed with serial amounts of cSCK with different N/P ratio. Incubated in PBS for 30 min. Native PAGE gel.

References

1.   Ha, T., et al., *Probing the interaction between two single molecules: fluorescence resonance energy transfer between a single donor and a single acceptor.* Proc Natl Acad Sci U S A, 1996. **93**(13): p. 6264-8.

2.   Haugland, R.P., J. Yguerabide, and L. Stryer, *Dependence of the kinetics of singlet-singlet energy transfer on spectral overlap.* Proc Natl Acad Sci U S A, 1969. **63**(1): p. 23-30.

3.   Cardullo, R.A., et al., *Detection of nucleic acid hybridization by nonradiative fluorescence resonance energy transfer.* Proc Natl Acad Sci U S A, 1988. **85**(23): p. 8790-4.

4.   Piston, D.W. and G.J. Kremers, *Fluorescent protein FRET: the good, the bad and the ugly.* Trends Biochem Sci, 2007. **32**(9): p. 407-14.

5.   Hoch, D.A., J.J. Stratton, and L.M. Gloss, *Protein-protein Forster resonance energy transfer analysis of nucleosome core particles containing H2A and H2A.Z.* J Mol Biol, 2007. **371**(4): p. 971-88.

6.   Duan, M.R. and M.J. Smerdon, *UV damage in DNA promotes nucleosome unwrapping.* J Biol Chem. **285**(34): p. 26295-303.

7.   Wilson, G.M., et al., *Phosphorylation of p40AUF1 regulates binding to A + U-rich mRNA-destabilizing elements and protein-induced changes in ribonucleoprotein structure.* J Biol Chem, 2003. **278**(35): p. 33039-48.

8.   Han, B., et al., *Quantification of iNOS mRNA with reverse transcription polymerase chain reaction directly from cell lysates.* Nitric Oxide, 1999. **3**(4): p. 281-91.

9.   Shi, N., R.J. Boado, and W.M. Pardridge, *Antisense imaging of gene expression in the brain in vivo.* Proc Natl Acad Sci U S A, 2000. **97**(26): p. 14709-14.

10.   Suzuki, T., et al., *Imaging endogenous gene expression in brain cancer in vivo with 111In-peptide nucleic acid antisense radiopharmaceuticals and brain drug-targeting technology.* J Nucl Med, 2004. **45**(10): p. 1766-75.

11.   Wittwer, C.T., et al., *Continuous fluorescence monitoring of rapid cycle DNA amplification.* Biotechniques, 1997. **22**(1): p. 130-1, 134-8.

12.   Jensen, K.K., et al., *Kinetics for hybridization of peptide nucleic acids (PNA) with DNA and RNA studied with the BIAcore technique.* Biochemistry, 1997. **36**(16): p. 5072-7.

13.   Ratilainen, T., et al., *Thermodynamics of sequence-specific binding of PNA to DNA.* Biochemistry, 2000. **39**(26): p. 7781-91.

14.   Kaihatsu, K., B.A. Janowski, and D.R. Corey, *Recognition of chromosomal DNA by PNAs.* Chem Biol, 2004. **11**(6): p. 749-58.

15.   Bonham, M.A., et al., *An assessment of the antisense properties of RNase H-competent and steric-blocking oligomers.* Nucleic Acids Res, 1995. **23**(7): p. 1197-203.

16.   Robertson, K.L., et al., *Fluorescent PNA probes as hybridization labels for biological RNA.* Biochemistry, 2006. **45**(19): p. 6066-74.

17.   Blanco, A.M., et al., *A FRET-based assay for characterization of alternative splicing events using peptide nucleic acid fluorescence in situ hybridization.* Nucleic Acids Res, 2009. **37**(17): p. e116.

18.   Tsuji, A., et al., *Development of a time-resolved fluorometric method for observing hybridization in living cells using fluorescence resonance energy transfer.* Biophys J, 2001. **81**(1): p. 501-15.

19.   Tsuji, A., et al., *Direct observation of specific messenger RNA in a single living cell under a fluorescence microscope.* Biophys J, 2000. **78**(6): p. 3260-74.

20.   Chen, A.K., et al., *Ratiometric bimolecular beacons for the sensitive detection of RNA in single living cells.* Nucleic Acids Res. **38**(14): p. e148.

21.   Santangelo, P.J., et al., *Dual FRET molecular beacons for mRNA detection in living cells.* Nucleic Acids Res, 2004. **32**(6): p. e57.

22.   Abe, H. and E.T. Kool, *Flow cytometric detection of specific RNAs in native human cells with quenched autoligating FRET probes.* Proc Natl Acad Sci U S A, 2006. **103**(2): p. 263-8.

23.   Varkouhi, A.K., et al., *Endosomal escape pathways for delivery of biologicals.* J Control Release. **151**(3): p. 220-8.

24.   Dominska, M. and D.M. Dykxhoorn, *Breaking down the barriers: siRNA delivery and endosome escape.* J Cell Sci. **123**(Pt 8): p. 1183-9.

25.   Koppelhus, U. and P.E. Nielsen, *Cellular delivery of peptide nucleic acid (PNA).* Adv Drug Deliv Rev, 2003. **55**(2): p. 267-80.

26.   Zhang, K., et al., *Well-defined cationic shell crosslinked nanoparticles for efficient delivery of DNA or peptide nucleic acids.* Proc Am Thorac Soc, 2009. **6**(5): p. 450-7.

27. Zhang, K., et al., *Cationic shell-crosslinked knedel-like nanoparticles for highly efficient gene and oligonucleotide transfection of mammalian cells.* Biomaterials, 2009. **30**(5): p. 968-77.

28. Fang, H., et al., *Cationic shell-cross-linked knedel-like (cSCK) nanoparticles for highly efficient PNA delivery.* Mol Pharm, 2009. **6**(2): p. 615-26.

29. Lowenstein, C.J., et al., *Macrophage nitric oxide synthase gene: two upstream regions mediate induction by interferon gamma and lipopolysaccharide.* Proc Natl Acad Sci U S A, 1993. **90**(20): p. 9730-4.

30. Shakeel, S., S. Karim, and A. Ali, *Peptide nucleic acid (PNA) — a review.* Journal of Chemical Technology & Biotechnology, 2006. **81**(6): p. 892-899.

31. Oquare, B.Y. and J.S. Taylor, *Synthesis of peptide nucleic acid FRET probes via an orthogonally protected building block for post-synthetic labeling of peptide nucleic acids at the 5-position of uracil.* Bioconjug Chem, 2008. **19**(11): p. 2196-204.

32. Fang, H., Y. Shen, and J.S. Taylor, *Native mRNA antisense-accessible sites library for the selection of antisense oligonucleotides, PNAs, and siRNAs.* RNA. **16**(7): p. 1429-35.

33. Nazarenko, I., et al., *Effect of primary and secondary structure of oligodeoxyribonucleotides on the fluorescent properties of conjugated dyes.* Nucleic Acids Res, 2002. **30**(9): p. 2089-195.

Chapter Five

Summary, conclusion and future studies

Methods for detecting and imaging gene expression *in vivo* would be of great use for fundamental research and biomedical applications. To image mRNA in vivo is a challenging task, due to the low abundance of mRNAs [1], their secondary structure [2] and difficulty in getting the required nucleic acid probes inside cells. The overall goal of this dissertation was to develop methods and techniques for detecting and imaging mRNA both *in vitro* and in living cells that could ultimately be used *in vivo*. We have explored three approaches to achieve this goal: (1) aptamer tagged transgenic mRNA imaging; (2) strand-displacement activated PNA probes; and (3) adjacent PNA FRET probes.

We first investigated the use of malachite green (MG) to image MG binding aptamer tagged transgenes in living cells. Two major advantages of using MG for detecting transgene RNA are that the MG binding aptamer can increase the fluorescence of MG up to 2000 fold [3], and that (2) the transgene can be engineered to contain multiple repeats of the aptamer, thereby enhancing the fluorescence signal. We investigated the ability of using the MG aptamer system to image and detect transgenic mRNA in living cells utilizing constructs developed by Dr. Huafeng Fang. These constructs consisted of a β-adrenergic receptor gene fused to green fluorescent protein (GFP) gene to which was appended multiple repeats of the Malachite binding aptamer. This vector was successfully transfected into MDCK cells, as verified from fluorescence from the GFP protein. We were then able to show that the transgene mRNA could be successfully detected in the presence of MG in solution and in total RNA extracted from transfected cells. We have shown by confocal microscopy that transfected cells expressing GFP could also be imaged by fluorescence from the MG molecules. Although

MG has been reported to show around 2000 times increase in fluorescence upon binding to the aptamer in vitro, we only observed 22-fold increase in fluorescence for MG upon binding to the aptamer in cellular RNA extracts, and only 1.3-fold increase in living cells. The weaker than expected signal could be attributed to overloading of the cells with MG or to non-specific binding of MG to other cellular components. It is also possible that there were very few aptamer tagged mRNAs being expressed which were outnumbered by excess amounts of MG molecules inside cells, We did find, however, that the signal to noise ratio increased with incubation time after MG was removed from the media, presumably because the unbound MG molecules could exit cells via free diffusion. Incubating cells for a longer time (more than 24 h) was not desirable because MG remaining inside cells can be toxic [4, 5]. In the future however, we could explore the use of tagged mRNAs with a specific sequence that can hybridize to nucleic acid probes such as molecular beacons, strand-displacement probes or FRET probes described in Chapters 3 and 4. This method could be useful for studying mRNA transport, localization and be used to detect abnormal expression of certain mRNAs in cancer cells.

Our next approach towards mRNA imaging was to investigate the use of strand-displacement activated PNA probes to image inducible nitric oxide synthase (iNOS) mRNA in living cells. iNOS is an enzyme that catalyzes the production of NO in eukaryotic species. Its expression is induced under inflammatory conditions or upon environmental stimulation [6]. One of the research goals for the Program of Excellence in Nanotechnology (PEN) grant that we were working on is to be able to image iNOS expression in acute lung injury (ALI). We used mouse macrophage RAW 264.7 cells as a model system for imaging iNOS mRNA expression. We first determined that there are

about 700 copies of iNOS mRNA per cell, and upon stimulation with lipopolysaccharide (LPS) and γ-interferon (γ-IFN), this number increases up to 100-fold to about 70,000 copies. We then designed a 23-mer antisense peptide nucleic acid probe (PNA) bearing a fluorescein dye (FAM), whose fluorescence could be quenched by Dabcyl [plus] attached to a complementary 17-mer DNA strand when hybridized to the PNA. In the presence of the target mRNA, the shorter DNA strand was displaced by the longer complementary section on the iNOS mRNA resulting in restoration of fluorescence to the PNA. We have shown that the strand-displacement probe can detect target complementary DNA as well as *in vitro* transcribed mRNA in solution. We have also shown that the probe can be used to image iNOS mRNA in fixed cells, although the fluorescent intensity of the probes only increased 3.8-fold after stimulation of the cells and not the 100-fold expected from the RT-PCR assay. The lower than expected increase could be attributed to potential mRNA loss during the sample preparation and high background signal from non-specifically bound probes. We then used cSCK nanoparticles to deliver the strand-displacement probes inside cells and were able to image the fluorescence of the probe upon displacement by the iNOS mRNA. The matched probe showed 16.6-fold increase in fluorescence for stimulated cells compared to the nonstimulated cells under the same treatment while a control probe showed 4.1-fold increase in fluorescence in stimulated cells compared to the nonstimulated cells treated with matched probe. In conclusion, we were able to show that the strand-displacement PNA probes could be used to image the iNOS mRNA *in vitro*, in situ and in living cells. However, the difference in expression level reported by the nucleic acid probes in living cells is not as high as measured by RT-

159

PCR. This may be due to a high background caused by nonspecific binding of the probes in various cellular compartments.

Although the strand-displacement probes have been shown to be able to image iNOS mRNA in living cells, the high relative background signal makes it difficult to quantify the expression level. We therefore explored another way to reduce the background noise and increase the sensitivity that involves binary FRET probes. With binary FRET probes, a signal can only be detected upon simultaneous hybridization of a donor and an acceptor probe to adjacent sites on a target mRNA. We therefore synthesized 15-mer PNA FRET pairs bearing a donor (FAM or Cy3) and an acceptor (Cy5) fluorophore, respectively. We showed that such FRET probes could be used to detect iNOS mRNA *in vitro*. We have also delivered these FRET probes into living RAW 264.7 cells with cSCK nanoparticles. The PNA probes were first annealed to partially complementary 13-mer DNAs and mixed with the cationic cSCK nanoparticles to form polyplexes via electrostatic interactions. The mixtures were then incubated with living cells and the FRET images of the iNOS mRNA were obtained by confocal microscopy. Wavelength scans were also performed to obtain the FRET spectra of the images. Cells expressing high levels of iNOS mRNA showed an enhanced FRET signal that is 3.8 times greater than cells expressing low levels of iNOS mRNA. Probes consisting of a FRET donor sequence and mismatched PNA-Cy5 showed almost no FRET in living cells, further confirming that the FRET signal was due to hybridization of the probes to iNOS mRNA, and not to formation of polyplexes with the cSCK nanoparticles.

In conclusion, this thesis has demonstrated our ability to image mRNA expression in living cells by either transgene aptamers or peptide nucleic acid probes utilizing cSCK

nanoparticles for intracellular delivery. There are some issues, however, that remain to be solved before one can quantitatively image mRNA expression *in vivo,* which is the long term goal of this research.

One important problem to solve is the more efficient intracellular delivery of the nucleic acid probes to the target mRNAs in the cytoplasm. We have shown that cSCK nanoparticles can deliver the PNA/DNA duplexes into the cells, though based on confocal microcopy studies, the delivery is not very fast or efficient (requiring 24 h incubation). Cells were also not homogeneously transfected, resulting in large deviations in signal intensity between cells. We noticed that while higher doses of cSCK nanoparticles could facilitate higher internalization of the probes, the higher doses also caused significant cellular toxicity [7]. Current efforts under the PEN program are to develop nanoparticles that can achieve faster delivery and that have lower toxicity, such as acetalated dextran (AC-DEX) nanoparticles, comb-shaped nanoparticles, and cSCK nanoparticles modified by cell targeting peptides, etc.

Another problem is the endosomal entrapment of the probes, which prevents the probes from reaching the target mRNA in the cytoplasm. Although the quenched strand-displacement probes and the FRET probes can minimize the signal from unbound probes, the absolute signal intensity will depend on the efficiency by which the probes enter the cytoplasm. Therefore, mechanisms that can improve release of the unbound probes from the endosomes should help to increase the sensitivity of the probes. For example, Engelman et al have reported the discovery of a pH Low Insertion Peptide (pHLIP), which changes its structure at pH6-6.5 and inserts its C terminus through bilayer lipid membrane [8]. Such a peptide has been used to deliver cellular impermeable molecules

including PNAs across the membrane of cancerous cells when attached to the C-terminus [9, 10]. In future studies, such a peptide could be conjugated to PNAs via a disulfide bond and help translocate the probes from endosomes to the cytoplasm when the endosomes acidify. The disulfide bond will then be cleaved in the cytoplasm and the probes will be released.

To further improve of the optical probes for *in vivo* imaging, it will be necessary to use fluorescent molecules that can emit in near infrared (NIR) range. Unlike radioactive probes, whose signal can penetrate through deep tissues without much loss, fluorescence in the UV-Vis range is prone to be absorbed by organs and tissues. However, tissues have much less absorption and scattering for NIR light, making NIR dyes more suitable for *in vivo* imaging [11, 12]. Dr. Achilefu's group at Washington University School of Medicine that is participating in the PEN program, have developed infrared dyes that can be used for molecular imaging and *in vivo* studies [13, 14]. In the future, those NIR dyes could be conjugated to the PNA probes and used for *in vivo* mRNA imaging.

One final improvement would be to further decrease the signal from unbound probes. One approach to doing this would be to combine the strand-displacement probe with the binary FRET probes developed in this thesis. Just like the dual FRET probes, which utilize molecular beacons to quench fluorescence from unbound probes [15], two strand-displacement probes could be employed to image mRNA in living cells (**Figure 5.1**). Both the donor and acceptor probes would remain quenched when there is no target mRNA present, but in the presence of the target mRNA, both quencher strands would be displaced thereby activating the donor and acceptor for FRET. Such dual strand-

displacement probes would be expected to have better signal to noise ratio than the individual strand displacement or binary FRET systems studied.
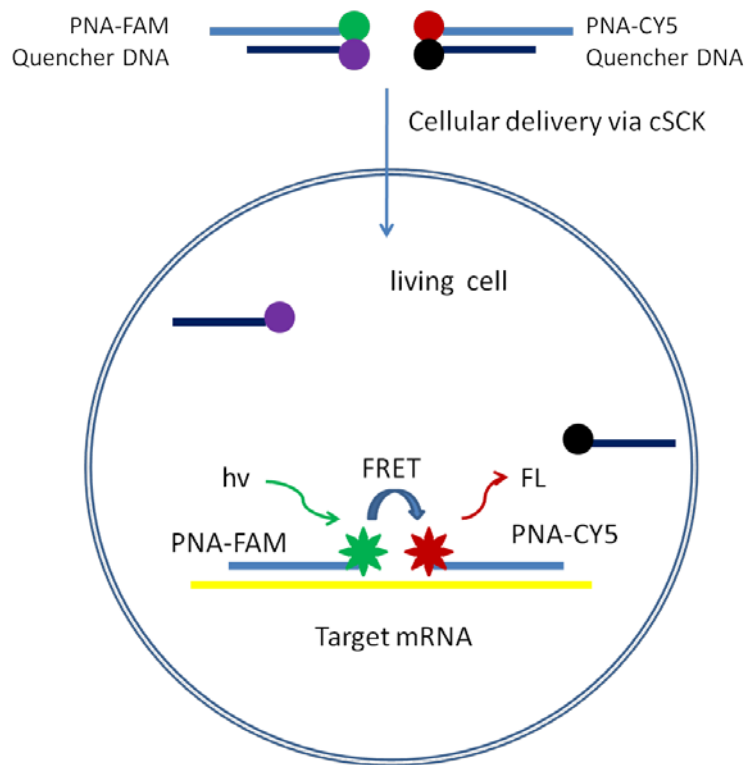

Figure 5.1: Schematic representation of dual strand-displacement FRET probes.

Reference

1.   Lewis, M.R. and F. Jia, *Antisense imaging: and miles to go before we sleep?* J Cell Biochem, 2003. **90**(3): p. 464-72.

2.   Gifford, L.K., et al., *Identification of antisense nucleic acid hybridization sites in mRNA molecules with self-quenching fluorescent reporter molecules.* Nucleic Acids Res, 2005. **33**(3): p. e28.

3.   Babendure, J.R., S.R. Adams, and R.Y. Tsien, *Aptamers switch on fluorescence of triphenylmethane dyes.* J Am Chem Soc, 2003. **125**(48): p. 14716-7.

4.   Kraus, G.A., et al., *Fluorinated analogs of malachite green: synthesis and toxicity.* Molecules, 2008. **13**(4): p. 986-94.

5.   Panandiker, A., G.B. Maru, and K.V. Rao, *Dose-response effects of malachite green on free radical formation, lipid peroxidation and DNA damage in Syrian hamster embryo cells and their modulation by antioxidants.* Carcinogenesis, 1994. **15**(11): p. 2445-8.

6.   Aktan, F., *iNOS-mediated nitric oxide production and its regulation.* Life Sci, 2004. **75**(6): p. 639-53.

7.   Zhang, K., et al., *Well-defined cationic shell crosslinked nanoparticles for efficient delivery of DNA or peptide nucleic acids.* Proc Am Thorac Soc, 2009. **6**(5): p. 450-7.

8.   Reshetnyak, Y.K., et al., *Translocation of molecules into cells by pH-dependent insertion of a transmembrane helix.* Proc Natl Acad Sci U S A, 2006. **103**(17): p. 6460-5.

9.   An, M., et al., *pH-(low)-insertion-peptide (pHLIP) translocation of membrane impermeable phalloidin toxin inhibits cancer cell proliferation.* Proc Natl Acad Sci U S A. **107**(47): p. 20246-50.

10.   Thevenin, D., M. An, and D.M. Engelman, *pHLIP-mediated translocation of membrane-impermeable molecules into cells.* Chem Biol, 2009. **16**(7): p. 754-62.

11.   Ntziachristos, V., C. Bremer, and R. Weissleder, *Fluorescence imaging with near-infrared light: new technological advances that enable in vivo molecular imaging.* Eur Radiol, 2003. **13**(1): p. 195-208.

12.   Zhu, B., et al., *Reduction of excitation light leakage to improve near-infrared fluorescence imaging for tissue surface and deep tissue imaging.* Med Phys. **37**(11): p. 5961-70.

13.   Almutairi, A., et al., *Biodegradable pH-sensing dendritic nanoprobes for near-infrared fluorescence lifetime and intensity imaging.* J Am Chem Soc, 2008. **130**(2): p. 444-5.

14.   Zhang, Z., et al., *Activatable Molecular Systems Using Homologous Near-Infrared Fluorescent Probes for Monitoring Enzyme Activities in Vitro, in Cellulo, and in Vivo.* Mol Pharm, 2009.

15.   Santangelo, P.J., et al., *Dual FRET molecular beacons for mRNA detection in living cells.* Nucleic Acids Res, 2004. **32**(6): p. e57.